Development of Efficient Flowsheet and Transient Modeling for Nuclear Heat Coupled Sulfur Iodine Cyclefor Hydrogen Production

Project No. 06-060

Award No. DE-FC07-06ID14749

Final Report
For Period
March 13, 2007 - March 12, 2010

By

Shripad T. Revankar, Nicholas R. Brown
Cheikhou Kane, and Seungmin Oh

May 2010

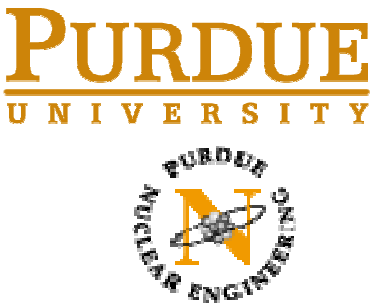

Contact: Dr. Shripad T. Revankar
School of Nuclear Engineering
Purdue University
West Lafayette, IN 47907-1290

765-496-1782

shripad@ecn.purdue.edu

Executive Summary

The realization of the hydrogen as an energy carrier for future power sources relies on a practical method of producing hydrogen in large scale with no emission of green house gases. Hydrogen is an energy carrier which can be produced by a thermochemical water splitting process. The Sulfur-Iodine (SI) process is an example of a water splitting method using iodine and sulfur as recycling agents. The SI cycle consists of three chemical reactions expressed as the following equations.

Section I (Bunsen reaction): $I_2+SO_2+2H_2O \rightarrow 2HI+H_2SO_4$

Section II (Sulfuric acid decomposition): $H_2SO_4 \rightarrow H_2O+SO_2+1/2O_2$

Section III (Hydrogen Iodide decomposition): $2HI \rightarrow H_2+I_2$

In the SI cycle, all process fluids are recycled and no greenhouse gases are emitted. Also, the SI cycle has been fully flow sheeted and operated at the bench scale in the US and Japan. This cycle has the highest efficiency (~52%) of any process that has been fully flow sheeted. However, the integrated SI cycle is not yet fully demonstrated and the process economics are not yet verified.

In this report, the following major subtasks were completed (i) Simulation of Sulfur Iodine Thermochemical Hydrogen Production Plant Coupled To High Temperature Heat Source, (iii)

Model for Nuclear Plant and Interface System and (ii) Transient Analysis for the Coupled System,

First a simplified model for the SI cycle is developed with chemical kinetics models of the three main SI reactions: the Bunsen reaction, sulfuric acid decomposition, and hydriodic acid decomposition. Each reaction was modeled with single control volume reaction chamber. The simplified model uses basic heat and mass balance for each of the main three reactions. For sulfuric acid decomposition and hydriodic acid decomposition, reaction heat, latent heat and sensible heat were considered. Since Bunsen reaction is exothermic and its overall energy contribution is small, its heat energy is neglected. However the inputs and output streams from the Bunsen reaction are accounted in

balancing the total stream mass flow rates from the SI cycle. The heat transfer between the reactor coolant (in this case helium) and the chemical reaction chamber was modeled with transient energy balance equations. The steady-state and transient behavior of the coupled system is studied with the model and the results of the study presented. It was determined from the study that the hydriodic acid decomposition step is the rate limiting step of the entire SI cycle.

In the model for nuclear plant and interfaces system, a simplified transient model of the Sulfur-Iodine (SI) cycle was coupled to a THERMIX thermal hydraulic model of the Pebble Bed Modular Reactor 268 (PBMR 268) and a point kinetics model. A control volume approach was used in analysis of the chemical plant. A steady state solution of the SI cycle model and THERMIX model was attained. A transient analysis of the couple system was carried out. A transient was initiated via reactivity insertion in a simple point kinetics model. Results from a nuclear reactor driven transient are presented, as well as suggestions for future work regarding chemical plant induced transients

Table of Contents

List of Figures

List of Tables

1. Project Objectives

The objective of Nuclear Hydrogen Initiative (NHI) program of the Department of Energy (DOE) is to operate the nuclear hydrogen production plant to produce hydrogen at a cost competitive with other alternative transportation fuels by the year 2017 (DOE 2005). The NHI program is focused on the Hydrogen production technologies that are compatible with nuclear energy systems and do not produce greenhouse gases. For the hydrogen production technology, several options are considered including steam methane reforming, electrolysis, thermochemical cycles, and high-temperature electrolysis. The steam methane reforming and electrolysis methods are not much interested in the NHI program due to the production of greenhouse gases and low efficiency. The thermochemical cycles and high-temperature electrolysis methods are expected to provide a similar theoretical efficiency in a range of 40-60%. However, the thermochemical cycles are considered as a best suited process with the nuclear heat source in terms of cost of hydrogen production and minimal environmental impact (Elder et al. 2005; Kubo et al. 2004a).

Among the thermochemical cycles, a well established Sulfur-Iodine (SI) process developed at General Atomics (Besenbruch 1982) and first described in the mid 1970's has been considered in U.S., Japan and France for hydrogen production using high temperature heat from nuclear reactor (Brown et al. 2002; Forsberg 2003; Yan et al. 2003). In a recent NERI supported project SI cycle flowsheet development was carried out using ASPEN PLUS, a commercial available process simulation program (Brown et al. 2003).

Though recently closed loop bench scale SI cycle has been demonstrated that several challenges remain in this technology such as maintaining stable operation (Kubo et al. 2004b), enhancing the efficiencies of the processes in the cycle (Goldstein et al. 2005; Yildiz and Kazimi 2003), thermodynamic data for the reactions for various operating conditions (Mathias 2005), coupling to high-temperature nuclear reactor and transient behavior of the coupled SI cycle and reactor. Several alternates to the SI cycles have been proposed in the literature specifically in the HI and H_2SO_4 decomposition processes and separation of the product gases (Goldstein et al. 2005; Kasahara et al. 2004; Kubo et al. 2004b; Nomura et al. 2004; Öztürk et al. 1995). These alternatives to the SI cycles will be

explored in this research and optimized flow sheet development will be carried out. Models will be developed to study transient performance of the closed loop SI cycle.

The main goal of the proposed project is to develop flowsheet for the closed loop SI cycle using current advances in the acid decomposition and product gas separation for high thermal efficiency and development of methods for transient analysis of the cycle. Specific objectives of the proposed project are: (i) to perform benchmark flowsheet analysis of the baseline GA SI cycle, (ii) to investigate and implement the membrane techniques to the HI and H_2SO_4 decomposition and separation processes, (iii) to perform comparative flowsheet analysis of the modified cycles, (iv) to develop component-wise models of the SI cycle for application to the transient analysis and (v) to perform preliminary analysis of transient behavior of the closed loop SI cycle. The objectives of this project address R&D needs of the Nuclear Hydrogen Initiative (NHI) Program Elements 3.1 Thermochemical Cycles and 3.3 Reactor-Hydrogen Production Process Interface.

2. Introduction

2.1 Hydrogen Production Using Nuclear Power

The demand for energy continues to rise due to the continuing increase in world population and the growing demand by the developing countries in order to improve their living standards. A large portion of the world's energy demand is met by the fossil fuels because of availability and existing infrastructure. However, it is estimated that the world's fossil fuel production will soon start declining. Also, pollution and greenhouse issues resulting from the use of fossil fuels require novel sustainable energy sources. Various non-fossil energy sources, such as solar, ocean-thermal, wind, waves, thermonuclear, geothermal, etc., are being considered as possible sources of energy.

There has been significant recent research on the hydrogen energy concept, in which hydrogen is used as a main energy carrier. The replacement of conventional combustion of fossil fuels by the electrochemical combustion of hydrogen has long been regarded as highly desirable from energetic, economic, and environmental viewpoints. In addition, availability of energy resources is an important national security issue. The energy output from combustion of hydrogen (about 118 MJ/kg at 298 K) is much higher than that of gasoline (about 44 MJ/kg). Also the byproduct of the hydrogen combustion is only water, which is a great environmental advantage of hydrogen compared to the fossil fuels. Recent development and use of fuel-cell powered vehicles has generated impetus to conduct research on the production, transmission, storage, and distribution of hydrogen.

The main sources of hydrogen are natural gas and petroleum. Hydrogen is separated by the removal of carbon monoxide or carbon dioxide from steam reformation processes. These are not of primary interest, because their reserves are diminishing and large amounts of greenhouse gases are emitted. The other major source of hydrogen is water, which is quite abundant. Hydrogen can be produced by decomposing water, i.e., breaking the chemical bonds of water. The decomposition of water can be effected by electrolysis, direct thermal decomposition, chemical reaction, and thermochemical cycles. Among those methods, the thermochemical water decomposition by closed cycle processes has received increasing attention. Thermochemical water decomposition cycle concept was proposed by Funk and Reinstrom (Funk and Reinstrom 1966). In a thermochemical

process, thermal energy is transformed into chemical energy (hydrogen), without first converting heat to mechanical energy and then to electrical energy as is the case with electrolysis. In an electrolysis plant, the steam process, by which the heat from the primary energy source is converted into electrical energy, is at best 40% efficient, and the electrolysis process is at best 90% efficient. This leads to an overall process efficiency from source heat to potential energy in product hydrogen of 36%. The initial projected theoretical efficiency of the thermochemical cycles under investigation is near 50%.

The high heat of combustion of hydrogen to water means that the thermochemical decomposition of water requires a large amount of energy. One of the large scale energy sources is nuclear energy. If nuclear energy is to be used for hydrogen production, the nuclear reactor must deliver the heat at conditions that match the requirements imposed by the hydrogen production process. The viability of hydrogen production from nuclear power ultimately depends upon the economics, which, in turn, depend upon both the proposed methods of hydrogen production and the available reactors.

Hydrogen can be produced by direct thermochemical processes in which the net reaction is heat plus water yields hydrogen and oxygen. For low production costs, however, high temperatures are required to ensure rapid chemical kinetics and high conversion efficiencies, which result in small plant size with low capital costs.

Many types of thermochemical processes for hydrogen production have been proposed (Brown et al. 2003; Yalcin 1989). The Sulfur-Iodine (SI) or Iodine-Sulfur (IS) cycle is currently the leading candidate, which has been studied extensively by the General Atomics (GA) (Brown et al. 2003; Norman et al. 1982) and the Japan Atomic Energy Research Institute (JAERI) (Kubo et al. 2004b; Kubo et al. 2004a; Nomura et al. 2005). In the present study, GA's SI cycle is chosen as a reference process.

2.2 Sulfur-Iodine Cycle

The SI cycle consists of three chemical reactions expressed as the following equations,

$$I_2+SO_2+2H_2O \rightarrow 2HI+H_2SO_4 \text{ (Bunsen reaction)} \quad (1.1)$$

$$H_2SO_4 \rightarrow H_2O+SO_2+1/2O_2 \text{ (Sulfuric acid decomposition)} \quad (1.2)$$

$$2HI \rightarrow H_2+I_2 \text{ (Hydrogen Iodide decomposition)} \quad (1.3)$$

Figure 2.1 presents the concept of the SI cycle. Eq. (1.1) is called Bunsen reaction and proceeds in liquid phase. This reaction produces two kinds of acid, sulfuric acid (H_2SO_4) and hydriodic acid in solution (HI) from sulfur dioxide (SO_2), iodine (I_2) and water (H_2O). The mixed acid separates into two types of acid of its own accord (liquid–liquid separation). The acid, which is rich in HI, is HI_x phase (HI_x solution), while the acid, which is rich in H_2SO_4, is the H_2SO_4 phase. After separation of the acids, they are purified, concentrated and decomposed in the other two reactions. Eq. (1.2) is the H_2SO_4 decomposition reaction that produces oxygen, sulfur dioxide, and water. Eq. (1.3) is the HI decomposition reaction which produces hydrogen and iodine. With the exception of hydrogen and oxygen, the other products in Eqs. (1.2) and (1.3) can be reused in the Bunsen reaction step as the reactant material. The endothermic H_2SO_4 decomposition reaction can be operated at about 800~1000°C. The decomposition of hydriodic acid involves an endothermic reaction around 400~500 C. The Bunsen reaction occurs exothermically at temperatures of about 100 C. Heat source of two endothermic acid decomposition reactions in the SI cycle can be provided by the nuclear heat as shown in Figure 2.2 schematically.

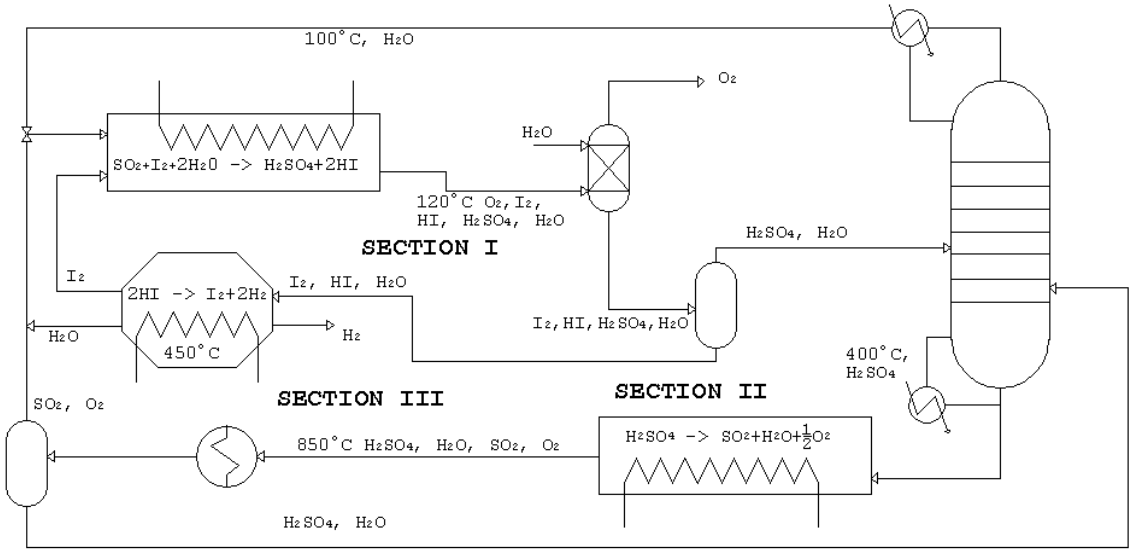

Figure 2. 1 Schematic diagram of sulfur-iodine cycle

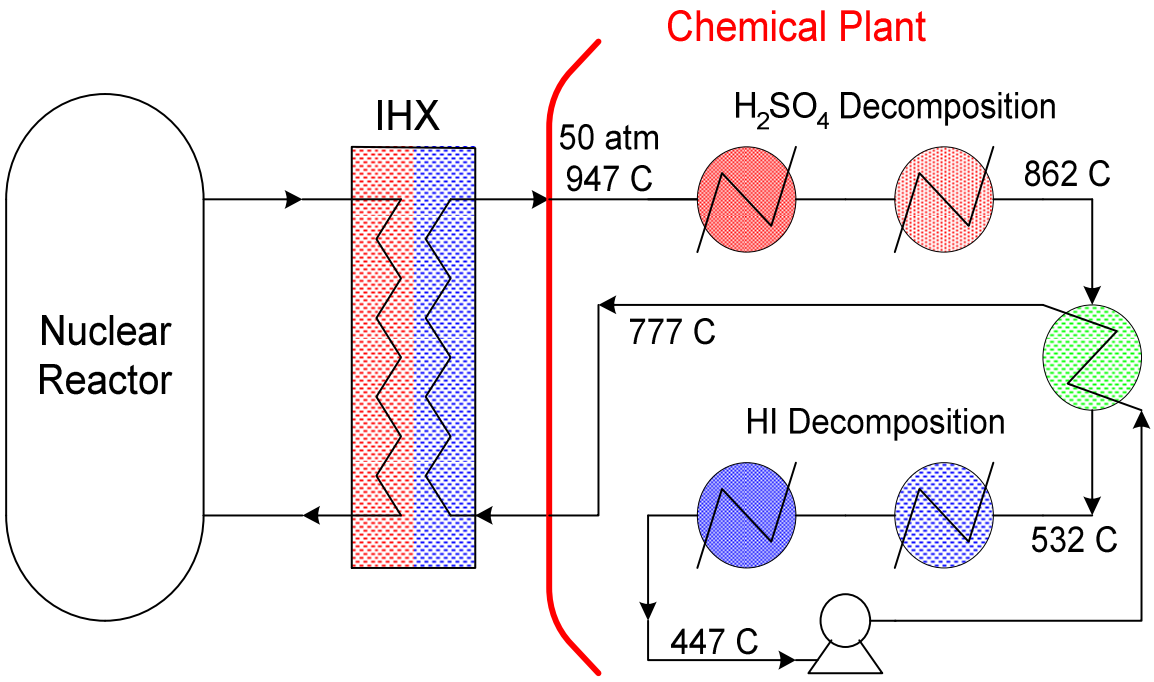

Figure 2. 2 Schematic diagram of nuclear-chemical plant

The net reaction of the SI cycle is the water splitting into hydrogen and oxygen expressed as the following equations.

$$H_2O \rightarrow H_2 + \tfrac{1}{2}O_2 \text{ (net reaction)} \qquad (1.4)$$

In the SI cycle, all process fluids are recycled and no greenhouse gases are emitted. Also, the SI cycle has been fully flow sheeted and operated at the bench scale in the US and Japan. This cycle has the highest efficiency (~52%) of any process that has been fully flow sheeted. Since the hydrogen is produced at high pressure, it eliminates the necessity of compressing the hydrogen for pipeline transmission or other downstream processing. One of the most challenging issues regarding the SI cycle are the material issues, which originate from the high process temperature (800~1000 C) and the corrosive reactants such as the sulfuric acid and hydrogen iodide. Also, the integrated SI cycle is still in the development stage.

2.3 Sulfur-Iodine Cycle Simulation Using ASPEN PLUS

In this report, the SI cycle simulation results using ASPEN PLUS code version 12 are presented. The present simulations followed the methodology applied to the GA's flowsheet (Brown et al. 2003). A step-by-step simulation is conducted. To minimize the convergence problem in a complex system of the SI thermochemical process, the simulation is performed initially for the single component. If adjacent components are converged, then they are combined and simulated. Finally, the simulation for the whole Section is conducted.

As background information, a detailed discussion on the SI cycle proposed by the GA is presented in chapter 3. In chapter 4, a step-by-step simulation for the SI cycle is presented.

3. General Atomics SI cycle

General Atomics (GA) developed the SI cycle which offers the potential for efficient, cost-effective, large-scale production of hydrogen from water, in which the primary energy input is high temperature heat from an advanced nuclear reactor (Brown et al. 2003). The selection of the SI cycle was based on a detailed literature search of published thermochemical cycles, a screening procedure using the criteria developed to rate each cycle, and a detailed analysis. The SI cycle is the cycle with the highest reported efficiency based on an integrated flowsheet. Also, various researchers have pointed out improvements that should increase the already high efficiency of this cycle and, in addition, lower the capital cost. As the SI cycle had both the highest predicted efficiency and the most potential for further improvement, it was selected for the hydrogen production method.

GA developed the SI process model based on the earlier GA's SI cycle flowsheet (Norman et al. 1982). They divided the SI cycle into three sections and named the Bunsen reaction in Eq. (1.1) as Section I, the H_2SO_4 decomposition process in Eq. (1.2) as Section II, and HI decomposition process in Eq. (1.3) as Section III. Figure 1.1 shows the SI cycle flow diagram. Sulfuric acid and hydrogen iodide are generated in the low temperature exothermic Bunsen reaction (Section I). Sulfuric acid is decomposed at high temperature endothermic reaction (Section II) and hydrogen iodide at medium temperature endothermic reaction (Section III). There are significant chemical separations associated with each chemical reaction. Water is the primary solvent in the system and iodine is also an important solvent in the Bunsen reaction.

GA's earlier SI flowsheets were developed using hand calculation and the thermodynamic models available at that time could not deal with the non-ideality of even the simplest part of the process. For the recent SI model, GA used Aspen Plus®, the process simulation program, which has the best implementation of electrolytic solution thermodynamics available. Aspen Plus® incorporates the capability of modeling electrolytes via several different modeling techniques including an electrolytic version of the Non-Random Two Liquid (NRTL) technique. An electrolytic NRTL (ELECNRTL) model can handle everything from concentrated electrolytes through dilute electrolytes to

non-polar species, such as iodine.

Initially, they tried to develop new models for each Section of SI cycle. However, there was no valid model covering the range of temperature, pressure and composition needed to describe the thermochemistry of the SI cycle even for the simple system H_2SO_4/H_2O. With the services of Aspen Technology, licenser of Aspen Plus, they developed the NRTL sulfuric acid model and it was used to model Section II of the flowsheet. However, they were unable to develop Aspen Plus models for $HI/I_2/H_2O$ system (Section III) or the $H_2SO_4/HI/I_2/H_2O$ system (Section I). The current state of the equilibrium data for the $HI/I_2/H_2O$ system appears to be inadequate to be able to develop a model that will successfully converge. So, the flowsheets for Sections I and III were based on earlier analyses, calculated by hand without a chemical simulation computer program. For Section III, HI decomposition, they use the reactive distillation process proposed by Roth and Knoche (Roth and Knoche 1989). For Section I, they started with the GA's earlier flowsheet (Norman et al. 1982) and calculated the compositions after accounting for the large recycle flows from Section III.

Final flowsheets developed by GA were based on assumed peak process temperature of 827°C. This temperature could be attained using proposed 850°C High Temperature Gas Reactor (HTGR) outlet temperature and a high effectiveness compact heat exchanger. The complete design at this temperature achieved 42% thermal efficiency. They estimated that 52% efficiency could be achieved at higher peak process temperature of 900°C This would require about 950°C reactor outlet temperature.

3.1 Bunsen Reaction

When the SI cycle was initially investigated in the mid 1970's, it was rejected by early workers due to difficulties encountered separating the hydrogen iodide and sulfuric acid produced in Bunsen reaction. Attempts to use distillation were useless as sulfuric acid and hydrogen iodide react according to the reverse of Bunsen reaction when their mixture is heated. The key to successful implementation of the cycle was the recognition that using an excess of molten iodine would result in a two-phase solution, a light phase

containing mainly sulfuric acid and a heavy phase containing hydrogen iodide and iodine.

A flowsheet for Section I is presented in Figure 3.1. The composition of streams exiting Section I can be predicted from thermodynamic arguments but the properties of streams recycled back to Section I can only be determined after completing detailed flowsheets of Sections II and III. The ELECNRTL thermodynamic model was insufficient to perform a strictly thermodynamic model so the Section I flowsheet was adapted from previous flowsheets (Norman et al. 1982) but modified the flow rates to match the current versions of Sections II and III.

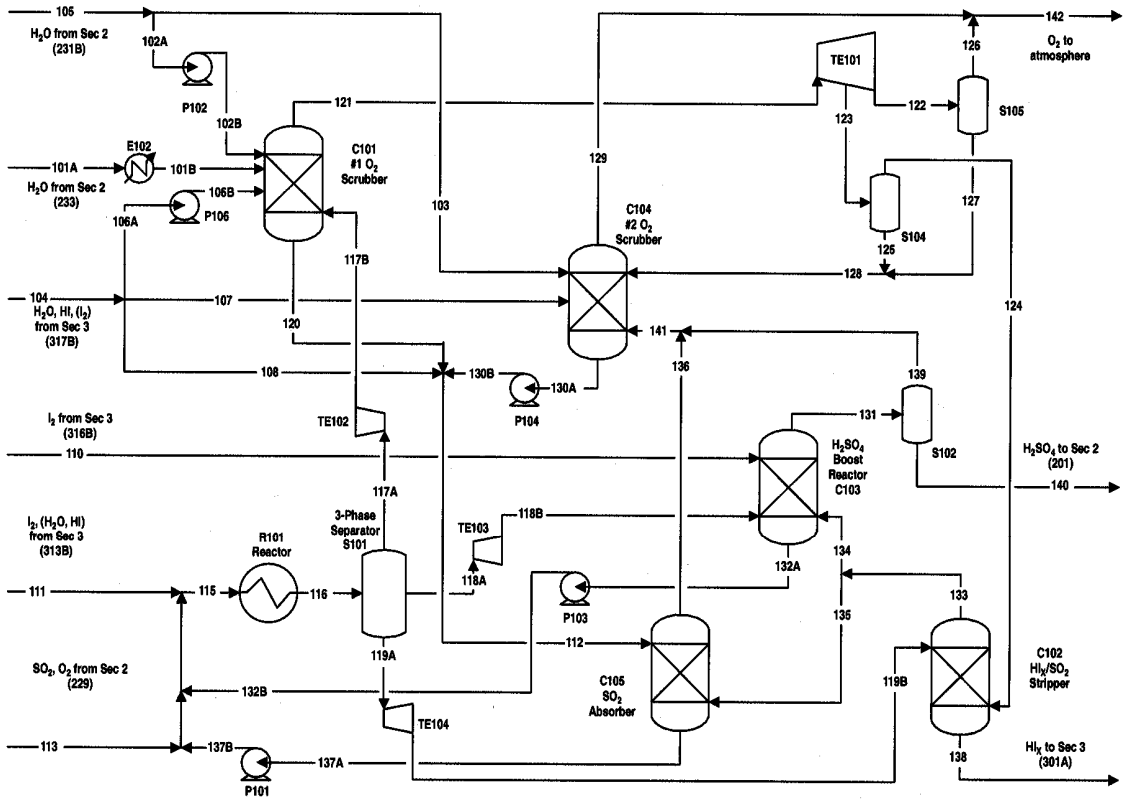

Figure 3. 1 GA Section I flowsheet (Brown et al. 2003)

The majority of the Bunsen reaction: $SO_2 + I_2 + 2H_2O \rightarrow H_2SO_4 + 2HI$ takes place in the heat exchange reactor (R101) at 7 bars. This reaction also takes place in the primary oxygen scrubber (C101), the secondary oxygen scrubber (C104), and the H_2SO_4 boost reactor (C103). The output from the heat exchange reactor consists of three phases, which are separated in S101 and processed separately. The gas phase contains residual SO_2 in

O_2. The SO_2 is removed by chemical reaction in C101: most of the O_2 is vented but a portion is recycled and used to strip the SO_2 remaining in the dense HIx ($HI/I_2/H_2O$) liquid (119A). The SO_2, stripped from the HIx in C102, is used to react water out of the light liquid phase (118A) in the H_2SO_4 boost reactor (C103). The sulfuric acid stream enters the boost reactor at 15 and exists at 20 mol%. The iodine stream (110) used in the boost reactor exits the bottom containing the HI formed in the boost reactor, along with the water required to solubilize the HI, and is pumped (P103) to the heat exchanger reactor. The overhead liquid product of the boost reactor (131/140) passes to Section II, where the H_2SO4 is concentrated and decomposed. Any SO_2 remaining in the sulfuric acid is returned to Section I, along with water flashed from the sulfuric acid (101A).

The gaseous product (131/139) of the boost reactor is scrubbed in the secondary scrubber, along with the exhaust (136) of the SO_2 Absorber (C105). The gaseous product (129) of the secondary O_2 scrubber exits the process along with the vent (126) from the primary O_2 scrubber. The combined vent (142) contains one-half mole of oxygen for every mole of hydrogen produced in the overall process. The liquid products of the two oxygen scrubbers (120/130B) are combined with a portion (108) of the HI/H_2O recycled from Section III (104), and the combined stream (112) is used to adsorb much of the SO_2 stripped from the HI_x.

3.2 Sulfuric Acid Decomposition

The flowsheet for Section II is shown in Figure 3.2. The purpose of Section II is to concentrate the sulfuric acid received from Section I and decompose the concentrated sulfuric acid, producing sulfur dioxide (SO_2) and oxygen ($H_2SO_4 \rightarrow H_2O+SO_2+1/2O_2$). It is important to concentrate the sulfuric acid before decomposing it. First, less material heated to high temperatures means less sensible heat must be supplied, which means smaller heat exchangers and less cost. Secondly, there is a thermodynamic loss associated with the differential temperature across heat exchangers and lower heat transfer means higher thermodynamic efficiency. Also, the heat of solvating sulfuric acid must be supplied at some point in the course of getting the sulfuric acid to the decomposition

conditions. In concentrating the sulfuric acid, the pressures and, thus, the temperatures at which the water is removed from the sulfuric acid can be adjusted, permitting thermodynamic optimization of the overall concentration and decomposition process.

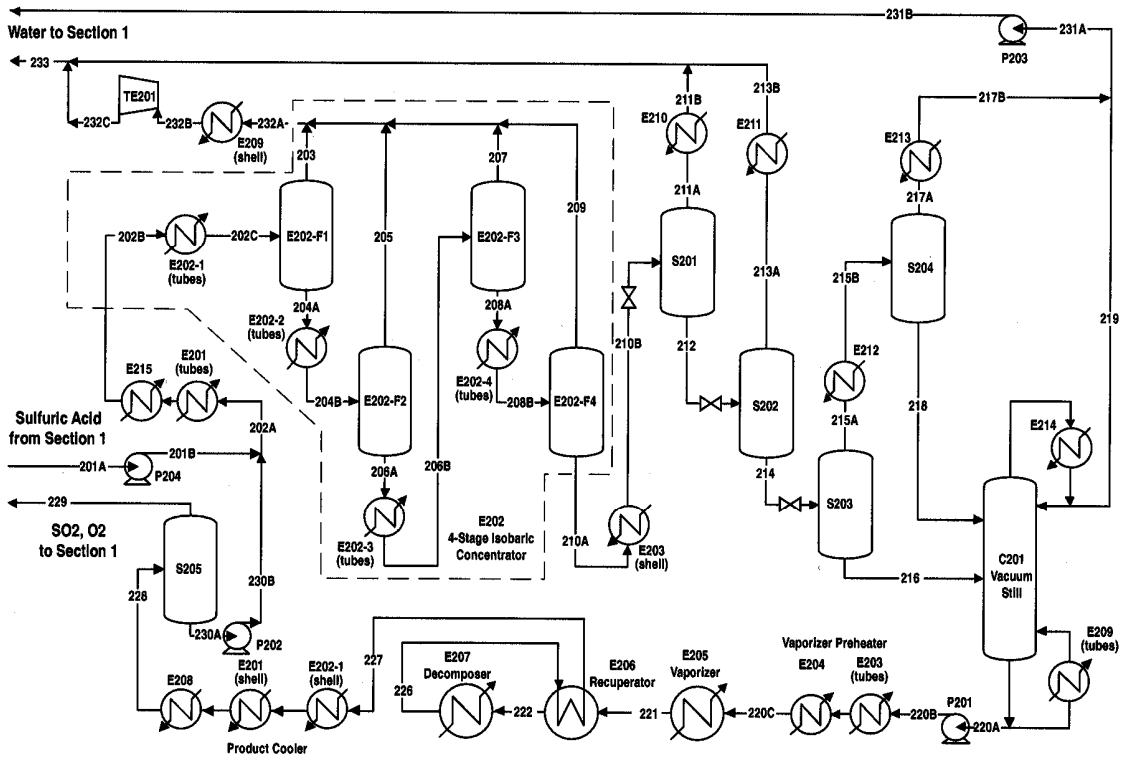

Figure 3. 2 GA Section II flowsheet (Brown et al. 2003)

3.2.1 Concentration of Sulfuric Acid

The inlet sulfuric acid of 20 mol%, along with internally recycled sulfuric acid, is concentrated to 40 mol% in a high pressure four-stage isobaric concentrator (E202). The feed to Section II (201A) and the recycle stream (230A) are pumped up to the operating pressure of the isobaric concentrator (35 atm) and preheated together before entering the concentrator. The sulfuric acid solution flows through four connected and heated chambers. Water is boiled off in each chamber so that both the temperature and the acid concentration of the solution increase as the solution flows through the concentrator. The water vapor boiled off in each chamber is mixed above the chambers and leaves as a single stream. The small amount of sulfur dioxide remaining in the inlet sulfuric acid is

also removed with the water. The sensible and latent heat in this stream will be used elsewhere in this section.

The liquid product of the isobaric concentrator (210A) is further concentrated in a series of three reduced pressure flashes (S201, S202, S203) at 8 bar, 2 bar and 50 Torr before entering the 50 Torr vacuum still (C201). Prior to the first flash, some heat is removed in E203 for use later in the process, the subsequent flashes are adiabatic. The feed to the vacuum still (216) is 56 mol% sulfuric acid. The vapor from the final adiabatic flash passes through a partial condenser. The condensate from the partial condenser (218) is feed to the vacuum still at a position appropriate to its composition (47 mol% H_2SO_4).

The pressures of the distillation column and the isobaric concentrator were chosen such that the column reboiler temperature is low enough to utilize heat recovered upon condensing the isobaric concentrator vapor stream. That is, a balance must be struck between the pressure of the isobaric flash and the pressure of the distillation column in order to use this heat. As the pressure of the isobaric flash increases, the temperature of heat recovered from the vapor stream also increases. As the column pressure is decreased, the required temperature of heat required goes down. All other considerations equal, the operating pressures should be as low as practical, although a higher helium temperature from the nuclear reactor might allow higher overall process efficiencies at higher pressures.

The overhead from the vacuum still, nearly pure water, is returned to Section I. The bottom product of the distillation column (220A) is azeotropic sulfuric acid (~90 mol% H_2SO_4) liquid at 212°C. The concentrated sulfuric acid is pumped from the column pressure up to the 7 bar pressure used in the sulfuric acid decomposition portion of the process.

3.2.2 Decomposition of Sulfuric Acid

Before the sulfuric acid can be decomposed, it must first be heated to the vaporization temperature and vaporized. All of these steps occur at 7 bars. The first step in the reaction sequence is the vaporization of the concentrated sulfuric acid stream. Some of the heat required to preheat the stream prior to vaporization is recovered from the liquid product of the isobaric concentrator but the remainder of the heat required for heating, vaporizing, and decomposing the sulfuric acid is provided by the high temperature helium from the nuclear reactor. Some of the sulfuric acid decomposes into SO_3 and water as it is vaporized and this reaction proceeds further as the vaporized stream is heated in the recuperator (E206). The recuperator retrieves much of the heat remaining after sulfuric acid decomposition. Physically, the recuperator is similar to a shell and tube heat exchanger, with the hot fluid flows on the tube side and the cool fluid flows on the shell side. Most of the sulfuric acid has decomposed into SO_3 and water by the exit of the recuperator (222).

The decomposer (E207) is modeled using printed circuit heat exchanger (PCHE) with catalyst deposited on the wall of the exchanger on the process side. The highest process temperature (827°C) in the whole SI cycle is realized in the decomposer. The catalytic wall reactor has the continuous temperature profile. Not only is the catalytic wall heat exchanger simpler to operate, it reduces the temperature difference between the hot helium and the decomposed acid compared with even a multi-staged fluidized bed. For a given process outlet temperature, the helium temperature can be lowered and thus the operating temperature of the nuclear reactor.

The reactor outlet stream (226) is cooled in the recuperator, transferring heat to the decomposer feed, as mentioned previously. The reaction products are further cooled and the heat is recovered for use within this Section in the product cooler. The product cooler is physically divided into three heat exchangers. Part of the recovered heat is used for the first stage of the isobaric concentrator and the remainder is used to preheat the concentrator feed. Unrecoverable heat is lost to cooling water. The liquid condensed in the product cooler is recycled to the isobaric concentrator and the gas phase, consisting

primarily of SO_2 and O_2 is recycled to Section I.

3.3 Hydrogen Iodide Decomposition

GA's earlier flowsheets developed in 1979 and 1981 (Norman et al. 1982) used phosphoric acid (H_3PO_4) to extract the water from the HI_x ($HI/I_2/H_2O$) solution resulting from the Bunsen reaction. It was indicated that over 40% of the total capital cost of the SI process was associated with the phosphoric acid concentration step.

There have been a number of suggestions as to methods of modifying the process to reduce the capital cost. The methods proposed included the use of liquid hydrogen bromide (HBr), at elevated pressure, to extract the hydrogen iodide from the HI_x; and reactive distillation of the HI_x. The analysis of the hydrogen bromide indicated some promise but the scheme was never evaluated in depth. At the time (1981), the vapor-liquid equilibrium (VLE) measurements required to evaluate the reactive distillation scheme had not been made. Measurements of VLE for the system $HI/I_2/H_2O$ were made in Germany and German researchers (Roth & Knoche 1989, Engels et al. 1987, Engels and Knoche 1986) produced a partial flowsheet that indicated that reactive distillation could work.

GA evaluated the possible flowsheet variations and decided to pursue the reactive distillation scenario as the primary effort but maintain the variation H_3PO_4 as a backup. The HBr variation also remains a potential alternative but thermodynamic data on the system $HI/HBr/I_2/H_2O$ is sparse. Therefore, the laboratory investigations on this system will be necessary to make an evaluation of the system.

3.3.1 Reactive Distillation

GA's HI decomposition process is based on the reactive distillation flowsheet developed by Roth and Knoche (1989). So the details of the reactive distillation process are explained in this chapter.

Since GA's HI concentration and decomposition scheme developed in 1981 seems to be the most expensive and energy consuming step, an alternative has been developed, in

which HI is decomposed directly from liquid $H_2O/HI/I_2$ solution under high pressure and temperature.

To develop an alternative for the original GA's HI decomposition process, the thermodynamic data of the quaternary system $H_2O/HI/I_2/H_2$ must be known. The vapor pressure of this system with HI concentration up to 17 mol% in the liquid phase and temperature up to 580K is measured by Engels and Knoche (1986). It was found that the relative vapor pressure minima of this quaternary system show a strong temperature dependency for low iodine contents in the liquid. Remarkable hydrogen pressures were only found in the equilibrium vapor of solutions with HI contents higher than the pseudo-azeotropic compositions. These results lead to develop a model to investigate direct dissociation of HI.

Figure 3.3 shows the distillation column proposed by Roth and Knoche (Roth and Knoche 1989). The $H_2O/HI/I_2$ stream coming from the Bunsen reaction (Section I) is the feed stream of the distillation column. As mentioned above the remarkable hydrogen pressure are only found in the vapor over solution with HI content higher than the azeotropic mole fraction. It determines the minimum temperature and pressure of the feed stream, which are 22 bar and 262°C.

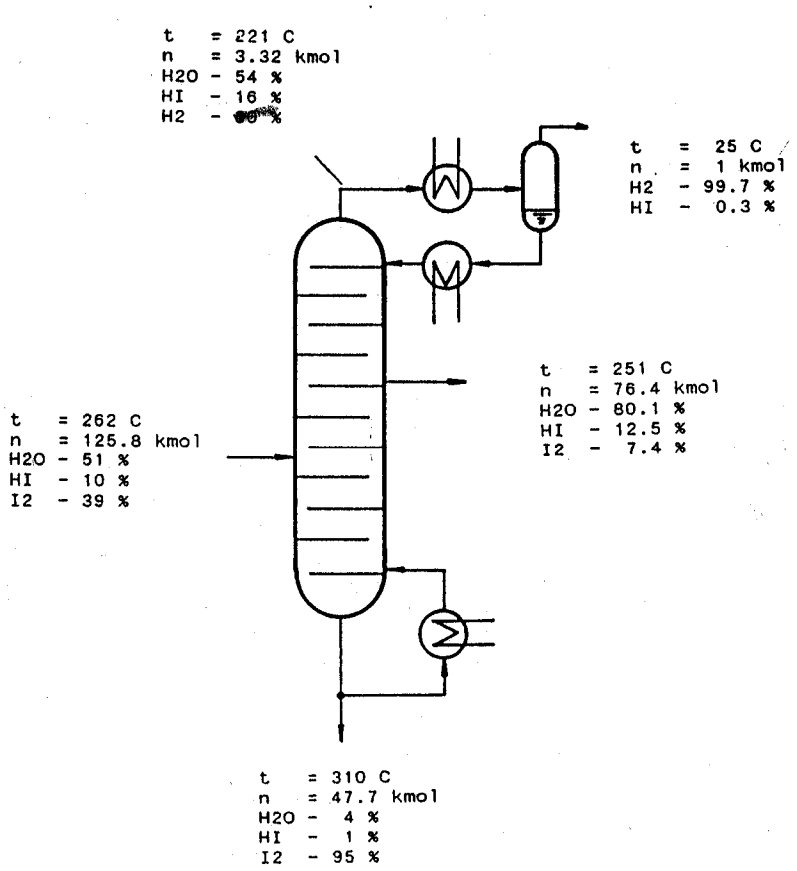

Figure 3. 3 Distillation column (Roth & Knoche 1989)

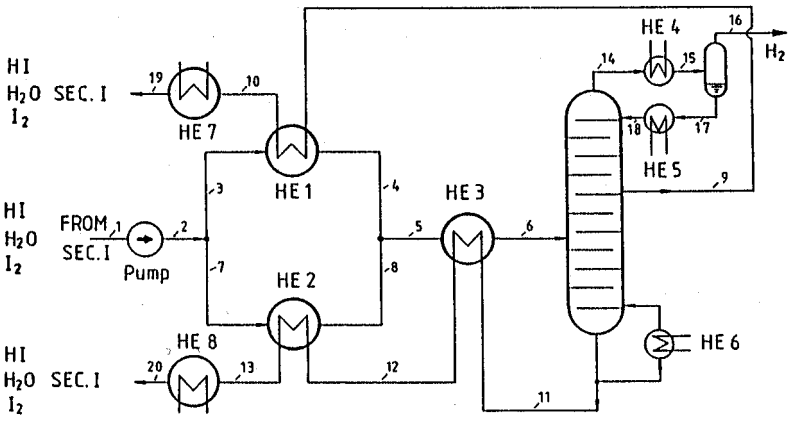

Figure 3. 4 HI decomposition flowsheet (Roth & Knoche 1989)

Figure 3.4 shows the HI decomposition flowsheet. The stream coming from Bunsen reaction is pumped to 22 bar and preheated to the boiling temperature of 262°C and then

enters the distillation column. The product from the bottom of column consists of mostly iodine and small part of water and HI. To close the water balance, a side stream must be taken out of the column. This stream consists of water, HI and a small amount of iodine. The ratio of HI/H_2O mole fractions of the side stream must be lower than the ratio of the feed stream. Also the HI mole fraction of the side stream must be high enough to get an equilibrium vapor with a sufficient HI pressure. These two conditions are the reason for the high mole numbers of the feed stream. Per 1 kmol hydrogen production, it needs a feed stream of 125.8 kmol. This very large feed stream requires a large amount of heat. The product from the top of the column consists of hydrogen and HI. The water and iodine content is negligible.

From the phase equilibrium of the quaternary system $H_2O/HI/I_2/H_2$ at a pressure of 22 bar, they found that high hydrogen mole fractions with low iodine content and temperature about 220°C or lower.

The flowsheet developed by Roth and Knoche (1989) can be connected to Section I of the GA process. The main advantage of this flowsheet compared with the GA proposal using the phosphoric acid to extract water from HIx solution is that there is only a little electric energy needed to drive pumps. For the GA's phosphoric acid method, a large amount of electric energy is required for the reconcentration of the phosphoric acid.

3.3.2 GA's HI Decomposition Process

As in the case of sulfuric acid decomposition, GA tried to regress the VLE and LLE data for the system $HI/I_2/H_2O$. However, they failed to obtain the useful results since the VLE data is incomplete. The available data (Engels and Knoche 1986) gives the total vapor pressure above $HI/I_2/H_2O$ solutions, but not the vapor pressures of the individual components. Furthermore, as the hydrogen iodide was decomposing under the measurement conditions, the total vapor pressure measurements included the equilibrium hydrogen pressure. So, GA's HI decomposition process (Brown et al. 2003) used the reactive distillation flowsheet presented by Roth and Knoche (1989).

The reactive distillation Section III flowsheet is present in Figure 3.5. Compared with Fig. 2.4, one can find the same structure between two flowsheets. The $HI/I_2/H_2O$ product of Section I is pumped up to 22 bars and recuperatively heated to the feed temperature of

the reactive distillation column (C301) in a network of heat exchangers (E301/E302/E303). This heat is recovered from the two liquid products of the distillation column, the bottom stream (305A) containing most of the iodine, and the side outlet (306A) containing most of the water and undecomposed hydrogen iodide.

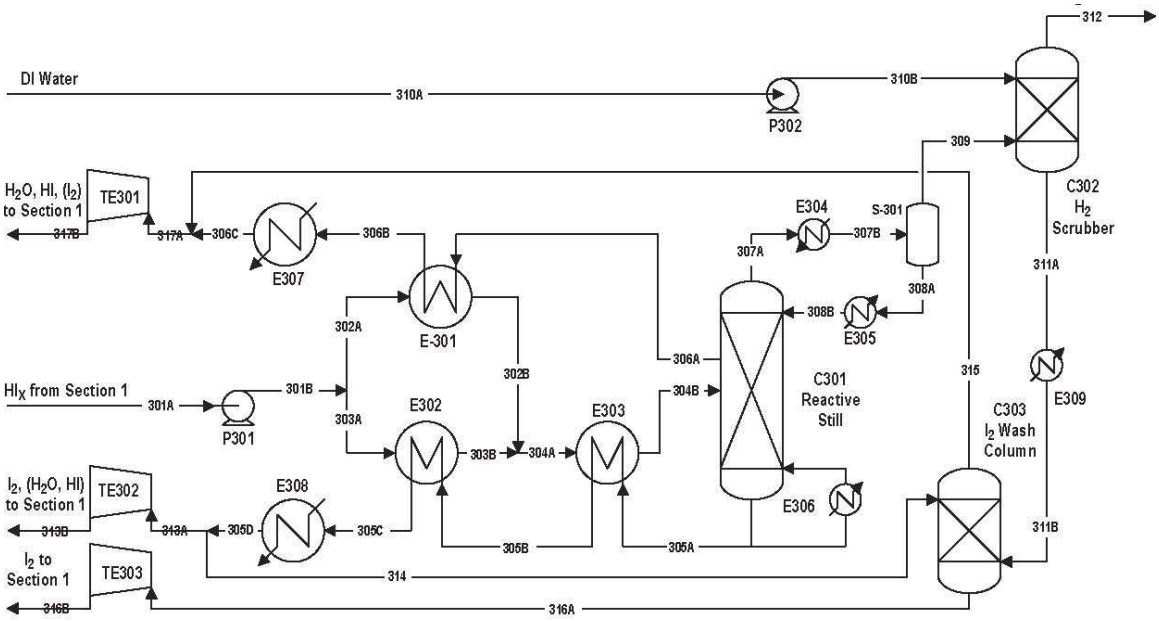

Figure 3. 5 GA Section III flowsheet (Brown et al. 2003)

The overhead product of the column is scrubbed in a packed column (C302) with water to remove the residual hydrogen iodide from the hydrogen. The high pressure (22 bars) and low temperature (25°C) of the scrubber result in a relatively low water content (0.14 mol%) in the hydrogen product. Fresh deionized water, the overall water input to the process, is used to scrub the product hydrogen.

It is uneconomic and unnecessary to remove all of the water and hydrogen iodide from the still bottoms but it is necessary to provide a small amount of pure iodine for the boost reactor in Section I. The scrub water (311A) is used to wash a portion of the bottoms in a packed column. The column was modeled as a single LLE stage using the model for HI/I2/H2O previously discussed.

The still must have a side product to remove the water that accompanies the HI in the feed. The side product contains a significant amount of hydrogen iodide and some iodine.

The total amount returned to Section I, from the side product and still bottoms, is five/sixths of the HI fed to Section III. For every mole of HI decomposed, five moles of HI are recycled unreacted and each mole of HI in the feed is accompanied by almost 4 moles of I_2 and over 5 moles of water. Even so, this version of the process is more efficient than the version using H_3PO_4 as it is not necessary to vaporize the water.

4. ASPEN PLUS Simulation for SI Cycle

In this chapter, the ASPEN PLUS simulations results for the SI cycle are presented. The present simulations followed the methodology applied to the GA's flowsheet (Brown et al. 2003). A step-by-step simulation is conducted. To minimize the convergence problem in a complex system of the SI thermochemical process and to investigate the component-wise characteristics, the simulation is performed initially for the single component such as flash drum, distillation column, and chemical reactor. If adjacent components are converged, then they are combined and simulated. Finally, the simulation for the whole Section is conducted.

The simulations for Section I, II, and III are also performed based on the GA's flowsheet reported in Brown et al. (2003).

4.1 Section I – Bunsen Reaction

4.1.1 RCSTR Simulation and Three Phase Separator Simulation

A combined system with a Bunsen reactor (R-101) and a three phase separator (S-102) as shown in Figure 4.1 is simulated using ASPEN PLUS. The same inlet and operating conditions are specified in the inlet stream (115), the Bunsen reactor, and the three phase separator. The Bunsen reactor is simulated with RCSTR (Rigorous Continuous Stirred Tank Reactor). The RCSTR rigorously models a Continuous Stirred Tank Reactor (CSTR), which is one of the steady-state ideal flow reactors. In this reactor, the contents are well stirred and uniform throughout. Thus the exit stream from this reactor has the same composition as the fluid within the reactor. It can be used when reaction kinetics are known. RCSTR can model equilibrium reactions simultaneously with rate-based reactions.

In the three phase separator, there is one gas-phase outlet stream (117A) and two liquid-phase outlet streams (118A and 119A). Through the bottom outlet (119A), a concentrated mixture of HI, I2, SO2 flows and it is forwarded to Section III, HI decomposition reaction. Through the side outlet (118A), a concentrated H2SO4 acid flows and it is forwarded to Section II, H2SO4 decomposition reaction. Through the top outlet (117A), mainly O2 gas is separated.

The continuous reactors with the three phase separator (Figure 4.1.) were first simulated and the results are presented in Table 4.1. The results are compared with the General Atomics results. The molar flow rate, phase status, operating pressure, and temperature at each stream are listed in the table.

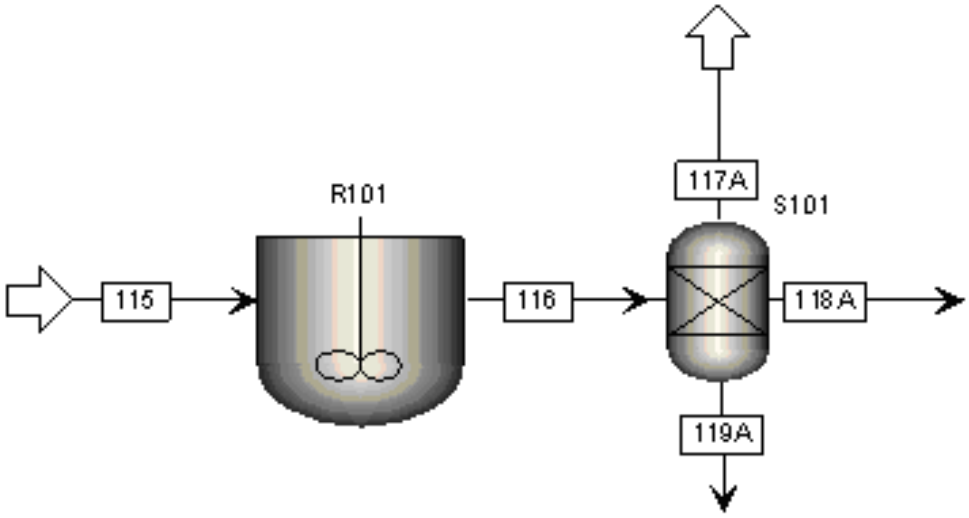

Figure 4.1. Bunsen reactor and three phase separator

Table 4.1 Results of Bunsen reactor and three phase's separator

Stream	H2O	I2	HI	SO2	H2SO4	O2	Total	Phase	P(bar)	T, K
115	72.7279	48.7791	10.9846	2.266	0.2173	0.5	135.47	V+L	7	393
116	71.2535	48.0419	12.4590	1.5288	0.9545	0.5	134.74	L	7	393
GA_116	71.2535	48.0419	12.4590	1.5288	0.9545	0.5	134.74	L	7	393
117A	0.0338	0.0075	0	0.1424	0	0.5	0.68	V	7	393
GA_117A	0.0338	0.0075	0	0.1424	0	0.5	0.68	V	7	393
118A	5.152	0	0	0.0154	0.9544	0	6.12	L	7	393
GA_118A	5.152	0	0	0.0154	0.9544	0	6.12	L	7	393
119A	66.0677	48.0344	12.4590	1.3710	0.0001	0	127.93	L	7	393
GA_119A	66.0677	48.0344	12.4590	1.3710	0.0001	0	127.93	L	7	393

The analysis of the data shows that the GA results are perfectible reproduced, indicating that both thermodynamics are the same.

Some parameters studies are also performed in the Bunsen reaction such as the pressure and the temperature influence (Figure 4.2, Figure 4.3)

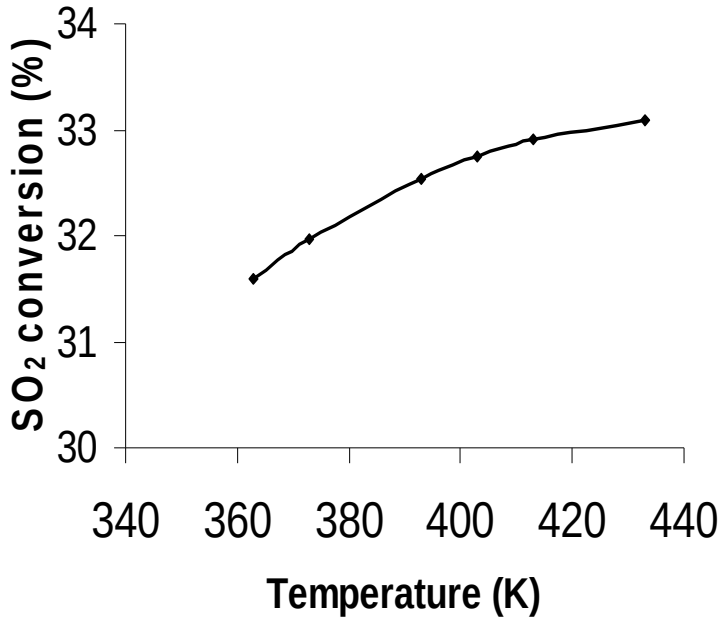

Figure 4.2 Effect of reaction temperature in the Bunsen reactor. SO2 consumption versus temperature.

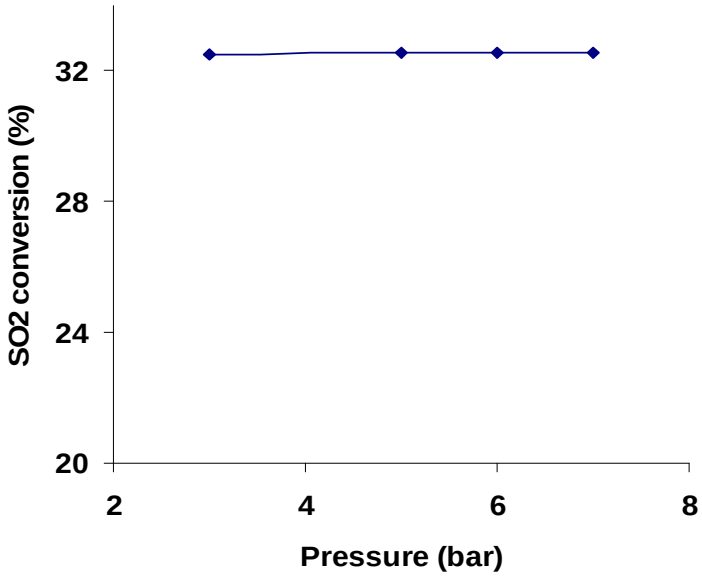

Figure 4.3 Effect of reaction temperature in the Bunsen reactor. SO2 consumption versus pressure.

Figure 4.2 shows that by increasing the temperature in the Bunsen reactor (R101), SO_2 conversion can be improved. In the opposite, the pressure has no influence in the Bunsen reaction according to Figure 4.3.

4.1.2 Stream 118 and 119 Process Simulation

Once the Bunsen reactor and the three phase separator were converged and the results validated, a step-by-step simulation method were adopted in order to get the whole flow sheet converged. One part of the flow sheet where the streams 118A and 119A are processed was first simulated and the flowsheet is presented in Figure 4.4. and the results are compared with the GA results in Table 4.2. The GA results are in red color in the table.

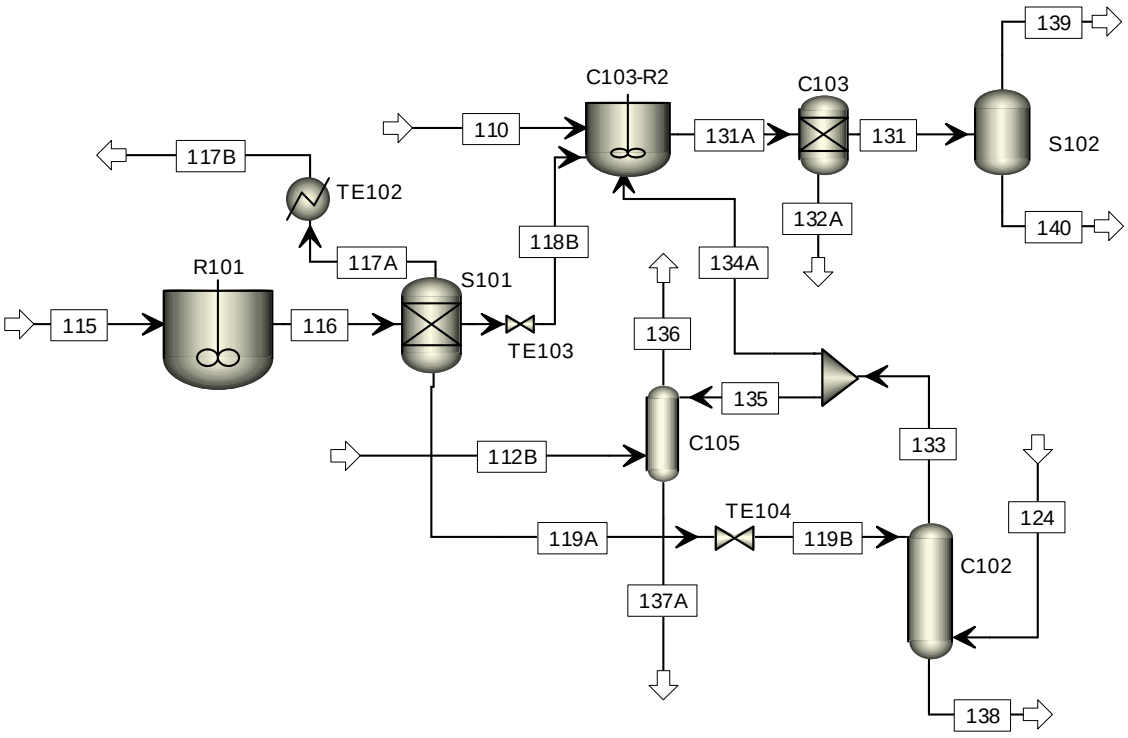

Figure 4.4 Parts of the flow sheet where the streams 118A and 119A are processed.

Table 4.2 Simulation results of the Bunsen reactor

N	Stream	H2SO4 (kmol/h)	HI (kmol/h)	I2 (kmol/h)	H2O (kmol/h)	SO2 (kmol/h)	O2 (kmol/h)	Total (kmol/h)	Phase	Pres.(bar)	Temp. K
1	**131**	1.015	0	0.019	4.138	0.048	0.016	5.235	L	1.85	384.5
1	**GA_131**	1.0234	0	0.0184	4.1377	0.0475	0.0155	5.2425	L	1.85	384.5
2	**132A**	0	0.122	0.811	0.91	0.024	0	1.867	L	1.85	384.5
2	**GA_132A**	0	0.1389	0.796	0.9252	0.0155	0	1.8756	L	1.85	384.5
3	**133**	0	0	0.113	0	1.371	0.182	1.667	V	1.85	390.6
3	**GA_133**	0	0	0.0271	0.3731	1.371	0.1825	1.9537	V	1.85	393
4	**135**	0	0	0.104	0	1.254	0.167	1.525	V	1.85	390.6
4	**GA_135**	0	0	0.0248	0.3414	1.2545	0.167	1.7877	V	1.85	393
5	**136**	0	0	0.006	0	1.254	0.167	1.428	V	1.85	368.2
5	**GA_136**	0	0	0.0003	0.036	0.0001	0.167	0.2034	V	1.85	369.6
6	**137A**	0.215	9.982	5.616	67.262	0	0	83.075	L	1.85	369.2
6	**GA_137A**	0.2173	9.9875	5.5408	67.5643	1.2544	0	84.5643	L	1.85	369.6
7	**138**	0	12.459	47.921	66.07	0	0	126.451	L	1.85	390.5
7	**GA_138**	0	12.459	48.0073	65.6973	0	0	126.1636	L	1.85	393
8	**139**	0.003	0	0.011	0.012	0.048	0.016	0.09	L+V	1.85	384.5
8	**GA_139**	0	0	0.0184	0.0434	0.0436	0.0155	0.1209	V	1.85	384.5
9	**140**	1.012	0	0.008	4.125	0	0	5.145	V	1.85	384.5
9	**GA_140**	1.0234	0	0	4.0943	0.0039	0	5.1216	L	1.85	384.5

The analysis of the results (Table 4.2) indicated that the GA data reproducibility was obtained.

4.1.3 Simulation of Section I

The same methodology was followed for the simulation of the whole flowsheet (Figure 4.5). The simulation of the oxygen scrubber (C 101) was preceded by a series of reactors such as the Bunsen reactor in order to achieve the SO2 conversion in sulfuric acid. The residual SO_2 is transformed in the scrubber. The number of the reactors used in the present analysis is 4. This number depends on the reactors volume. The results for the whole flow sheet are presented in Table 4.3 and the GA results are shown in Table 4.4.

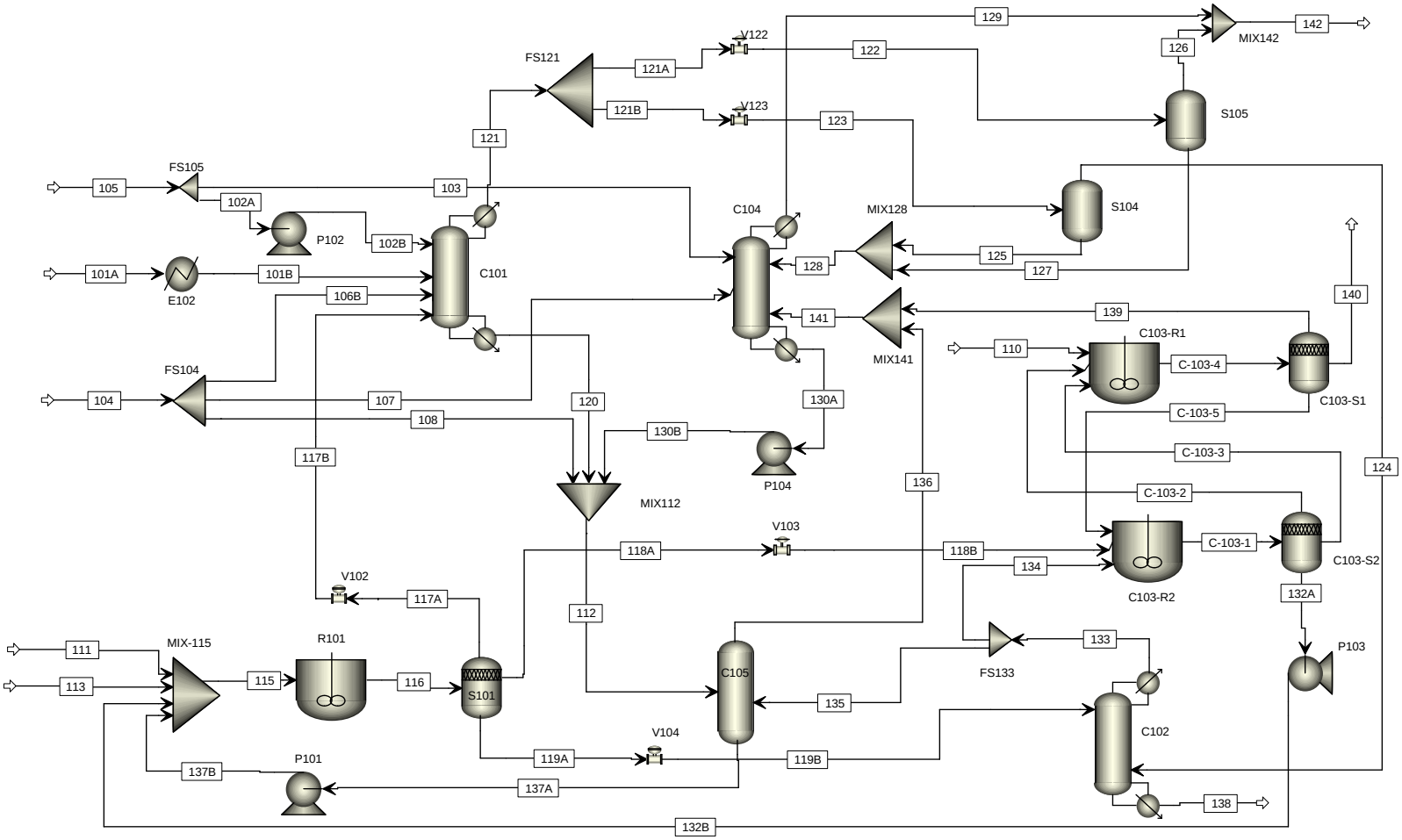

Figure 4.5. Section I Complete Flow Sheet

Table 4.3 Present Analysis Results for HI Decomposition

Stream	H2SO4 (kmol/h)	HI (kmol/h)	I2 (kmol/h)	H2O (kmol/h)	SO2 (kmol/h)	O2 (kmol/h)	Total Flow (kmol/h)	Phase	Press. (bar)	Temp. (K)
101A	0.022	0	0	3.458	0.008	0	3.488	L	4.2	393.1
101B	0.022	0	0	3.458	0.008	0	3.488	L	4.2	359.6
102A	0	0	0	0.319	0	0	0.319	L	1.01	311.2
102B	0	0	0	0.319	0	0	0.319	L	4.4	311.3
103	0	0	0	1.285	0	0	1.286	L	1.01	311.2
104	0	9.6	5.684	62.494	0	0	77.778	L	4.2	368.5
105	0	0	0	1.603	0	0	1.605	L	1.01	311.1
106	0	0.288	0.17	1.874	0	0	2.333	L	1.85	311.1
107	0	0.081	0.048	0.525	0	0	0.653	L	1.01	368.5
107A	0	0.081	0.048	0.525	0	0	0.653	L	4.2	368.5
108	0	9.231	5.466	60.095	0	0	74.792	L	4.2	368.5
110	0	0.001	0.881	0.017	0	0	0.899	L	1.85	393
111	0	0.858	42.442	4.206	0	0	47.506	L	1.85	393
112	0.215	9.982	5.518	67.262	0	0	82.978	L	1.85	368.2
113	0	0	0	0.033	0.996	0.5	1.529	V	7	393
115	0.217	10.985	48.779	72.728	2.266	0.5	135.475	L+V	7	393
116	0.955	12.459	48.042	71.253	1.529	0.5	134.738	L	7	393
117A	0	0	0.007	0.034	0.142	0.5	0.684	V	7	393
117B	0	0	0.007	0.034	0.142	0.5	0.684	V	4.2	354.2
118A	0.954	0	0	5.152	0.015	0	6.122	L	7	393
118B	0.954	0	0	5.152	0.015	0	6.122	L	1.85	393.1
119A	0	12.459	48.034	66.068	1.371	0	127.932	L	7	393
119B	0	12.459	48.034	66.068	1.371	0	127.932	L	1.85	393
120	0.17	0.583	0.029	5.373	0	0	6.156	L	4.2	384.4
121	0	0.002	0	0.015	0.002	0.5	0.519	L+V	4.2	384.4
122	0	0.001	0	0.01	0.001	0.317	0.33	V	1.01	238.8
123	0	0.001	0	0.006	0.001	0.182	0.189	L+V	1.85	289
124	0	0	0	0.003	0.001	0.182	0.186	L+V	1.85	289
125	0	0	0	0.003	0	0	0.003	L	1.85	289
126	0	0.001	0	0.005	0.001	0.317	0.325	L+V	1.01	289
127	0	0	0	0.004	0	0	0.005	L	1.01	289
128	0	0	0	0.072	0	0	0.072	L	1.01	289
129	0	0	0	trace	0	0.183	0.183	V	1.01	305.3
130A	0.044	0.168	0.023	1.874	0	0	2.109	L	1.01	346.4
130B	0.045	0.168	0.023	1.795	0	0	2.03	L	1.85	393
131	1.015	0	0.019	4.138	0.048	0.016	5.235	L	1.85	384.5
132A	0	0.122	0.811	0.91	0.024	0	1.867	L	1.85	384.5
132B	0	0.122	0.811	0.91	0.024	0	1.867	L	7	385.3
133	0	0	0.113	0	1.371	0.182	1.667	V	1.85	390.6
134	0	0	0.01	0	0.117	0.016	0.142	V	1.85	390.6
135	0	0	0.104	0	1.254	0.167	1.525	V	1.85	390.6
136	0	0	0.006	0	1.254	0.167	1.428	V	1.85	368.2
137A	0.215	9.982	5.616	67.262	0	0	83.075	L	1.85	369.2
137B	0.215	9.982	5.616	67.262	0	0	83.075	L	7	369.7
138	0	12.459	47.921	66.07	0	0	126.451	L	1.85	390.5
139	0.003	0	0.011	0.012	0.048	0.016	0.09	L+V	1.85	384.5
140	1.012	0	0.008	4.125	0	0	5.145	L	1.85	384.5

Table 4.4.GA Results for HI decomposition

Stream	H2SO4 (kmol/h)	HI (kmol/h)	I2 (kmol/h)	H2O (kmol/h)	SO2 (kmol/h)	O2 (kmol/h)	Total Flow (kmol/h)	Phase	Press. (bar)	Temp. (K)
101A	0.0222	0	0	3.4582	0.0078	0	3.4882	L	4.2	393.15
101B	0.0222	0	0	3.4582	0.0078	0	3.4882	L	4.2	359.6
102A	0.0002	0	0	0.3186	0	0	0.3188	L	1.01	311.15
102B	0.0002	0	0	0.3186	0	0	0.3188	L	4.4	311.15
103	0.001	0	0	1.2847	0	0	1.2857	L	1.01	311.15
104	0	9.5997	5.684	62.494	0	0	77.7777	L	4.2	368.51
105	0.0012	0	0	1.6033	0	0	1.6045	L	1.01	311.15
106	0	0.288	0.1705	1.8742	0	0	2.3327	L	1.85	311.15
107	0	0.0806	0.0477	0.5248	0	0	0.6531	L	1.01	368.51
108	0	9.2311	5.4658	60.095	0	0	74.7919	L	4.2	368.51
110	0	0.0011	0.881	0.017	0	0	0.8991	L	1.85	393
111	0	0.8582	42.4423	4.2056	0	0	47.5061	L	1.85	393
112	0.2173	9.9875	5.5163	67.2589	0	0	82.9800	L	1.85	
113	0	0	0	0.0328	0.9961	0.5	1.5289	V	7	393
115	0.2173	10.9846	48.7791	72.7279	2.266	0.5	135.4749	V+L	7	
116	0.9545	12.459	48.0419	71.2535	1.5288	0.5	134.7377	V+L	7	393
117A	0	0	0.0075	0.0338	0.1424	0.5	0.6837	V	7	393
117B	0	0	0.0075	0.0338	0.1424	0.5	0.6837	V	4.2	354.2
118A	0.9545	0	0	5.152	0.0154	0	6.1219	L	7	393
118B	0.9545	0	0	5.152	0.0154	0	6.1219	L	1.85	393
119A	0	12.459	48.0344	66.0677	1.371	0	127.9321	L	7	393
119B	0	12.459	48.0344	66.0677	1.371	0	127.9321	L	1.85	393
120	0.1726	0.5884	0.0278	5.3694	0	0	6.1582	L	4.2	384.4
121	0	0	0	0.015	0	0.5	0.5150	V	4.2	384.4
122	0	0	0	0.0095	0	0.3175	0.3270	V+L	1.01	
123	0	0	0	0.0055	0	0.1825	0.1880	V+L	1.85	289
124	0	0	0	0.0027	0	0.1825	0.1852	V	1.85	289
125	0	0	0	0.0028	0	0	0.0028	L	1.85	289
126	0	0	0	0.0051	0	0.3175	0.3226	V	1.01	
127	0	0	0	0.0044	0	0	0.0044	L	1.01	
128	0	0	0	0.0072	0	0	0.0072	L	1.01	
129	0	0	0	0.0142	0	0.1825	0.1967	V	1.01	313
130A	0.0447	0.168	0.0227	1.7945	0	0	2.0299	L	1.01	393
130B	0.0447	0.168	0.0227	1.7945	0	0	2.0299	L	1.85	393
131	1.0234	0	0.0184	4.1377	0.0475	0.0155	5.2425	L	1.85	384.5
132A	0	0.1389	0.796	0.9252	0.0155	0	1.8756	L	1.85	384.5
132B	0	0.1389	0.796	0.9252	0.0155	0	1.8756	L	7	384.5
133	0	0	0.0271	0.3731	1.371	0.1825	1.9537	V	1.85	393
134	0	0	0.0023	0.0317	0.1165	0.0155	0.1660	V	1.85	393
135	0	0	0.0248	0.3414	1.2545	0.167	1.7877	V	1.85	393
136	0	0	0.0003	0.036	0.0001	0.167	0.2034	V	1.85	369.6
137A	0.2173	9.9875	5.5408	67.5643	1.2544	0	84.5643	L	1.85	369.6
137B	0.2173	9.9875	5.5408	67.5643	1.2544	0	84.5643	L	7	369.6
138	0	12.459	48.0073	65.6973	0	0	126.1636	L	1.85	393
139	0	0	0.0184	0.0434	0.0436	0.0155	0.1209	V	1.85	384.5
140	1.0234	0	0	4.0943	0.0039	0	5.1216	L	1.85	384.5

4.2 Section II – H2SO4 Decomposition Reaction

4.2.1 GIBBS Reactor Simulation

The Gibbs reactor, denoted RGibbs in ASPEN, models single-phase chemical equilibrium, or simultaneous phase and chemical equilibria. RGibbs minimizes the Gibbs free energy, subject to atom balance constraints. This model does not require reaction stoichiometry. RGibbs can determine phase equilibrium without chemical reaction, particularly for multiple liquid phases. Any number of liquid phases is allowed in this model.

Four-stage H_2SO_4 decomposition reactors shown in Figure 4.6 are simulated with RGibbs model. The ASPEN simulation results are listed in Table 4.5. The results of the present simulation are very similar to those of the GA's simulation.

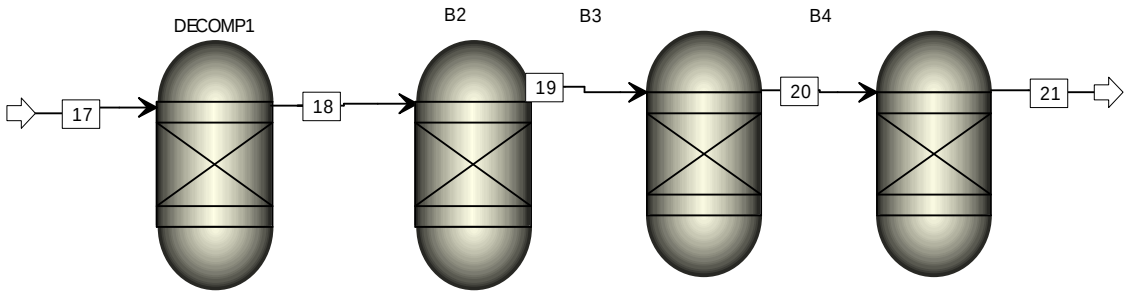

Figure 4.6. Gibbs reactor

Table 4.5 Results of Gibbs reactor-decomposition reactor

Stream	GA Stream	H2O	H2SO4	SO3	O2	SO2	Total	P, bar	T, K
17	222	1.490	0.291	1.315	0.000	0.000	3.096	7.09	796.85
18	223	1.700	0.081	1.261	0.132	0.264	3.439	7.09	875.05
	R-223	1.688	0.093	1.258	0.128	0.256	3.423	7.09	875.05
19	224	1.757	0.024	1.078	0.252	0.505	3.616	7.09	955.05
	R-224	1.739	0.042	1.564	0.000	0.000	3.345	7.09	955.05
20	225	1.773	0.009	0.841	0.379	0.757	3.758	7.09	1027.05
	R-225	1.772	0.009	0.838	0.379	0.759	3.757	7.09	1027.05
21	226	1.778	0.003	0.603	0.500	1.000	3.884	7.09	1100.15
	R-226	1.778	0.003	0.593	0.505	1.010	3.889	7.09	1100.15

4.2.2 Simulation for Section II

The whole H2SO4 decomposition reaction in Section II is modeled as in Figure 4.7. Table 4.6 shows the simulation results. For the comparison, Table 4.7 lists the GA's result from GA Report GA-A24285, Rev. 1, Table 3-2 (Brown et al. 2003). Figures 4.8-4.10 present the molar flow rate of each species at all streams. Stream numbers in x-axis of figures are listed in the first column of Tables 4.6 and 4.7. As shown in the tables and figures , the present results are very close to those of GA's results.

Some notable results are:

- 0.5 mole of O2 is generated at Stream No. 229 (outlet stream of Flash drum S205)

- The highest temperature is 1100.15 K (823 C) at Stream No. 226 (outlet stream of DECOMP4 and inlet stream of Recuperator)

- Main components: 4 isobaric concentrators (35 bar), 3 Flash drums, Preheaters, Recuperator, 4 Decomposition Reactors, Product Coolers

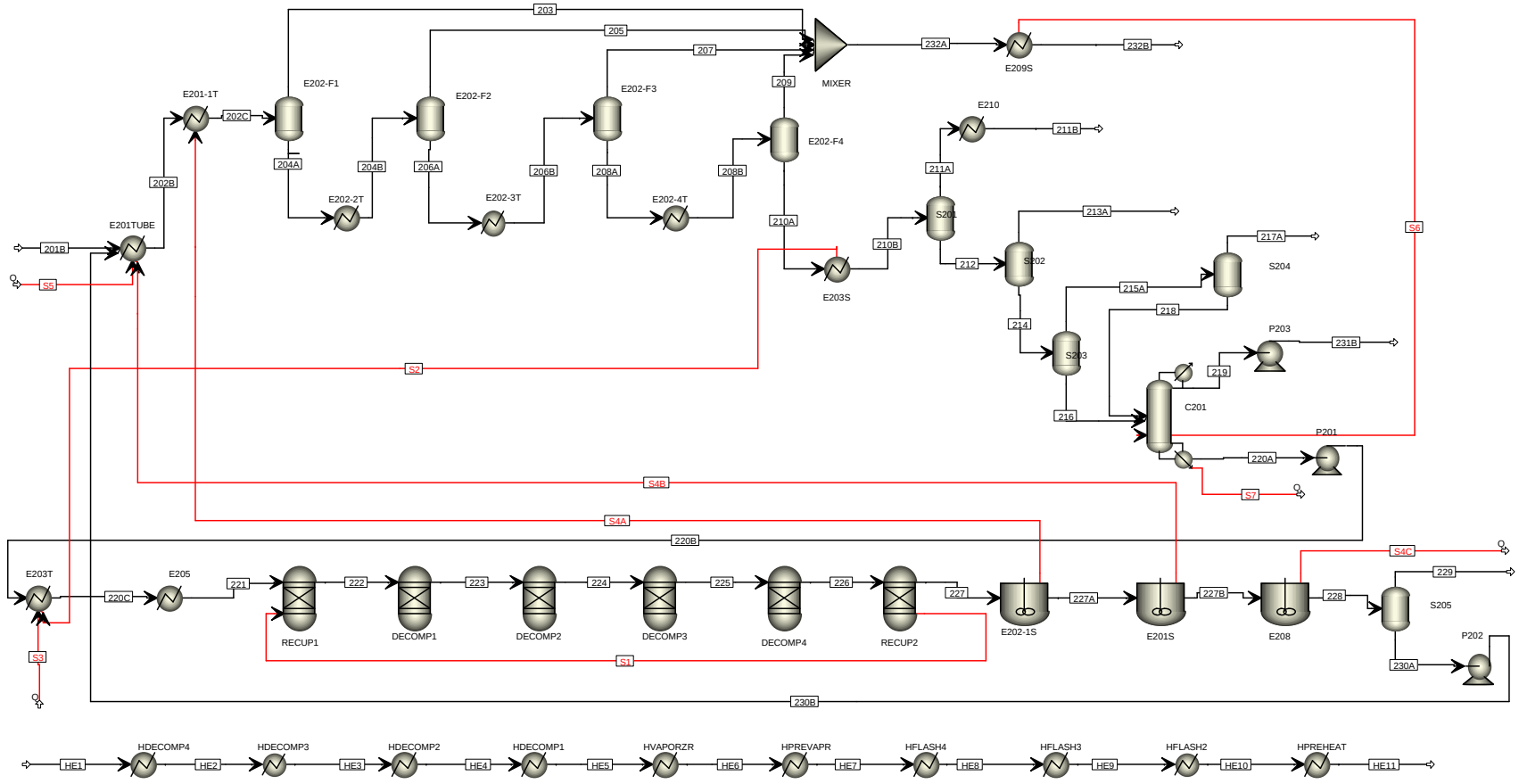

Figure 4.7 Section II simulation model

Table 4.6 Results of Section II simulation

Stream No.	GA Stream	H2O	H2SO4	SO3	O2	SO2	Total	P, atm	T, K	Vapor Frac.
1	201B	4.0943	1.0234	0	0	3.90E-03	5.1216	35	393.15	0
2	202B	5.195881	1.632039	6.10E-11	1.02E-05	7.64E-03	6.835574	35	374.565	0
3	202C	5.195881	1.632039	6.10E-11	1.02E-05	7.64E-03	6.835574	35	596.857	0.0823
4	203	0.558282	6.99E-04	2.31E-11	9.97E-06	3.55E-03	0.562539	35	596.857	1
5	204A	4.6376	1.63134	3.79E-11	2.71E-07	4.10E-03	6.273035	35	596.857	0
6	204B	4.6376	1.63134	3.79E-11	2.71E-07	4.10E-03	6.273035	35	619.15	0.20375
7	205	1.269376	5.69E-03	2.66E-11	2.69E-07	3.09E-03	1.278163	35	619.147	1
8	206A	3.368223	1.625646	1.13E-11	2.14E-09	1.00E-03	4.994872	35	619.147	0
9	206B	3.368223	1.625646	1.13E-11	2.14E-09	1.00E-03	4.994872	35	631.15	0.10134
10	207	0.501657	3.91E-03	6.19E-12	2.11E-09	6.02E-04	0.506169	35	631.15	1
11	208A	2.866566	1.621737	5.12E-12	3.53E-11	4.00E-04	4.488703	35	631.15	0
12	208B	2.866566	1.621737	5.12E-12	3.53E-11	4.00E-04	4.488703	35	644.15	0.0976
13	209	0.432208	5.65E-03	0	3.47E-11	2.46E-04	0.438099	35	644.15	1
14	210A	2.434359	1.616091	0	0	1.55E-04	4.050604	35	644.15	0
15	210B	2.434359	1.616091	0	0	1.55E-04	4.050604	35	581.15	0
16	211A	0.273085	2.09E-03	0	0	1.16E-04	0.275291	8	562.845	1
17	211B	0.273085	2.09E-03	0	0	1.16E-04	0.275291	8	393.15	0
18	212	2.161274	1.614	0	0	3.90E-05	3.775314	8	562.845	0
19	213A	0.382041	4.97E-03	0	0	3.73E-05	0.387044	2	517.112	1
20	214	1.779234	1.609035	0	0	1.65E-06	3.38827	2	517.112	0
21	215A	0.547586	0.013461	0	0	1.65E-06	0.561048	0.06579	432.894	1
22	216	1.231648	1.595574	0	0	3.29E-09	2.827222	0.06579	432.894	0
23	217A	0.533849	1.23E-03	0	0	1.65E-06	0.535084	0.06579	408.15	1
24	218	0.013736	0.012227	0	0	0	0.025964	0.06579	408.15	0
25	219	1.113293	4.97E-15	8.34E-29	0	3.29E-09	1.113293	0.06579	311.178	0
26	220A	0.132199	1.607695	1.07E-04	0	9.05E-24	1.74	0.06579	484.793	0
27	220B	0.132199	1.607695	1.07E-04	0	9.05E-24	1.74	7	485.642	0
28	220C	0.132199	1.607695	1.07E-04	0	9.05E-24	1.74	7	657.023	0
29	221	0.585631	1.151281	0.45503	0	0	2.194923	6.96982	684.15	0.99
30	222	1.453288	0.286605	1.321179	0	0	3.061072	7	797.232	1
31	223	1.659755	0.080138	1.263873	0.1318868	0.263774	3.399426	7	875	1
32	224	1.716166	0.023727	1.080286	0.2518856	0.503771	3.575836	7	955	1
33	225	1.731459	8.43E-03	0.843131	0.3781099	0.75622	3.717353	7	1027	1
34	226	1.736698	3.20E-03	0.605446	0.4995712	0.999142	3.844053	7	1100.15	1
35	227	1.405823	0.33407	0.274572	0.4995712	0.999142	3.513178	7	704.15	1
36	228	1.131251	0.608642	1.25E-10	0.4995712	0.999142	3.238607	7	393.15	0.47077
37	229	0.02967	2.21E-06	6.43E-11	0.499561	0.995399	1.524633	7	393.151	1
38	230A	1.101581	0.60864	6.10E-11	1.02E-05	3.74E-03	1.713974	7	393.151	0
39	230B	1.101581	0.60864	6.10E-11	1.02E-05	3.74E-03	1.713974	35	396.021	0
40	231B	1.113293	4.97E-15	8.34E-29	0	3.29E-09	1.113293	1	311.235	0
41	232A	2.761522	0.015949	5.59E-11	1.02E-05	7.49E-03	2.78497	35	622.567	0.99859
42	232B	2.745573	5.49E-10	5.59E-11	1.02E-05	7.49E-03	2.78497	35	393.15	0

Table 4.7 Section II GA results

Stream No.	GA Stream	H2O	H2SO4	SO3	O2	SO2	Total	Phase	P, atm	T, K
1	201B	4.0943	1.0234	0	0	0.0039	5.1216	L	35.00	393.15
2	202B	5.2361	1.6298	0	0	0.0078	6.8737	L+V	35.00	572.15
3	202C	5.2361	1.6298	0	0	0.0078	6.8737	L+V	35.00	603.15
4	203	1.0007	0.0018	0	0	0.0052	1.0077	V	35.00	603.15
5	204A	4.2354	1.628	0	0	0.0026	5.866	L	35.00	603.15
6	204B	4.2354	1.628	0	0	0.0026	5.866	L+V	35.00	619.15
7	205	0.8661	0.0038	0	0	0.0019	0.8718	V	35.00	619.15
8	206A	3.3693	1.6242	0	0	0.0007	4.9942	V	35.00	619.15
9	206B	3.3693	1.6242	0	0	0.0007	4.9942	L+V	35.00	631.15
10	207	0.5037	0.0039	0	0	0.0004	0.508	V	35.00	631.15
11	208A	2.8656	1.6203	0	0	0.0003	4.4862	L	35.00	631.15
12	208B	2.8656	1.6203	0	0	0.0003	4.4862	L+V	35.00	644.15
13	209	0.433	0.0056	0	0	0.0002	0.4388	V	35.00	644.15
14	210A	2.4326	1.6147	0	0	0.0001	4.0474	L	35.00	644.15
15	210B	2.4326	1.6147	0	0	0.0001	4.0474	L	35.00	581.15
16	211A	0.273	0.002	0	0	0.0001	0.2751	V	8.00	562.85
17	211B	0.273	0.002	0	0	0.0001	0.2751	L	8.00	393.15
18	212	2.1596	1.6127	0	0	0	3.7723	L	8.00	562.85
19	213A	0.3817	0.0051	0	0	0	0.3868	V	2.00	517.05
20	214	1.7779	1.6076	0	0	0	3.3855	L	2.00	517.05
21	215A	0.5471	0.0134	0	0	0	0.5605	V	0.069085	432.85
22	216	1.2308	1.5942	0	0	0	2.825	L	0.069085	432.85
23	217A	0.5335	0.0012	0	0	0	0.5347	V	0.069085	408.15
24	218	0.0136	0.0122	0	0	0	0.0258	L	0.069085	408.15
25	219	1.0698	0	0	0	0	1.0698	L	0.069085	311.15
26	220A	0.1746	1.6064	0	0	0	1.781	L	0.069085	485.25
27	220B	0.1746	1.6064	0	0	0	1.781	L	7.00	486.05
28	220C	0.1746	1.6064	0	0	0	1.781	L	7.00	684.15
29	221	0.6174	1.1636	0.4428	0	0	2.2238	L+V	7.00	684.15
30	222	1.4899	0.2911	1.3153	0	0	3.0963	V	7.00	796.85
31	223	1.7	0.081	1.261	0.1322	0.2644	3.4386	V	7.00	875.05
32	224	1.757	0.024	1.0776	0.2524	0.5048	3.6158	V	7.00	955.05
33	225	1.7725	0.0085	0.8405	0.3787	0.7574	3.7576	V	7.00	1027.05
34	226	1.7777	0.0033	0.6031	0.5	1	3.8841	V	7.00	1100.15
35	227	1.4456	0.3354	0.271	0.5	1	3.552	V	7.00	704.15
36	228	1.1746	0.6064	0	0.5	1	3.281	L+V	7.00	393.15
37	229	0.0328	0	0	0.5	0.9961	1.5289	V	7.00	393.15
38	230A	1.1418	0.6064	0	0	0.0039	1.7521	L	7.00	393.15
39	230B	1.1418	0.6064	0	0	0.0039	1.7521	L	35.00	396.05
40	231B	1.6033	0.0012	0	0	0	1.6045	L	1.01	311.25
41	232A	2.8035	0.0151	0	0	0.0077	2.8263	V	35.00	621.35
42	232B	2.788	0	0	0	0.0038	2.7918	L	35.00	393.15

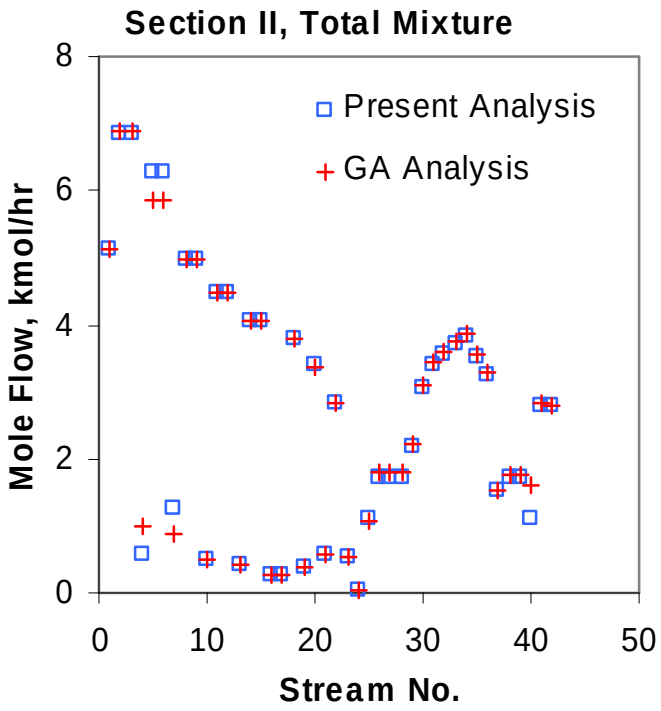

a) Total mixture

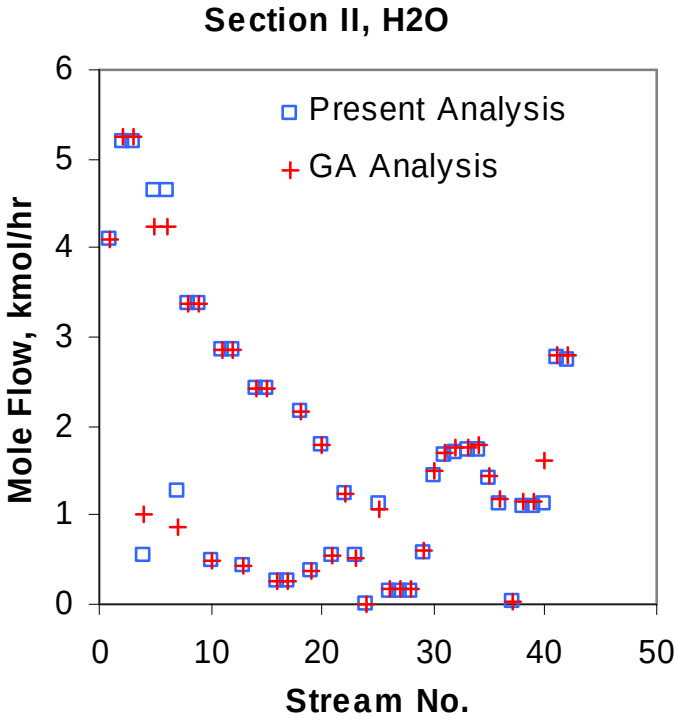

b) H2O

Figure 4.8 Comparison between GA and current ASPEN analysis

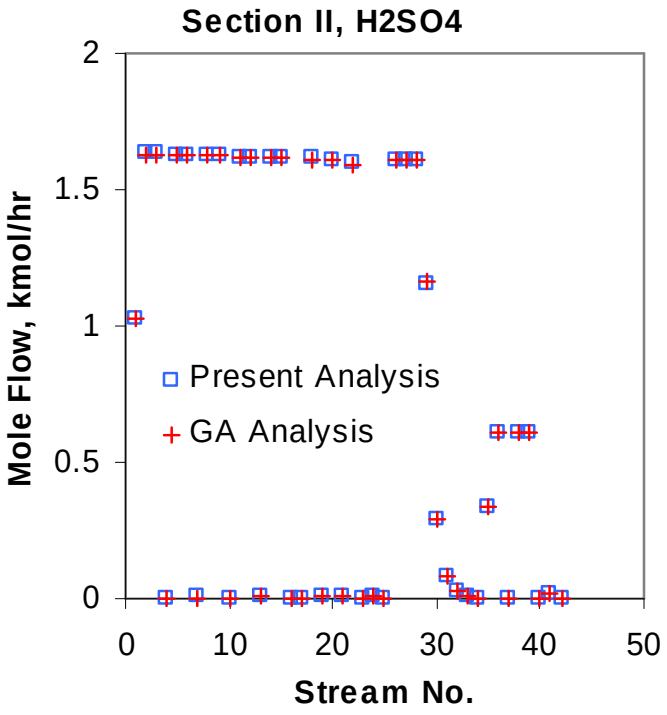

c) H2SO4

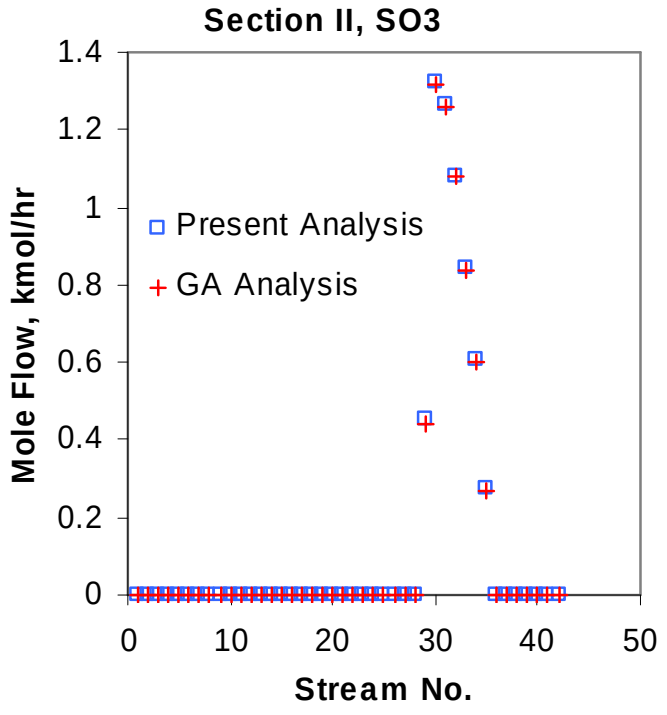

d) SO3

Figure 4.9 Comparison between GA and current ASPEN analysis (continued)

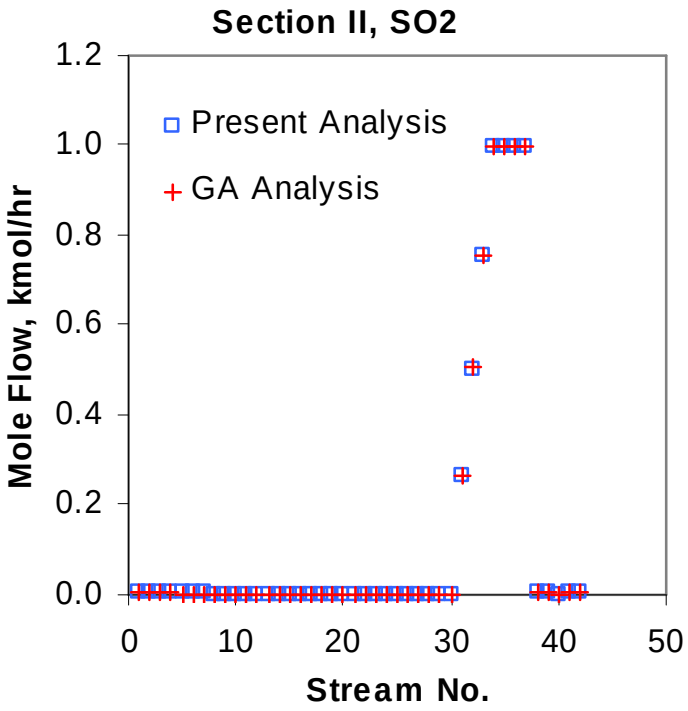

e) SO2

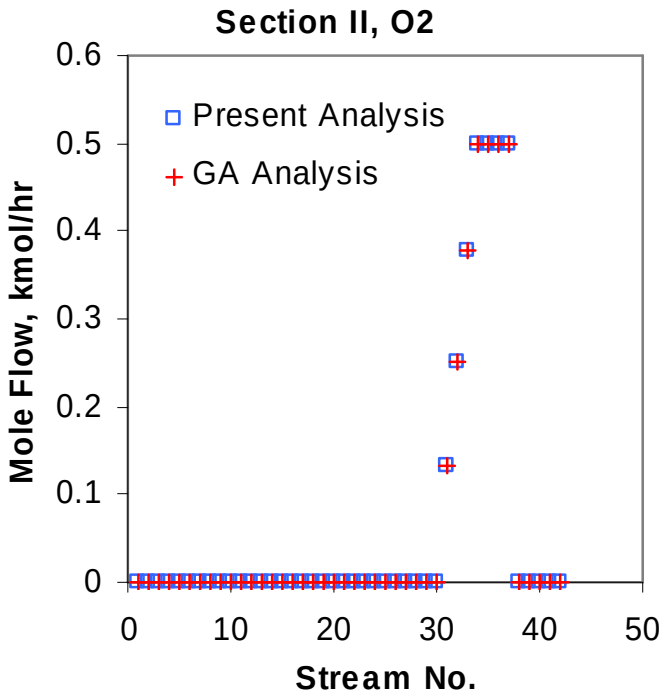

f) O2

Figure 4.10 Comparison between GA and current ASPEN analysis (continued)

4.3 Section III – HI Decomposition Simulation

4.3.1 Flowsheet Convergence

Aspen Plus was used to simulate the reactive distillation column for HI decomposition by following the methodology proposed by General Atomics. The simplified proposed flowsheet for the reactive distillation column is shown in Figure 4.11 and the whole flowsheet is represented in Figure 4.12. The column is constituted by 7stages including the condenser and the reboiler. The $HI/I_2/H_2O$ product stream from the Bunsen reaction is pressurized up to 22 bar and heated to the feed temperature of the reactive distillation column (C301) in a network of heat exchangers (type: shell and tubes) (E301/E302/E303). This heat is recovered from the two liquid products of the distillation column, the bottom stream (305A) containing most of the iodine, and the side outlet (306A) containing most of the water and undecomposed hydrogen iodine.

The overhead product of the column is scrubbed in a packed column (C302) with water to remove the residual hydrogen iodine from the hydrogen. The high pressure (22 bar) and low temperature (298 K) of the scrubber result in a relatively low water content in the hydrogen product. Fresh deionized water, the overall water input to the process, is used to scrub the product hydrogen. The scrub water (311A) is used to wash portion of the bottoms in a packed column.

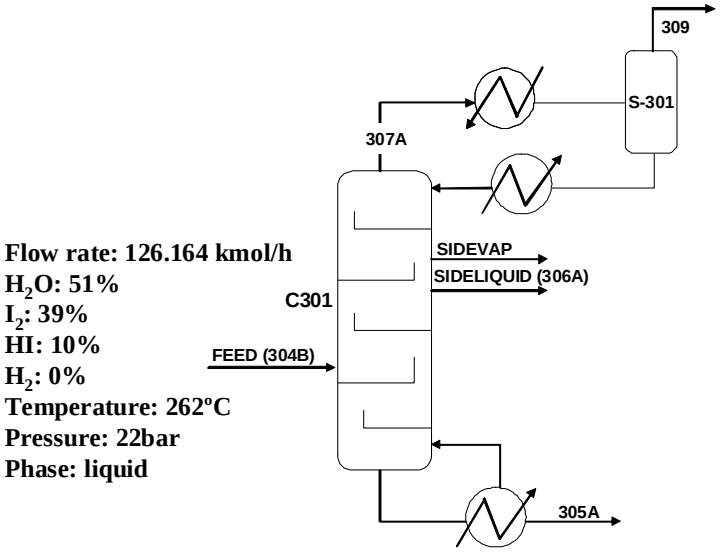

Figure 4.11 Simplified reactive distillation

The simulation was conducted first in the reactive distillation column only. The HI decomposition reaction takes place in all the 7 stages and the side liquid draw is adopted in this study; a high amount of liquid compared to the gas flow rate is extracted at the third stage. Once the convergence is achieved, the gas flow rate is decreased until no flow is observed. The feed from the Bunsen reaction is at its bubble temperature (262ºC) with a molar fraction of 51% of water, 39% of iodine and 10% of HI and is set at stage 5.

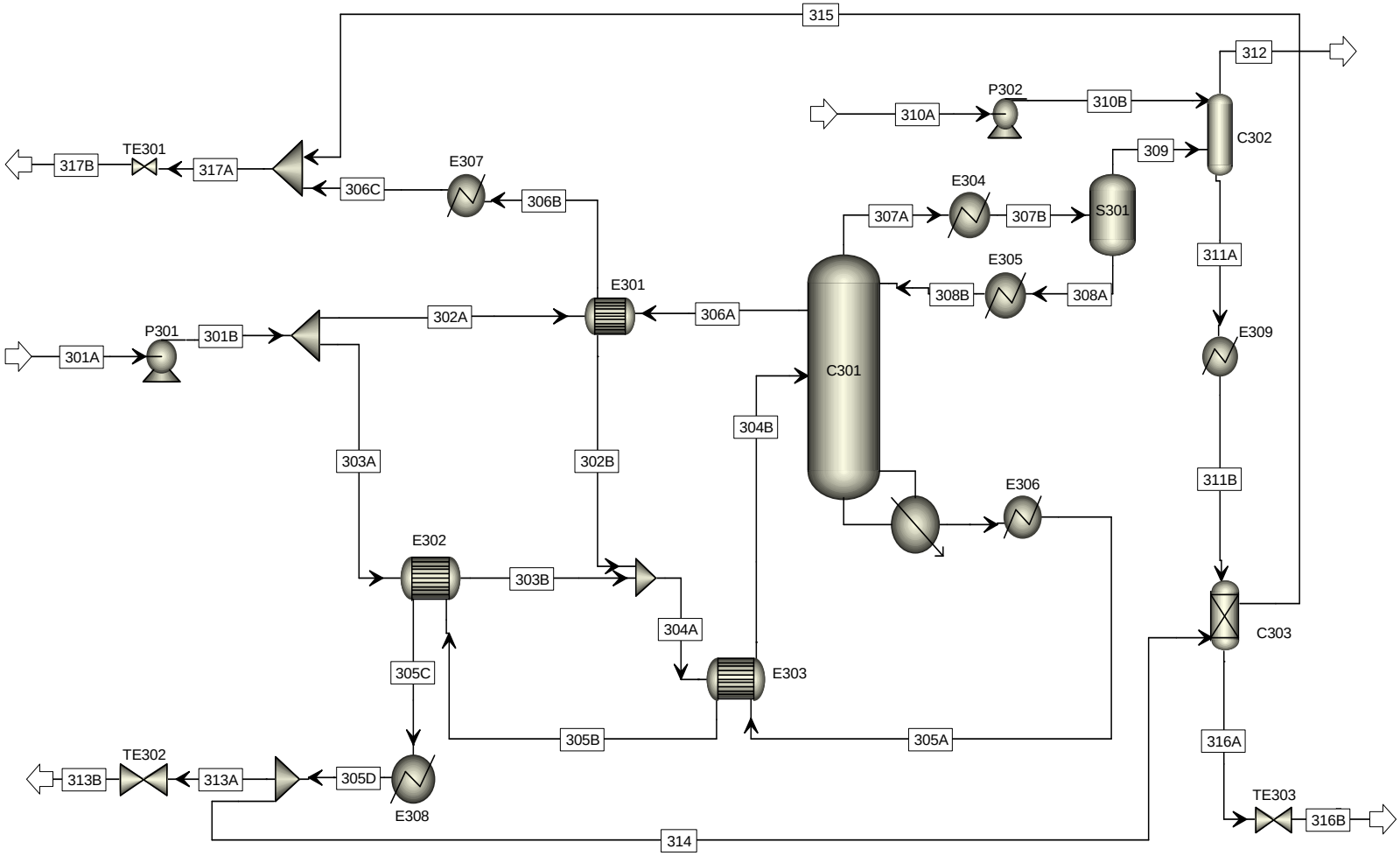

Figure 4.12 Complete HI decomposition flowsheet section (section III)

At the beginning of the calculations, the side liquid (sideliquid) flow rate is set at 50 kmol/h and the side vapor (sidevap) flow rate at 0.01 kmol/h. The convergence is achieved in a first time at 22 bar without the HI decomposition when the boil up rate is equal 40kmol/h. Once the convergence is achieved, the reaction rate of HI decomposition is added progressively from the bottom to the top of the column. A production of 1kmol/h of hydrogen was obtained when the boil up rate is set at 210 kmol/h. Then flow sheet simulations were carried out to obtain 1kmol/h of hydrogen production by varying boilup rates and side liquid flow rate in the column and the convergence of the whole flowsheet was achieved.

Once the flowsheet convergence was achieved parametric studies were conducted. The system pressure was varied from 22 bar to 40 bar. For each pressure, the boil up rates, side liquid flow composition, temperature, liquid vapor composition were determined for 1kmol/h of hydrogen production. The whole flowsheet was implemented once the convergence was achieved in the reactive distillation column.

The simulation results on stream composition, pressure, temperature, flow and phase are presented in Table 4.8 for the whole flowsheet. In this table the stream number 23 shows the hydrogen production rate.

Table 4.8 Present Analysis Results for HI Decomposition Simulation

No	Stream	H_2O (kmol/h)	I_2 (kmol/h)	HI (kmol/h)	H_2 (kmol/h)	Mole flow (kmol/h)	Phase	Pressure. (bar)	Temp. (K)
1	301A	65.697	48.007	12.459	0	126.164	L	1.85	393.1
2	301B	65.697	48.007	12.459	0	126.164	L	22	397.5
3	302A	41.061	30.005	7.787	0	78.852	L	22	397.5
4	302B	41.061	30.005	7.787	0	78.852	L	22	511
5	303A	24.636	18.003	4.672	0	47.311	L	22	397.5
6	303B	24.636	18.003	4.672	0	47.311	L	22	500
7	304A	65.697	48.007	12.459	0	126.164	L	22	507.1
8	304B	65.697	48.007	12.459	0	126.164	L	22	535.1
9	305A	5.224	41.895	1.414	0	48.533	L	22	583.1
10	305B	5.224	41.895	1.414	0	48.533	L	22	526.8
11	305C	5.224	41.895	1.414	0	48.533	L	22	414.7
12	305D	5.224	41.895	1.414	0	48.533	L	22	393.1
31	306A	60.471	7.112	9.047	0	76.63	L	22	521
13	306B	60.471	7.112	9.047	0	76.63	L	22	415.6
14	306C	60.471	7.112	9.047	0	76.63	L	22	368.1
15	307A	2.333	0	0	1	3.333	V	22	473.9
16	307B	2.333	0	0	1	3.333	V+L	22	298.1
17	308A	2.333	0	0	0	2.333	L	`22	298.1
18	308B	2.333	0	0	0	2.333	L	22	494.1
30	309	0.001	0	0	1	1.001	V	22	298.1
19	310A	1.021	0	0	0	1.021	L	1.013	298.1
20	310B	1.021	0	0	0	1.021	L	22	299.4
21	311A	1.021	0	0	0	1.021	L	22	298.9
22	311B	1.021	0	0	0	1.021	L	22	393.1
23	**312**	**0**	**0**	**0**	**1**	**1**	**V**	**22**	**299.3**
24	313A	5.117	41.031	1.385	0	47.532	L	22	393.1
25	314	0.108	0.864	0.029	0	1.001	L	22	393.1
26	315	1.112	0.095	0.029	0	1.236	L	22	398.9
27	316A	0.017	0.769	0	0	0.786	L	22	395.7
28	316B	0.017	0.769	0	0	0.786	L	7	395.7
29	317A	61.583	7.207	9.076	0	77.866	L	4.2	369.8

The vapor molar fractions and liquid molar fractions are presented in Figure 4.13. The results indicate that at the top of the column, water is predominant and no HI is present at Stage 1 in the vapor phase.

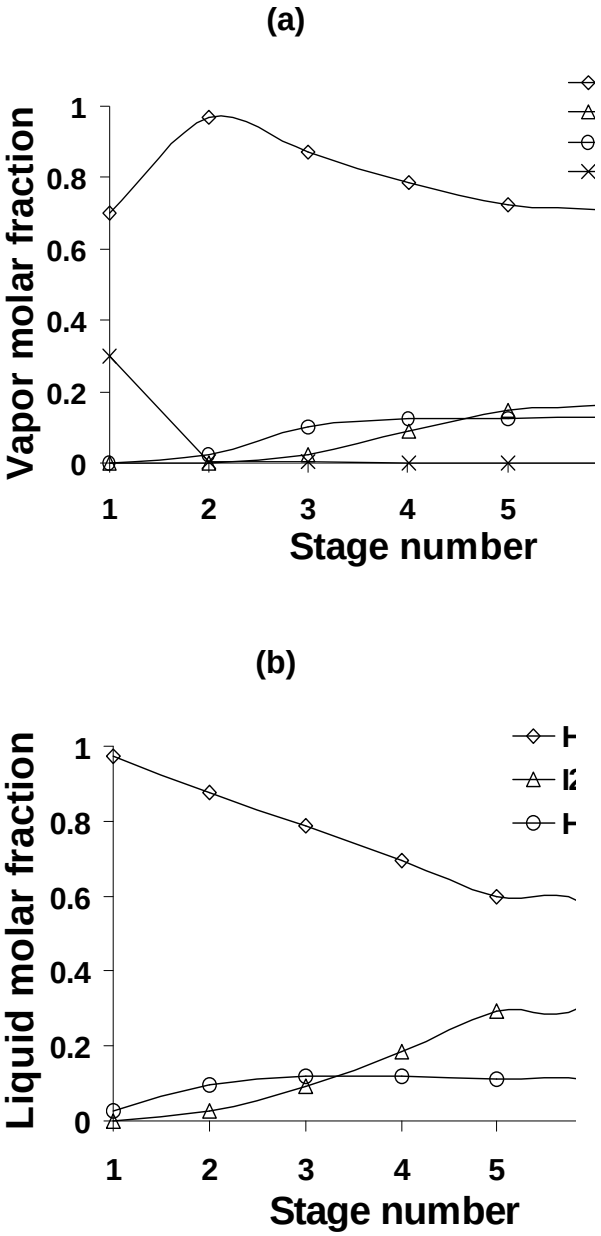

Figure 4.13 Vapor molar fraction (a) and liquid molar fraction (b) in the reactive distillation column when the hydrogen production rate is 1kmol/h

4.3.2 General Atomic Results Reproducibility

The present simulation results are compared with GA results. For comparison, referring to Figure 4.12, the same stream numbers as in GA are used to compare the results. For example,

stream number 304A from present results is compared with stream number 304A of the GA results as shown in Table 4.9. The comparisons are presented in Figures 4.14.-4.17 for component flow rates and stream temperatures.

Table 4.9 Stream Composition for the Reproducibility Study

No	Stream	H2O (kmol/h)	I_2 (kmol/h)	HI (kmol/h)	H_2 (kmol/h)	Mole Flow (kmol/h)	Phase	Press. (bar)	Temp. (K)
1	301A	65.697	48.007	12.459	0	126.164	L	1.85	393.1
2	302A	41.061	30.005	7.787	0	78.852	L	22	397.5
3	303A	24.636	18.003	4.672	0	47.311	L	22	397.5
4	304A	65.697	48.007	12.459	0	126.164	L	22	507.1
5	305A	5.224	41.895	1.414	0	48.533	L	22	583.1
6	306A	60.471	7.112	9.047	0	76.63	L	22	521
7	307A	2.333	0	0	1	3.333	V	22	473.9
8	308A	2.333	0	0	0	2.333	L	22	298.1
9	309	0.001	0	0	1	1.001	V	22	298.1
10	310A	1.021	0	0	0	1.021	L	1.013	298.1
11	311A	1.021	0	0	0	1.021	L	22	298.9
12	**312**	**0**	**0**	**0**	**1**	**1**	**V**	**22**	**299.3**
13	313A	5.117	41.031	1.385	0	47.532	L	22	393.1
14	314	0.108	0.864	0.029	0	1.001	L	22	393.1
15	315	1.112	0.095	0.029	0	1.236	L	22	398.9
16	316A	0.017	0.769	0	0	0.786	L	22	395.7
17	317A	61.583	7.207	9.076	0	77.866	L	4.2	369.8

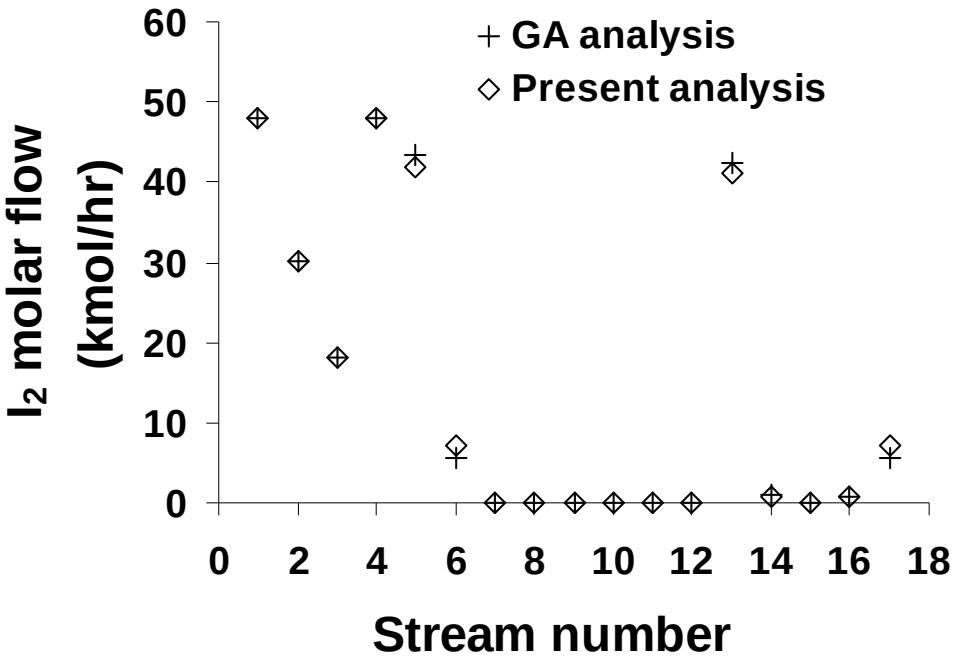

Figure 4.14 I2 flow rate in the flow sheet

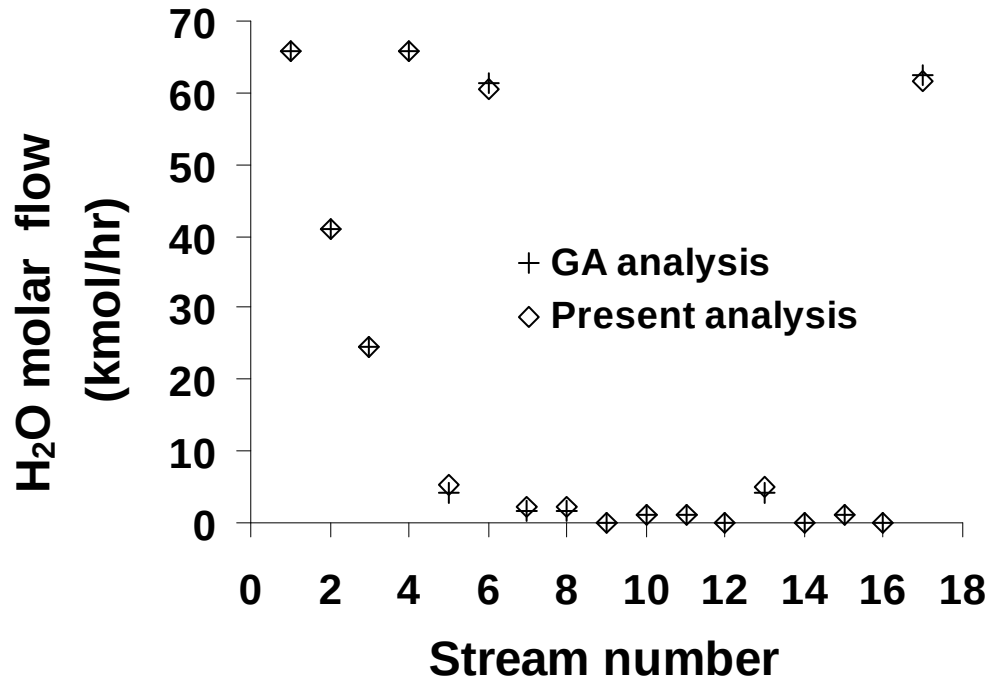

Figure 4.15 H2O flow rate in the flow sheet

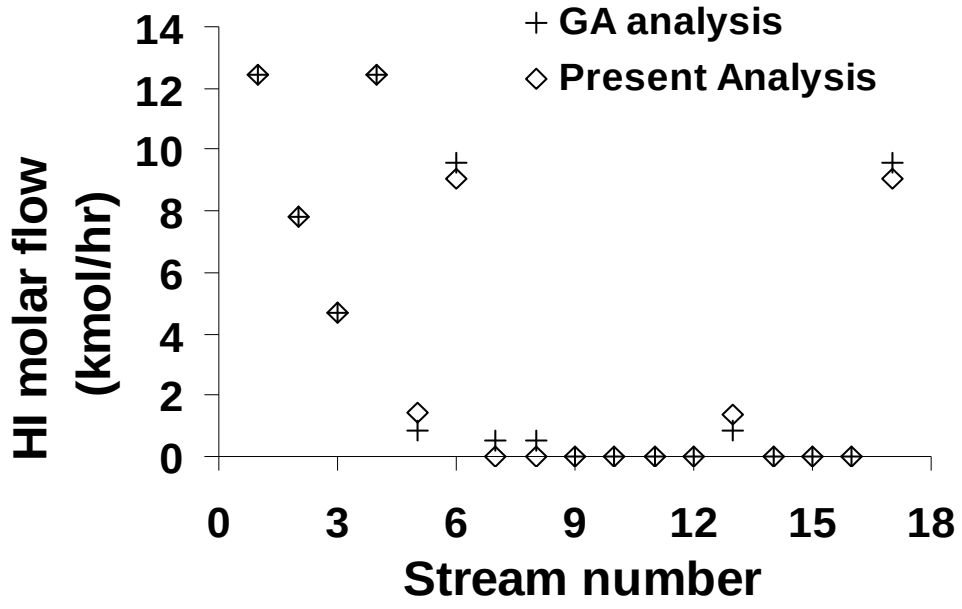

Figure 4.16 HI flow rate in the flow sheet

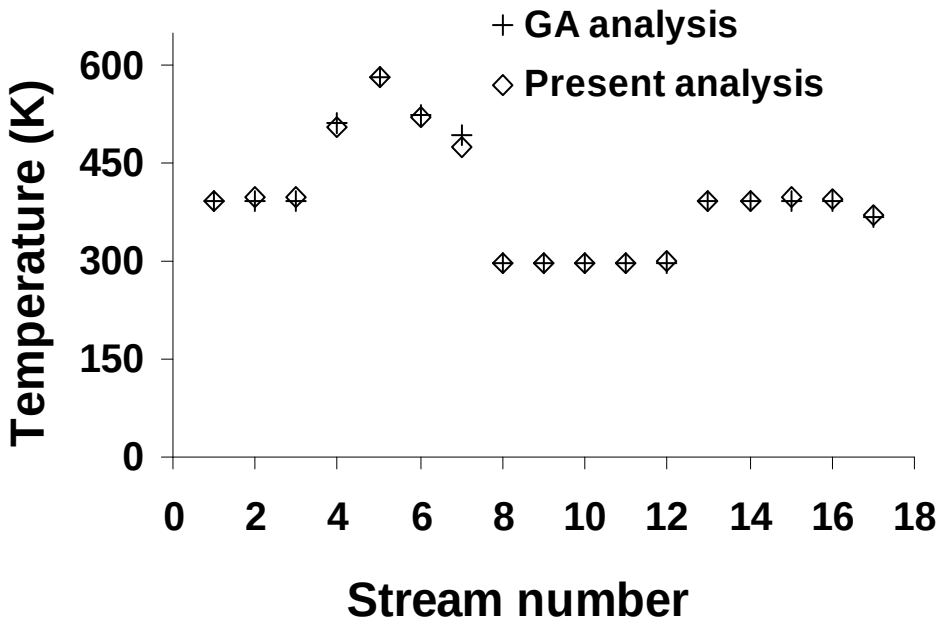

Figure 4.17 I2 flow rate in the flow sheet

The component flow rates of the present simulation compare very well with the GA results. A small difference is noted in the HI flow rate. This deviation may be due to the

difference in the temperature of the side liquid flow rate (stream 306A). Indeed, the temperature in the present analysis is 521K while in the GA analysis, this temperature is 524.15K.

4.3.3 Pressure Influence on the Operating Conditions

The influence of the pressure on the operating conditions was studied for a production of 1 kmol/h of hydrogen. Boil up rate dependence to the pressure in the reactive distillation when hydrogen production rate is 1 kmol/h is presented in Figure 4.18. From the figure, it is clear that if the pressure is increased for hydrogen production rate of 1kmol/h then the boil up rate must be decreased in order to maintain the same hydrogen production rate.

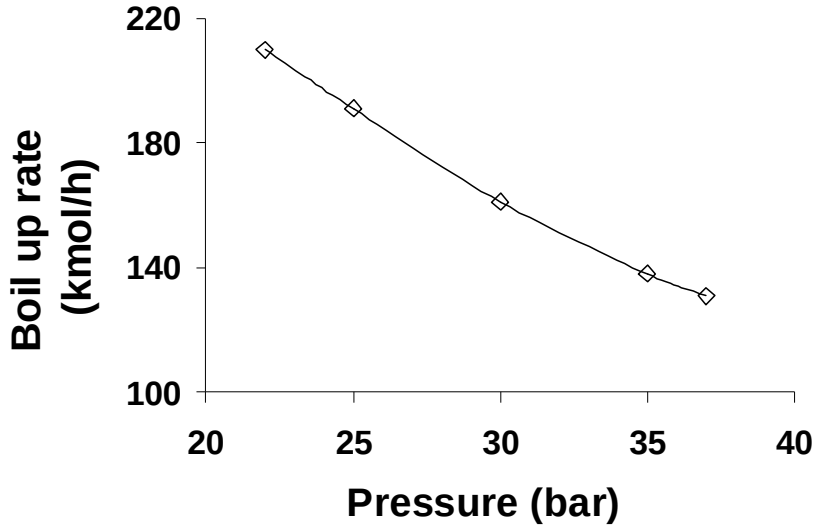

Figure 4.18 Boil up rate dependence to the pressure in the reactive distillation when hydrogen production rate is 1kmol/h.

Component flows of the side liquid (stream 306A) of the column are plotted in Figure 4.19.

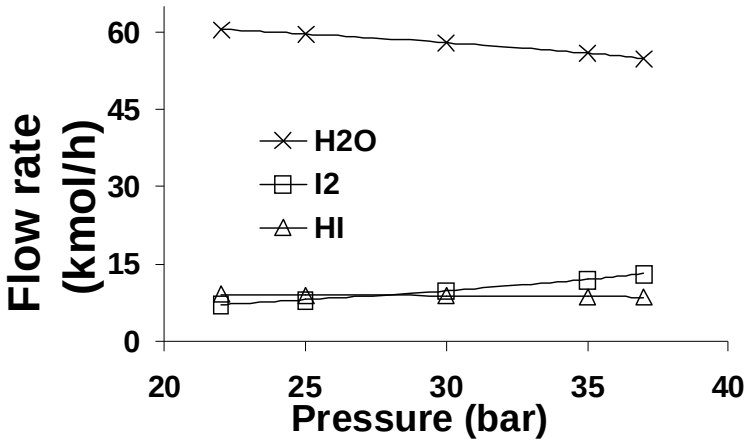

Figure 4.19 Stream 306A component flow dependence to the pressure

The results indicate that when the pressure in the column is increased, the water flow decreases at the side liquid flow while the iodine flow increases. However the HI flow rate is at steady level. At the bottom of the column, water flow rate increases with the increase in the pressure while iodine flow rate decreases.

4.4 Binary Parameter Estimation

The binary parameters were estimated by using Aspen plus with the NRTL activity coefficient model in order to build our proper model for the Section III of the SI cycle. The data were collected from different sources:

- The I_2-H_2O system has been studied by Kracek (Kracek 1931). The solubility of iodine in water was measured and a miscibility gap lying between the solid-liquid equilibrium point at 385.4 K and an upper temperature approximately 553 K was identified.
- Total pressures of HI-H_2O mixtures have been investigated by Wuster (Wuster 1979). This system exhibits an azeotrope whose precise composition depends on temperature and pressure. A synthesis of these data has been published by Engels and Knoche (1986). In the ternary HI-I_2-H_2O system, the liquid phase exhibits two immiscibility regions which are the extension of the partly miscible systems I_2-H_2O and HI-H_2O.

– The hydrogen solubility in pure liquid hydrogen iodide and iodine was measured by O'Keefe and Norman (O'Keefe and Norman 1982) and they found that this solubility obeys Henry's law.

Comparison between the experimental data and the model for the bubble pressure of the HI-H_2O binary is presented in Figure 4.20 at 373 K and 398 K.

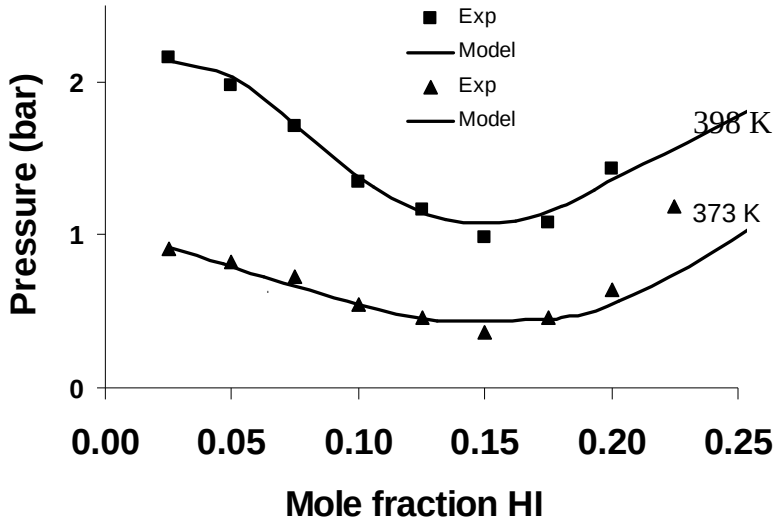

Figure 4.20 Bubble pressure of HI-H_2O mixture

Table 4.10 and Table 4.11 summarize the binary parameters estimated by the model.

Table 4.4.100 NRTL binary parameters estimated with Aspen Plus

Component i	HI	I_2	I_2
Component j	H_2O	HI	H_2O
Aij	-2.093	1.458	-4.678
Aji	4.126	0	-0.875
Bij	-819.078	173.318	3132.595
Bji	-573.903	0	2796.087
Cij	0.3	0.3	0.3
Tlower (C)	0	0	0
Tupper (C)	1000	1000	1000

Table 4.11 Henry's binary parameters estimated with Aspen Plus under pressure unit in bars.

Component i	H_2	H_2
Component j	HI	I_2
Aij	7.867	-286.355
Bij	0	0
Cij	0	0
Tlower (C)	0	0
Tupper (C)	65	65

We are currently working on the improvement of HI decomposition in the SI cycle by using the membranes techniques.

4.5 Membrane Separation Method for HI Decomposition

In order to increase the SI cycle efficiency, which depends mostly to the amount of heat input for the HI and sulfuric acid decomposition and the amount of water recycled to the Bunsen reaction, different methods have been proposed.

To reduce the excessive recycling agents, three membrane techniques have been proposed for the SI cycle process. An electrochemical cell (EC) method can reduce the amount of iodine (I_2) coming from the Bunsen reactor (Nomura et al. 2004; Nomura et al. 2005). HI separation and decomposition procedures are integrated into the Bunsen reactor membrane reactor. The H_2SO_4 solution and the HI solution are obtained separately at both sides of the cationic-exchange membrane. HI solution can be concentrated by using an electro-electrodialysis (EED) (Arifal et al. 2002; Onuki et al. 2001). This method is effective in reducing the amount of water recycled to the Bunsen reaction after the reactive distillation reaction. A hydrogen permselective membrane reactor (HPMR) can improve the conversion ratio of HI decomposition reaction (Hwang and Onuki 2001; Hwang et al. 1999).

The evaluation of the sulfur-iodine process featuring of the membranes techniques by total thermal efficiency is presented by Nomura et al. (Nomura et al. 2005). In their study, the comparisons are made between electro-electrodialysis (EED), electrochemical cell (EC) and hydrogen permselective membrane reactor (HPMR). The maximal thermal efficiency was found to be 40.8% at 12.5mol.kg$^{-1}_{(H2O)}$ of HI molality after the EED. For the electrochemical cell (EC)

the maximum thermal efficiency was 38.9% at 15.3mol.kg$^{-1}_{(H2O)}$ of H_2SO_4 molality after the EC. It was also shown that when the HPMR is used for HI decomposition, the conversion in one pass is about 76.4% while in the SI cycle the conversion is 20%. The amount of recycled HI was reduced by 91.5% using this membrane technique. It was noted that the total thermal efficiency was improved only 0.7% by the application of the HPMR.

Very recently, the removal of water from aqueous hydriodic acid (HI) by pervaporation using Nafion 117 membrane was also studied (Orme and Stewart 2007; Stewart et al. 2007). Water was successfully removed from the acid with a separation factor of 10^3 with respect to HI. For example, HI feeds were concentrated from approximately 1.7 to 5M and permeate concentration from 10^{-3} to 10^{-4} M. Membrane distillation (MD) was also applied for the concentration of hydriodic and sulfuric aqueous solution (Caputo et al. 2007). Two different membranes were investigated, direct contact membrane distillation (DCMD) with a polypropylene capillary membrane, and air-gap membrane distillation (AGMD) with polytetrafluoroethylene (PTFE) flat-sheet membrane. It has been demonstrated that H2SO4 concentration in feed was increased from 1.1 up to 7mol/L with DCMD and from 0.9 up to 10.1mol/L with AGMD. HI concentration was increased from 0.3 up to 7.0mol/L with the DCMD and from 0.3 up to 8mol/Lwith AGMD. The latter result shows that the HI concentration can be higher than the azeotropic concentration of the HI/H_2O (7.57mol/L). All the work will be focused on the HI decomposition section by using EED and or Pervaporation. The proposed modified flowsheet is presented in Figure 4.21.

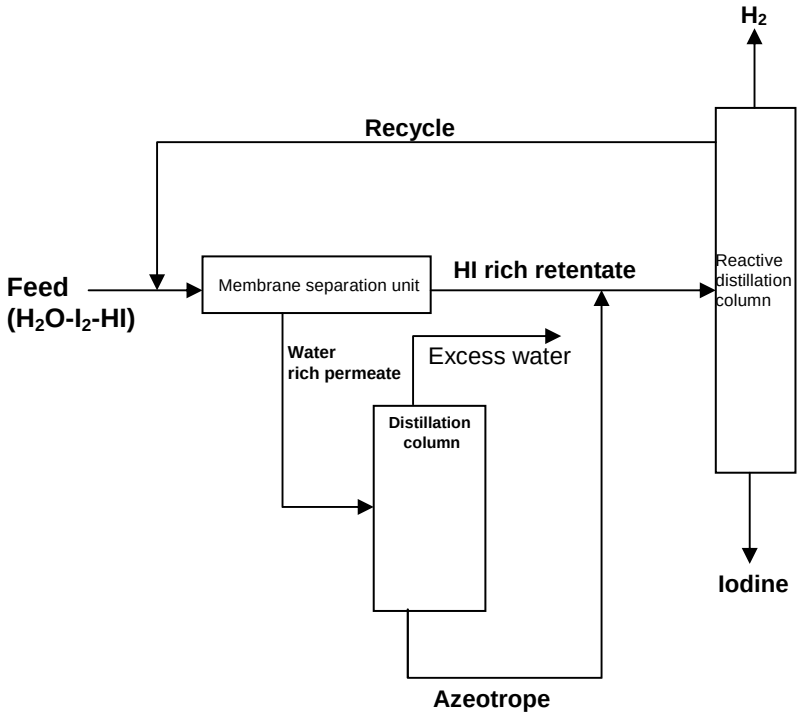

Figure 4.21 Schematic proposed modified HI decomposition flowsheet

5. Simulation of Sulfur Iodine Thermochemical Hydrogen Production Plant Coupled To High Temperature Heat Source

5.1 Introduction

In the present model the SI cycle is simplified in to three main reactions -Bunsen reaction, sulfuric acid decomposition and the hydriodic acid decomposition. Since Bunsen reaction is exothermic, it is not coupled to nuclear heat transport system. Thus Section I does not receive process heat input.

A mathematical model for the reaction chamber and all chemical processes is developed. The process heat from the nuclear reactor is simulated through the heat exchanger that is coupled to reaction chambers. Dynamic response of the coupled SI plant and high temperature reactor heat exchanger is examined for transients using the simplified model.

5.2 Simplified model

The first step in developing a transient model for the sulfur iodine cycle is to derive governing equations of mass, momentum, and energy. Governing equations applicable for a reaction chamber control volume with inlet and outlet flow are derived (Figure 3.1). The model is used to analyze the decomposition of sulfuric acid (H_2SO_4) and hydrogen iodide (HI) in the SI cycle. Transients initiated from high temperature helium side such as helium inlet temperature or helium inlet flow rate changes are simulated. It is assumed that all reaction chambers are well mixed, the chamber volumes are constant, and the chamber pressures are constant.

5.2.1 Extent of Reaction

The general chemical reaction can be written as

$$|\nu_1| A_1 + |\nu_2| A_2 + \ldots = \ldots + |\nu_{i-1}| A_{i-1} + |\nu_i| A_i \qquad (5.1)$$

where the $|\nu_i|$ are stoichiometric coefficients and the A_i stand for chemical species. The left hand side and right hand side of the equation are reactants and products, respectively. The ν_i are called stoichiometric numbers, which are positive for products and negative for reactants. For example, the hydrogen iodide decomposition reaction can be written as

$$2HI = H_2 + I_2$$

then $\nu_{HI} = -2$, $\nu_{H_2} = 1$, $\nu_{I_2} = 1$. Eq. (5.1) can be rearranged as

$$\sum_i \nu_i A_i = 0 \tag{5.2}$$

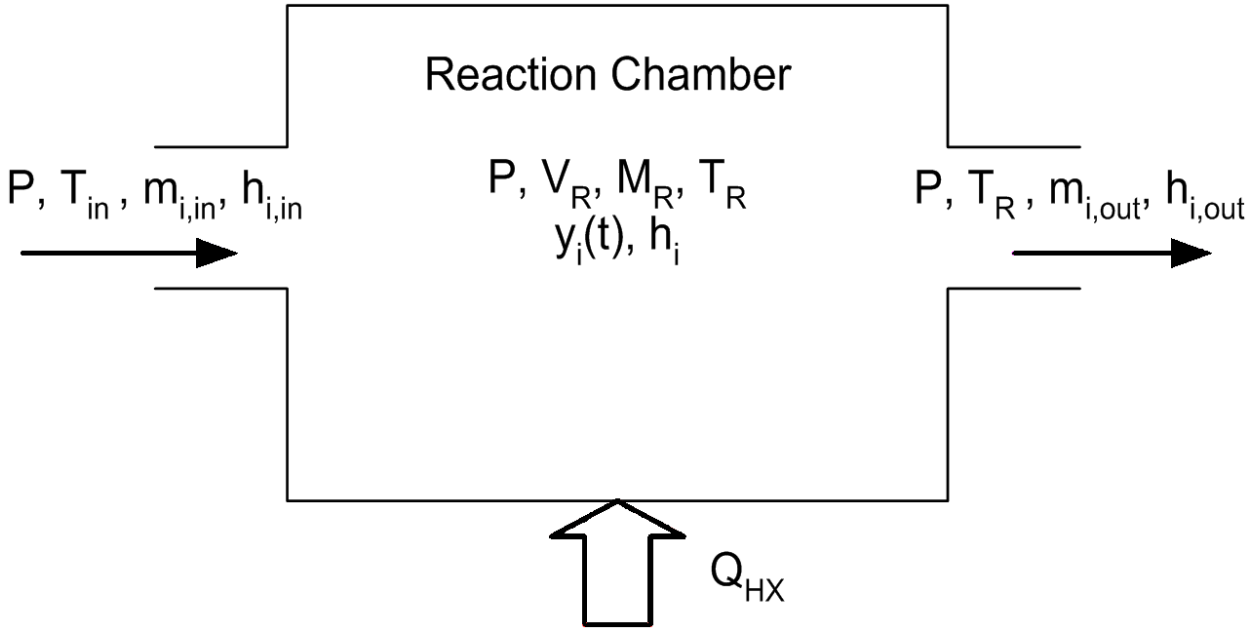

Figure 5.1 - Schematic diagram of a reaction chamber

In the reaction represented by Eq. (5.2), the changes in the numbers of moles of the species are directly proportional to the stoichiometric numbers.

$$\frac{dM_1}{\nu_1} = \frac{dM_2}{\nu_2} = \ldots = \frac{dM_{i-1}}{\nu_i} = \frac{dM_i}{\nu_i} \tag{5.3}$$

where the M_i are the numbers of moles of the species. Each term is related to an amount of reaction. Since all terms are equal, they can be represented by a single quantity *dX*.

$$dX = \frac{dM_1}{\nu_1} = \frac{dM_2}{\nu_2} = \ldots = \frac{dM_{i-1}}{\nu_{i-1}} = \frac{dM_i}{\nu_i} \tag{5.4}$$

The variable, *X*, is called the *molar extent of reaction*, which characterizes the extent or degree to which a reaction has taken place. The general relation between a differential change $dM_{i,RXN}$ in the number of moles of a reacting species and *dX* is

$$dM_i = \nu_i dX \tag{5.5}$$

The sum of the changes in the number of moles for all species is then

$$dM_{reaction} = \sum_i dM_i = \left(\sum_i \nu_i \right) dX = (\Delta \nu)\, dX \tag{5.6}$$

5.2.2 Balance Equation in a Reaction Chamber

A schematic diagram of one of the reaction chambers is shown in Figure 1.

5.2.2.1 The Molar Balance

The molar balance for each species in the reaction chamber can be written as,

$$\frac{dM_{i,R}}{dt} = m_{i,in} - m_{i,out} + \frac{dM_i}{dt} \tag{5.7}$$

where $M_{i,R}$ = the accumulation of moles of species i in the reaction chamber,

$m_{i,in}$ = the molar flow rate of species i into the reaction chamber,

$m_{i,out}$ = the molar flow rate of species i out of the reaction chamber,

M_i = the production rate of moles of species i due to reaction,

In equation (5.7), the M_i is defined as,

$$M_i = V_R \nu_i \frac{dC_i}{dt} \tag{5.8}$$

where M_i = the production rate of moles of species i due to reaction,

V_R = the reaction chamber volume,

$m_{i,out}$ = the molar flow rate of species i out of the reaction chamber,

C_i = the concentration of species i in the reaction chamber,

The total number of moles in reaction chamber and the total molar flow rate into and out of the chamber can be written as

$$M_R = \sum_i M_{i,R} \tag{5.9}$$

$$m_{in} = \sum_i m_{i,in} \tag{5.10}$$

$$m_{out} = \sum_i m_{i,out} \tag{5.11}$$

The molar fraction of each species in the reaction chamber is defined as

$$y_i = \frac{m_{i,out}}{m_{out}} \tag{5.12}$$

Combining equations,

$$\frac{d\left(y_i M_R\right)}{dt} = m_{i,in} - m_{i,out} + \nu_i \frac{dX}{dt} \tag{5.13}$$

This is the molar continuity equation for a species, *i*. In this equation, *dX/dt* is defined as,

$$\frac{dX}{dt} = \frac{1}{\nu_i}\frac{dM_i}{dt} = V_R\frac{dC_i}{dt} \tag{5.14}$$

Thus, equation (5.13) can be rewritten as,

$$\frac{d\left(y_i M_R\right)}{dt} = m_{i,in} - m_{i,out} + \nu_i V_R\frac{dC_i}{dt}$$

For the hydrogen iodide decomposition reaction, the molar balance equation for each species can be written as,

$$\frac{d\left(M_{HI,R}\right)}{dt} = m_{HI,in} - m_{HI,out} - \frac{dM_{HI}}{dt} = m_{HI,in} - m_{HI,out} - 2\frac{dX}{dt} \tag{5.15}$$

$$\frac{d\left(M_{H_2,R}\right)}{dt} = m_{H_2,in} - m_{H_2,out} + \frac{dM_{H_2}}{dt} = m_{H_2,in} - m_{H_2,out} + \frac{dX}{dt} \tag{5.16}$$

$$\frac{d\left(M_{I_2,R}\right)}{dt} = m_{I_2,in} - m_{I_2,out} + \frac{dM_{I_2}}{dt} = m_{I_2,in} - m_{I_2,out} + \frac{dX}{dt} \tag{5.17}$$

By summing the molar balance equation for species i in Eq. (5.12), global molar balance equation can be obtained as

$$\frac{dM_R}{dt} = m_{in} - m_{out} + \Delta\nu\frac{dX}{dt} \tag{5.18}$$

The left hand side of Eq. (5.12) can be expanded as

$$M_R\frac{dy_i}{dt} + y_i\frac{dM_R}{dt} = m_{i,in} - m_{i,out} + \nu_i\frac{dX}{dt} \tag{5.19}$$

Combining and simplifying, the above equations are written as

$$M_R\frac{dy_i}{dt} + y_i\left(m_{in} + \Delta\nu\frac{dX}{dt}\right) = m_{i,in} + \nu_i\frac{dX}{dt} \tag{5.20}$$

5.2.2.2 The Energy Balance

From the first law of thermodynamics for an open system with negligible kinetic and potential energy, the energy balance equation for the entire reaction chamber can be expressed as

$$\frac{dU}{dt} = \sum_i\left(m_{i,in}h_{i,in}\right) - \sum_i\left(m_{i,out}h_{i,out}\right) + \dot{Q}_{HX} \tag{5.21}$$

where U = total internal energy in the reaction chamber,

$h_{i,in}$ = the enthalpy of each reactant species entering the reaction chamber,

$h_{i,out}$ = the enthalpy of each reactant species exiting the reaction chamber,

$\dot{Q}_{HX}$ = the energy input from the heat exchanger.

Using the definition of enthalpy Eq. (15) can be written as

$$\frac{dH}{dt} = \sum_i \left(m_{i,in} h_{i,in} \right) - \sum_i \left(m_{i,out} h_{i,out} \right) + \dot{Q}_{HX} + V_R \frac{dP}{dt} \tag{5.22}$$

where $H = U + PV$ = total enthalpy in the reaction chamber,

P = pressure in the reaction chamber,

V_R = the reaction chamber volume.

For simplicity, the ideal gas mixture assumption is used in this model.

If $M_{i,R}$ moles of species i in this mixture occupy the same total volume alone at the same temperature, the pressure is

$$PV_R = M_R R T_R \tag{5.23}$$

Dividing the latter equation by the former gives

$$\frac{p_i}{P} = \frac{M_{i,R}}{M_R} = y_i \text{ or } p_i = y_i P \tag{5.24}$$

where y_i is the mole fraction of species i in the gas mixture, and p_i is known as the partial pressure of species i. The sum of the partial pressures equals to the total pressure.

An ideal gas is a model gas comprised of imaginary molecules of zero volume that do not interact. Each chemical species in an ideal-gas mixture therefore has its own private properties, uninfluenced by the presence of other species. This is the basis of Gibbs's theorem (Smith and Ness, 1987): A total thermodynamic property (*U, H, Cp, S, A, or G*) of an ideal-gas mixture is the sum of the total properties of the individual species, each evaluated at the mixture temperature but at its own partial pressure.

This is expressed mathematically for the enthalpy H by the equation

$$dH = \sum_i \left(y_i h_i \right) dM_R + M_R \sum_i \left(h_i dy_i \right) + M_R \sum_i \left(y_i dh_i \right) \tag{5.25}$$

where the superscript *ig* denotes an ideal-gas property. Since the molar enthalpy of an ideal gas is independent of pressure,

$$\overline{h^{ig}(T)} = \sum y_i h_i^{ig}(T) \tag{5.26}$$

The superscript ig will be dropped for the simplicity, hereafter.

The total enthalpy of the system can be related to the molar enthalpy using the ideal gas mixture relations.

$$H = M_R \cdot \bar{h} = \sum_i M_{i,R} \cdot h_i = M_R \sum_i y_i \cdot h_i \tag{5.27}$$

where $\bar{h}$ = the mixture molar enthalpy in the reaction chamber,

h_i = the molar enthalpy of each species i in the reaction chamber.

The expression for the change in the total enthalpy can be expanded as,

$$dH = \sum_i \left(y_i h_i \right) dM_R + M_R \sum_i \left(h_i dy_i \right) + M_R \sum_i \left(y_i dh_i \right) \tag{5.28}$$

By substitution Eq. (5.22) into Eq. (5.16), we can reduce the energy balance equation to dependence on more computationally relevant quantities.

$$\sum_i \left(y_i h_i \frac{dM_R}{dt} + M_R h_i \frac{dy_i}{dt} + M_R y_i \frac{dh_i}{dt} \right) = \sum_i \left(m_{i,in} h_{i,in} \right) - \sum_i \left(m_{i,out} h_{i,out} \right) + \dot{Q}_{HX} + V_R \frac{dP}{dt} \tag{5.29}$$

This expression may be further reduced via substitution,

$$\sum_i \begin{pmatrix} y_i h_i \left(m_{in} - m_{out} + \nu_i \frac{dX}{dt} \right) + M_R y_i \frac{dh_i}{dt} + \\ h_i \left(-y_i m_{in} - y_i \nu_i \frac{dX}{dt} + m_{i,in} + \nu_i \frac{dX}{dt} \right) \end{pmatrix} = \sum_i \left(m_{i,in} h_{i,in} \right) - \sum_i \left(m_{i,out} h_{i,out} \right) + \dot{Q}_{HX} + V_R \frac{dP}{dt} \tag{5.30}$$

The change in molar enthalpy of each species in the reaction chamber is then

$$dh_i = c_{p,i} dT_R \tag{5.31}$$

where $c_{P,i}$ = the molar specific heat at constant pressure,

dT_R = the temperature change in the reaction chamber.

The molar enthalpy of the outlet stream is assumed as one in the reaction chamber, $h_{i,out} = h_i$.

Then, the energy equation is further simplified as

$$M_R \sum_i y_i c_{p,i} \frac{dT_R}{dt} = \sum_i m_{i,in} \left(h_{i,in} - h_i \right) - \frac{dX}{dt} \sum_i \nu_i h_i + \dot{Q}_{HX} + V_R \frac{dP}{dt} \tag{5.32}$$

The heat of reaction and mixture specific heat are defined as

$$\Delta h_{reaction} = \sum_i \nu_i h_i \tag{5.35}$$

$$\overline{c_p} = \sum_i y_i c_{p,i} \tag{5.34}$$

Finally, the energy balance equation can be written as

$$M_R \overline{c_P} \frac{dT_R}{dt} = \sum_i m_{i,in}(h_{i,in} - h_i) - \Delta h_{RXN} \frac{dX}{dt} + \dot{Q}_{HX} + V_R \frac{dP}{dt} \tag{3.35}$$

To summarize, the continuity equation for the reaction chamber is,

$$M_R \frac{dy_i}{dt} + y_i \left(m_{in} + \Delta\nu \frac{dX}{dt} \right) = m_{i,in} + \nu_i \frac{dX}{dt}$$

As an equation of state, ideal gas law is used.

$$PV_R = M_R R T_R$$

where $C_R = M_R / V_R$ the molar concentration in the reaction chamber.

The energy equation for the reaction chamber is,

$$M_R \sum_i y_i c_{p,i} \frac{dT_R}{dt} = \sum_i m_{i,in}\left(h_{i,in} - h_i\right) - \frac{dX}{dt} \sum_i \nu_i h_i + \dot{Q}_{HX} + V_R \frac{dP}{dt}$$

The extent of reaction, X, can be related to the reaction temperature, T_R, as well as the species concentration, $C_i = y_i C_R$. Thus,

$$X = X\left(T_R, C_i\right) \tag{5.36}$$

The heat exchanger is modeled as a shell and pipe type heat exchanger. It is assumed that the pipes carry the nuclear heat with helium stream and the heat is transferred to the shell side which is the reaction chamber volume. The energy balance through heat exchanger is

$$\dot{Q}_{HX} = U \cdot A \cdot \Delta T = m_{He}(h_{He,in} - h_{He,out}) \tag{5.37}$$

where, U = overall heat transfer coefficient of heat exchanger

A = heat transfer surface area

ΔT = mean temperature difference in heat exchanger

m_{He} = molar flow rate of helium stream

$h_{He,in}$ = molar enthalpy of helium stream at inlet with Th_1,

$h_{He,out}$ = molar enthalpy of helium stream at outlet with Th_2

The unknowns in this system of equations are: M_R, X, y_i (i=1,2,,,n), m_{out}, P, T_R and Th_2 . We have (n+6) unknowns but only have (n+5) equations. We need one more equation to close

the problem. One missing equation is a momentum balance equation through the reaction chamber. We can construct the momentum balance for the reaction chamber with an appropriate consideration of pressure forces, viscous forces and gravitational forces. A realistic set-up of the momentum balance is related with specific process system design and control logics (piping configurations, pump performance and control logic, valve characteristics and control logic, etc). Such information is not available now and it is not appropriate for the purpose of this model, a simplified model. Instead of solving the momentum balance, a few possible model assumptions could be used for the present simplified model;

1. The pressure in the reaction chamber is constant (i.e. $\frac{dP}{dt} = 0$)
2. –Or- the total mole number in the chamber is constant (i.e. $\frac{dM_R}{dt} = 0$)
3. –Or- the outlet molar flow rate is constant (i.e. $\frac{dm_{out}}{dt} = 0$)

A reasonable assumption seems to be that, during a transient, the pressure in the reaction chamber does not change. We can expect that actual process system would have such pressure control logic in each reaction chamber. Therefore, constant pressure in the reaction chamber is assumed in the present analysis.

$$\frac{dP}{dt} = 0 \quad \text{or } P = \text{constant} \tag{5.38}$$

5.2.3 Chemical Reactions in SI Cycle

To close the governing equations derived in the previous section, the extent of reaction in Eq. (5.27) should be specified for each reaction. The main chemical reaction in the SI cycle is modeled with an appropriate simplification and the other chemical processes for the separation, concentration, and recycling are neglected or simplified. For section 1, the depletion rate of sulfur dioxide can be expressed as (Brown et al. 2003),

$$-\frac{d[SO_2]}{dt} = k_1 \cdot [I_2] \cdot [H_2O] \cdot [SO_2] \tag{5.39}$$

Thus, the depletion rate of sulfur dioxide is dependent on the reaction rate, as well as the concentration of each of the constituents.

For section 2, the analysis of the sulfuric acid decomposition is carried out in two steps. First, sulfuric acid is assumed to be decomposed into water and sulfur trioxide. Second, oxygen and sulfur dioxide are produced by the decomposition of sulfur trioxide (8). These steps are,

$$1)\ H_2SO_4 \longrightarrow H_2O + SO_3, \qquad 2)\ SO_3 \longrightarrow SO_2 + \frac{1}{2}O_2$$

From the chemical equilibrium calculation, the sulfuric acid decomposition (first reaction) is close to 100% at above 700 ^{o}C (Huang and A. T-Raissi, 2005). Therefore, 100% conversion is assumed in this model. Then, the chemical kinetics for section 2 is expressed as,

$$-\frac{d[H_2SO_4]}{dt} = -\frac{d[SO_3]}{dt} = k_2 \cdot [SO_3] \tag{5.40}$$

Because the reverse reaction rate of section 3 is substantial, the definition of Hydrogen Iodide depletion rate is significantly more complex. The HI decomposition reaction can be quantified via three coupled differential equations for the production of hydrogen and iodine and the depletion of hydrogen iodide. These expressions are,

$$\begin{aligned} &\frac{d[H_2]}{dt} = k_3 \cdot [HI]^2 - k_{-3} \cdot [H_2] \cdot [I_2]; \\ &\frac{d[H_2]}{dt} = \frac{d[I_2]}{dt}; \\ &\frac{1}{2}\frac{d[HI]}{dt} = k_{-3} \cdot [H_2] \cdot [I_2] - k_3 \cdot [HI]^2 \end{aligned} \tag{5.41}$$

These coupled equations for section 3 are solved using the Runge-Kutta method. Assuming each reaction is elementary; these reaction rate constants can be calculated using the following relationships,

$$k_1 = A_1 \exp\left(-\frac{E_1}{R}\left\{\frac{1}{T_1} - \frac{1}{T_0}\right\}\right), k_2 = A_2 \exp\left(-\frac{E_2}{RT_2}\right),$$

$$k_3 = A_3 \exp\left(-\frac{E_3}{RT_3}\right), \quad k_{-3} = A_{-3} \exp\left(-\frac{E_{-3}}{RT_3}\right) \tag{5. 42}$$

Table 5.1 summarizes each parameter in Eq. (5.39). The reaction constants (*A*'s and *k*'s) were obtained from reference (Oxtoby And N.H. Nachtrieb., 1986). Thus, a simple chemical model of the steady state and transient behavior of each reaction chamber has been described. This chemical reaction chamber model, when coupled to a relevant thermal model, constitutes a fully coupled simplified model of the SI cycle.

Table 5.1 Reaction rate parameters

Section 1: Bunsen reaction (Liquid Phase, 120 ^oC)	
Pre-Exponential Factor (A1)	3e-6 $L^2/(mol^2\ s)$
Activation Energy (E1)	4.187 kJ/mol
Section 2: H2SO4 decomposition (Gas Phase, 850 ^oC)	
Pre-Exponential Factor (A2)	6.8e4 s^{-1}
Activation Energy (E2)	73.1 kJ/mol
Section 3: HI decomposition (Gas Phase, 450 ^oC)	
Reverse Reaction	
Pre-Exponential Factor (A-3)	1.596e7 L/(mol s)
Activation Energy (E-3)	108 kJ/mol
Forward Reaction	
Pre-Exponential Factor (A3)	1e11 L/(mol s)
Activation Energy (E3)	184 kJ/mol

The reason for the large response time of Section III is that HI decomposition requires a very large volume. This large volume is due to the reverse reaction rate of HI decomposition which is on the same order as the forward reaction rate. In the simplified SI model, HI decomposition is the most challenging reaction in terms of chemical kinetics. In contrast, the chemical kinetics of the H_2SO_4 decomposition is straightforward, but there are many material difficulties due to high temperature and the highly corrosive nature of the solution. The long response time of Section III slows chemical plant feedback to the nuclear reactor. The contrast in response time between Section II and Section III is shown in Figure 2.

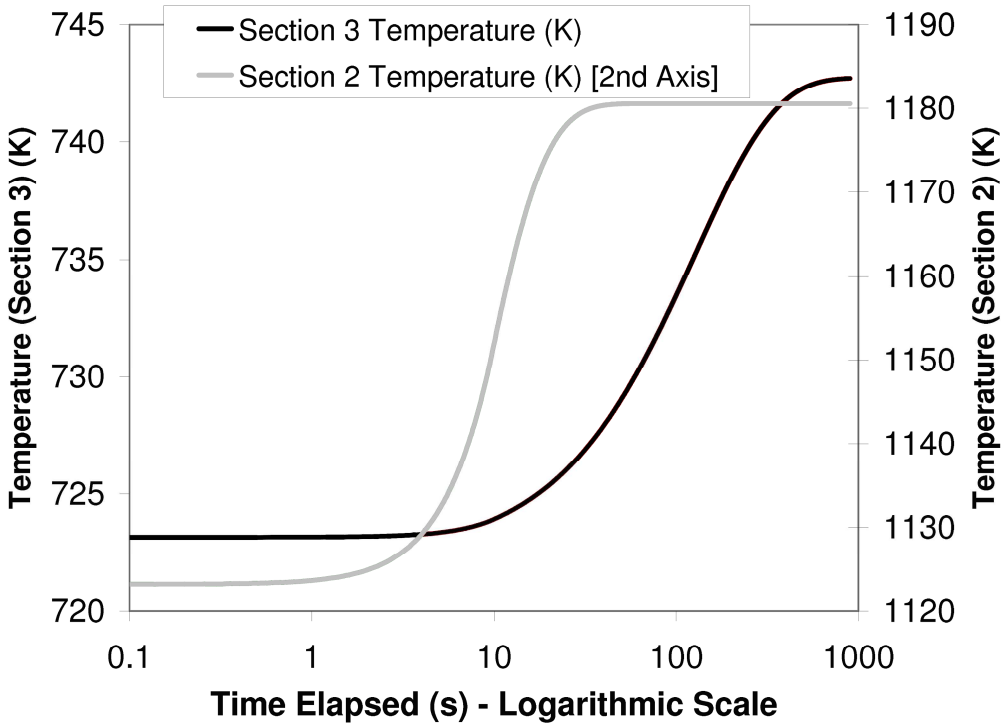

Figure 5.2 - Response time of Section 2 and Section 3

5.3 Model Implementation

To implement the transient model, a comprehensive steady state calculation must first be performed. The steady state analysis involves calculating a steady state hydrogen production rate based on reactor coolant and reactant flow rates and temperatures. After the initial steady state calculation, one of the relevant quantities, such as reactor coolant temperature, can be perturbed, and the resultant transient can be observed. The initial steady state condition can be obtained by fixing all but one of the relevant quantities. For example, a desired hydrogen production rate could be fixed, and the required coolant flow rate calculated. Alternatively the coolant flow rate could be fixed and the heat exchanger transfer area required calculated. Thus, there are a variety of potential steady state solutions that could be reached. A sample set of specific chemical species concentrations is shown in Table 5.2. The temperature and pressure for each sections were set based on the values from previous literature (Norman et al. 1982).

Table 5.2 Steady state concentrations

***Section I**: Bunsen reaction (Liquid Phase, 120 C, 7 bar)*

Components	Concentration, mol/m^3
SO_2	315.1
I_2	9901.5
H_2O	14685.0
HI	2567.8
H_2SO_4	206.1

***Section II**: H_2SO_4 decomposition (Gas Phase,850 C, 7.09 bar)*

Components	Concentration, mol/m^3
H_2SO_4	0.1
H_2O	34.7
SO_3	11.8
SO_2	19.5
O_2	9.8

Section III: HI decomposition (Gas Phase, 450 C, 22 bar)

Components	Concentration, mol/m^3
H_2	5.2
I_2	51.6
HI	161.1
H_2O	148.1

Once a steady state solution has been attained, a quantity, such as the nuclear reactor coolant flow rate or the coolant temperature, can be perturbed. Then, using the time dependent energy balance, continuity balance, reaction rates, and momentum assumption, the transient response of the SI-cycle system can be observed. The transient is modeled by introducing a perturbation and iterating with a small time step until convergence is achieved. A flowchart of the proposed transient model procedure is shown in Figure 5.3.

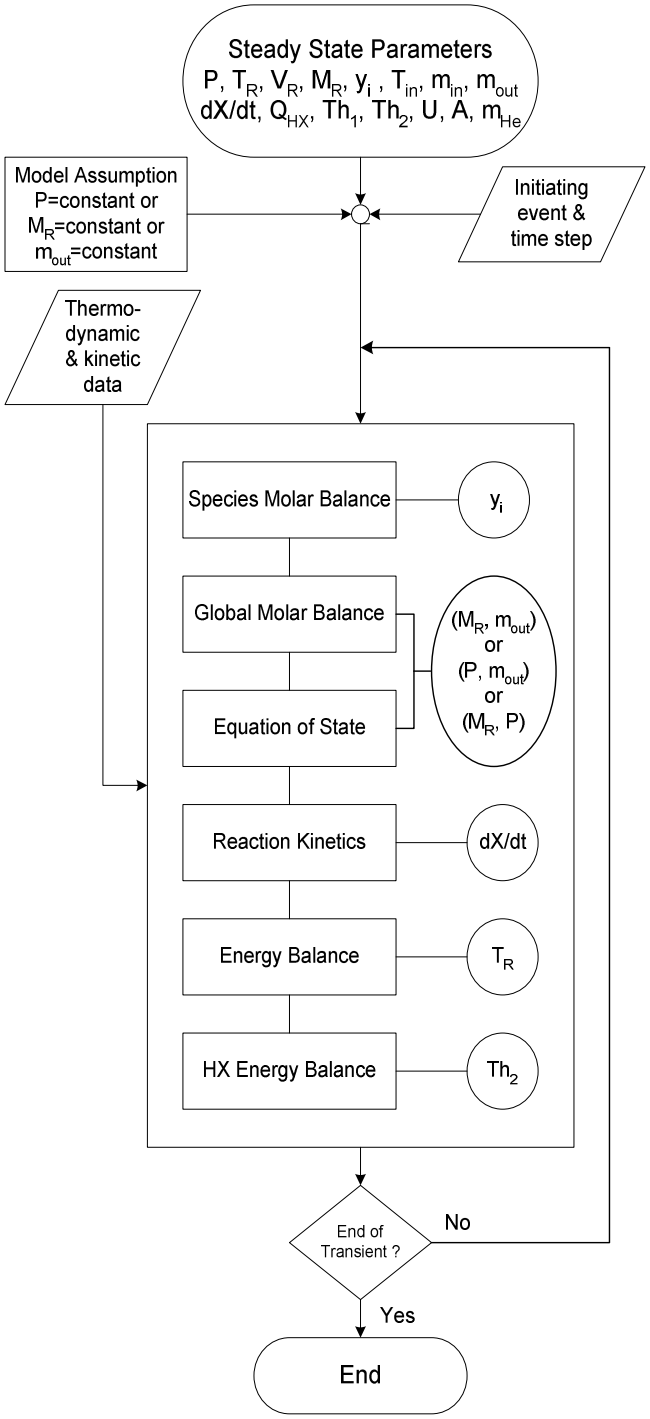

Figure 5.3 - Flowchart – transient analysis

5.4 Results and Discussion

Some of the most important transients in nuclear reactors are those such as a partial Loss-of-Coolant Accident, where some percentage of the reactor coolant is removed from the coolant

stream. This is a potentially severe reactor accident. Understanding the transient behavior of the chemical plant in such an event is an important nuclear safety question. Thus, a sudden change in coolant flow rate is an important perturbation in the transient analysis.

Occasionally, to prevent an out-of-control nuclear reaction, an emergency insertion of negative reactivity is necessitated. As a result of the reactivity removal, the outlet temperature of the reactor coolant will quickly drop. The change in chemical plant reaction rates and hydrogen production rate would be important to understand in such an event. In the following section, perturbations for helium inlet temperature and helium inlet flowrate are simulated as transient analyses. Thus perturbations in the process heat inlet coolant flow rate and inlet temperature are chosen as test cases because they are of interest in the analysis of high temperature gas cooled reactor.

The transient model for the reaction chamber is implemented in a series of MATLAB scripts based on the available thermodynamic and kinetic data (Oxtoby and Nachtrieb., 1986). For the steady state condition, it is assumed that two helium streams flow through each reaction chamber (Section 2 for H2SO4 decomposition and Section 3 for HI decomposition) with helium inlet temperature of 900^{o}C (1173.15K) and helium outlet temperature of 450^{o}C (723.15 K). Steady state helium flow rate can be determined from the steady state helium inlet and outlet temperatures using heat exchanger (HX) heat load (the heat required for two endothermic reactions in Section 2 and Section 3) and at assumed design hydrogen generation rate. For calculations hydrogen generation of 1 mol/s was first assumed. Steady state concentrations were derived from ASPENPlus calculation using the GA flowsheet (Brown et al. 2003). Then the corresponding heat exchanger heat loads are calculated. The reaction kinetics for each section determines the amount of reactants in each chamber. Thus for given pressure the reaction chamber volume is determined. The reaction chamber volume for Section 3 is very large compared to Section 2. This can then be scaled to any generation level.

In the current model implementation, there is no time delay between the event that initiates the transient and the response of the chemical plant. The thermal time constant and heat capacities of the, heat exchanger, chambers and piping are not modeled. Thus, the transient begins immediately following the perturbation. Therefore the transient results from the model show accelerated effects than the reality. Nevertheless, some understanding of the transient behavior of the SI-cycle may be gained from the model results. The interface between the

chemical plant and the nuclear reactor is the intermediate heat exchanger. Thus, in the simplified model, the interface between the two loops can be reduced to the heat transfer, Q, through the intermediate heat exchanger. Thus, to drive a transient in both loops, this heat transfer quantity, Q, must be changed in some way. The transient model for the reaction chamber is implemented in a series of MATLAB scripts based on the available thermodynamic and kinetic data. For the transient analysis, the following initiating events are assumed;

Helium Inlet Temperature Perturbation

Initiating Event = step(or ramp) increase (or decrease) in helium inlet temperature (Th1)

Case 1) 25 K step increase , Case 2) 5 K/s ramp increase for initial 5 seconds and remain constant afterward, Case 3) 5 K/s ramp decrease for initial 5 seconds and remain constant afterward, Case 4) 25 K step decrease

Helium Inlet Flowrate Perturbation

Initiating Event = step (or ramp) increase (or decrease) in helium inlet flow

Case 1) 10 % step increase , Case 2) 2 %/s ramp increase for initial 5 seconds and remain constant afterward, Case 3) 2 %/s ramp decrease for initial 5 seconds and remain constant afterward, Case 4) 10 % step decrease

Figures 5.4(a) and (b) show reaction chamber temperature in section 2 and 3. The reaction chamber temperature in section 2 quickly responds to the perturbation and the new steady state is reached within 20 seconds period. However, the response of section 3 is too slow to reach a new steady state condition for the same time frame. The section reaction chamber temperature change is slower because the volume of the chamber required for assumed hydrogen generation for section 3 is large. The reactions rates in Section 3 are slower are slower and hence require large chamber volume.

In Figure 5.5, the outlet molar flow rate from reaction chamber in section 2 and 3 are shown for the transient. The section 2 molar flow rate as a result of the transient reaches new steady state in 20 seconds time whereas for the section 3 the steady state is reached at more than 500 seconds. The slower response of the Section 3 molar flow rates is due to chemical kinetics.

In Figure 5.6 the oxygen mole fraction in section 2 is shown. In Figure 5.7 the hydrogen mole fraction is shown for the inlet helium temperature perturbation. The response of the reaction chamber temperatures for helium inlet flow rate perturbation is shown in Figure 5.8 for section 2 and 3. From these figures it is seen that the mole fraction change with time occur at

much slower rate in Section 3 than in Section 2. The response of the oxygen mole fraction in section 2 and the hydrogen mole fraction in section 3 are shown in Figures 5.9 and 5.10 respectively. The response of the section 2 is fast and that of the section 3 is slow for this initiating event as well. The differences in the response between two sections come from different reaction kinetics: The reaction kinetics in Section 3 is slow so that the reaction chamber volume for Section 3 is much bigger than for Section 2.

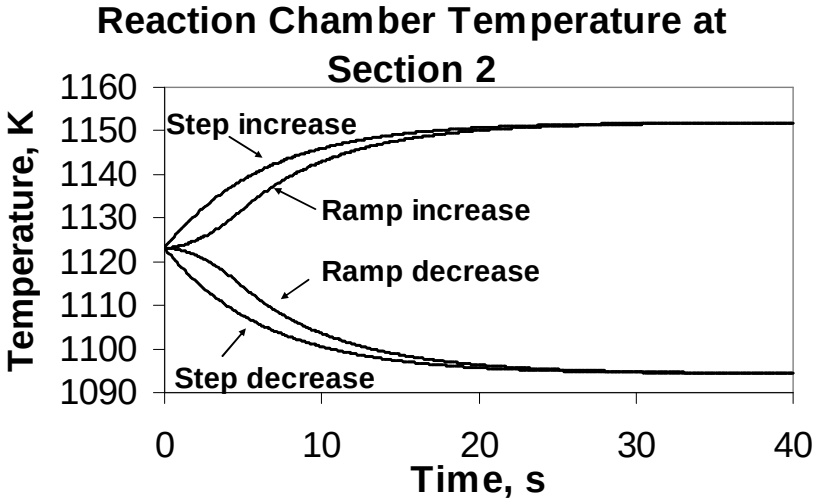

(a)

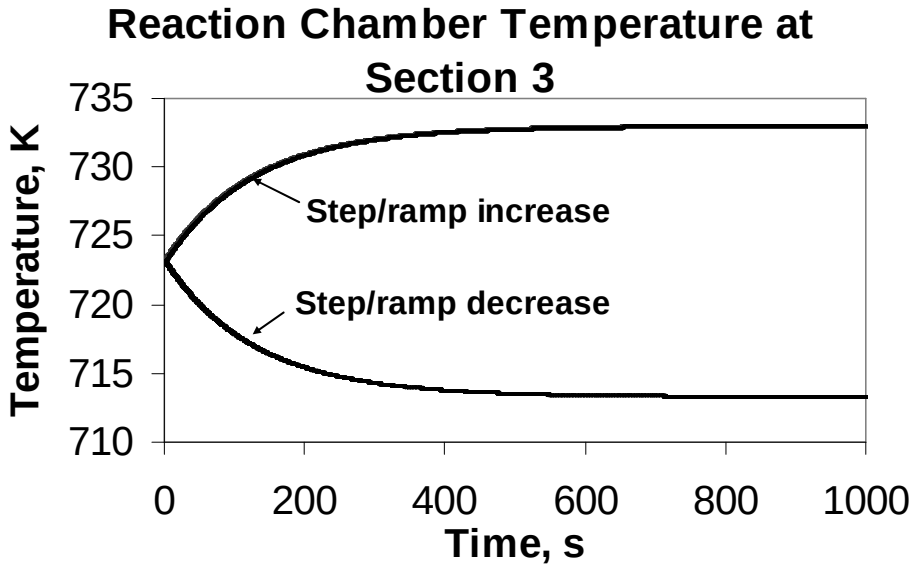

(b)

Figure 5.4 - a) Section 2 b)Section 3 Reaction chamber temperature for inlet helium temperature change events

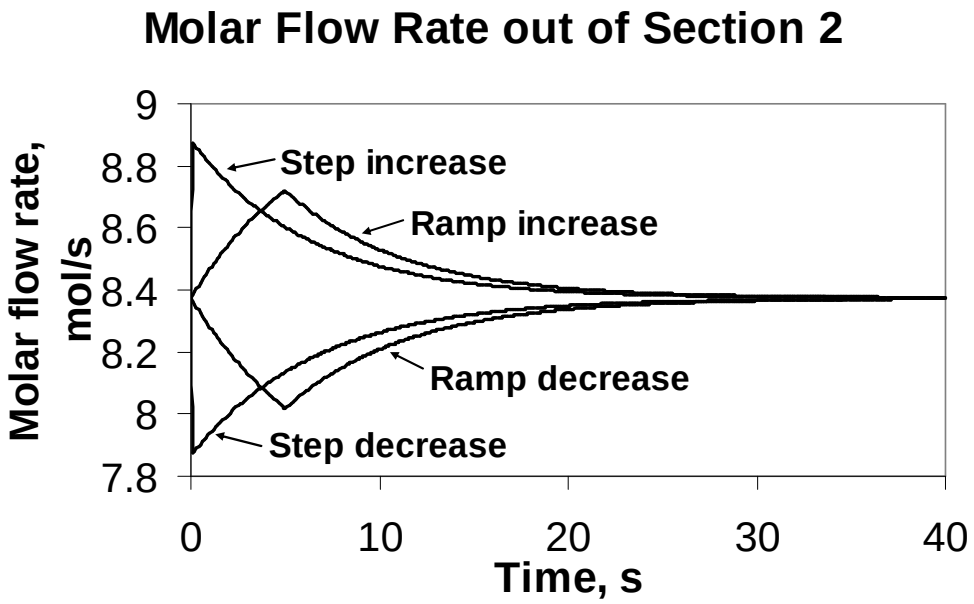

(a)

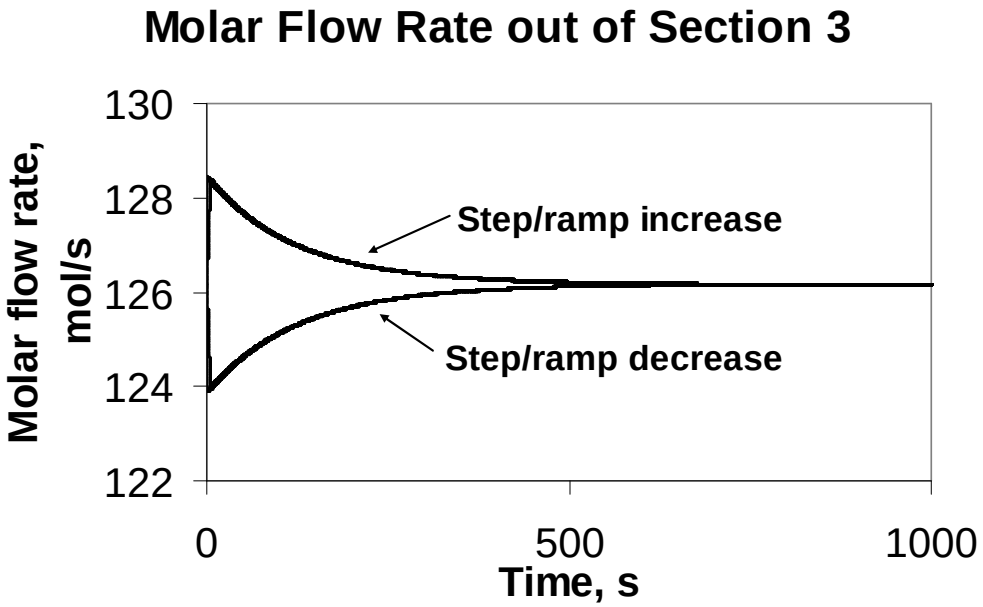

(b)

Figure 5.5 - a) Section 2 b)Section 3 Outlet molar flow from reaction chamber for Th1 change events

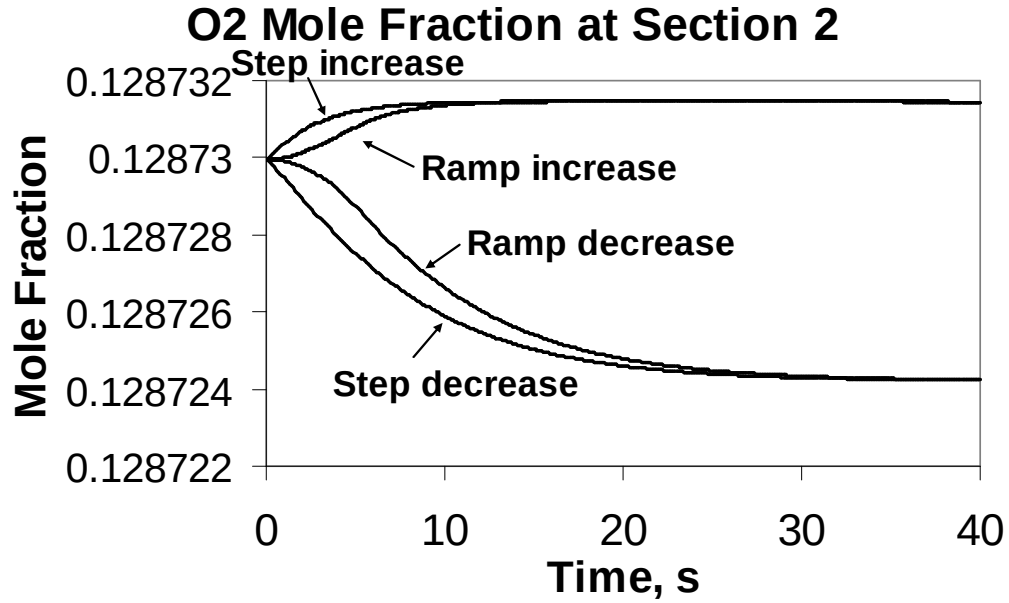

Figure 5.6 - Oxygen mole fraction at Section 2 for Th1 change events

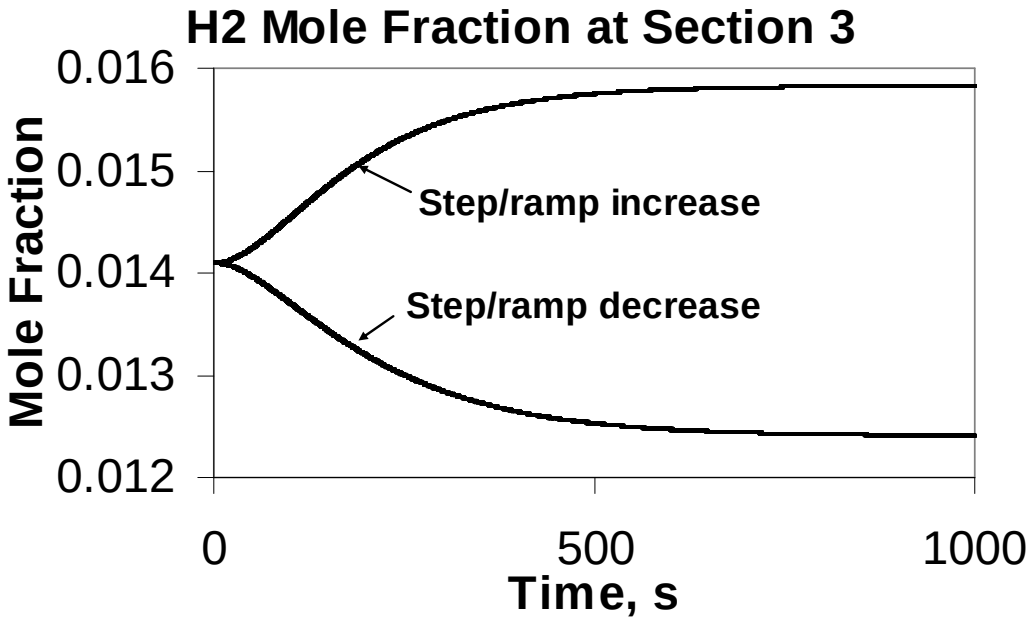

Figure 5.7 - Hydrogen mole fraction at Section 3 for Th1 change events

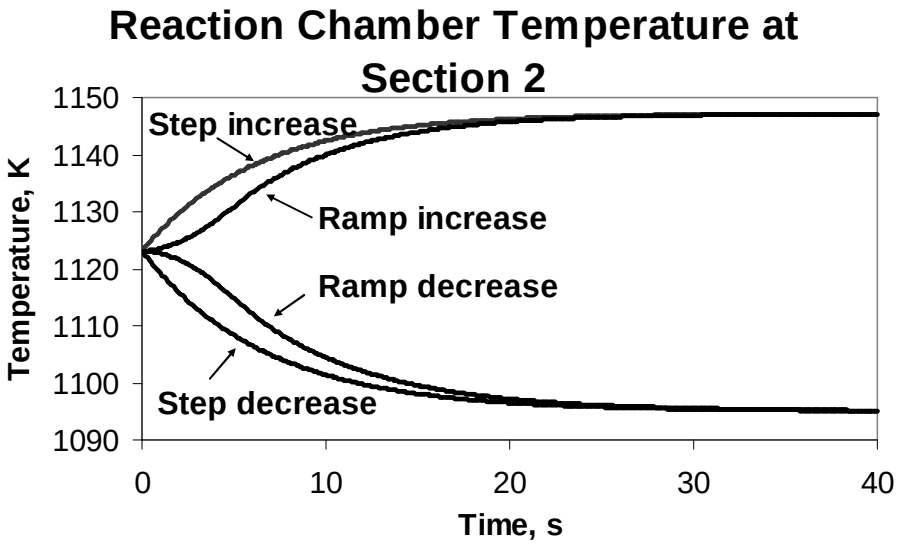

(a)

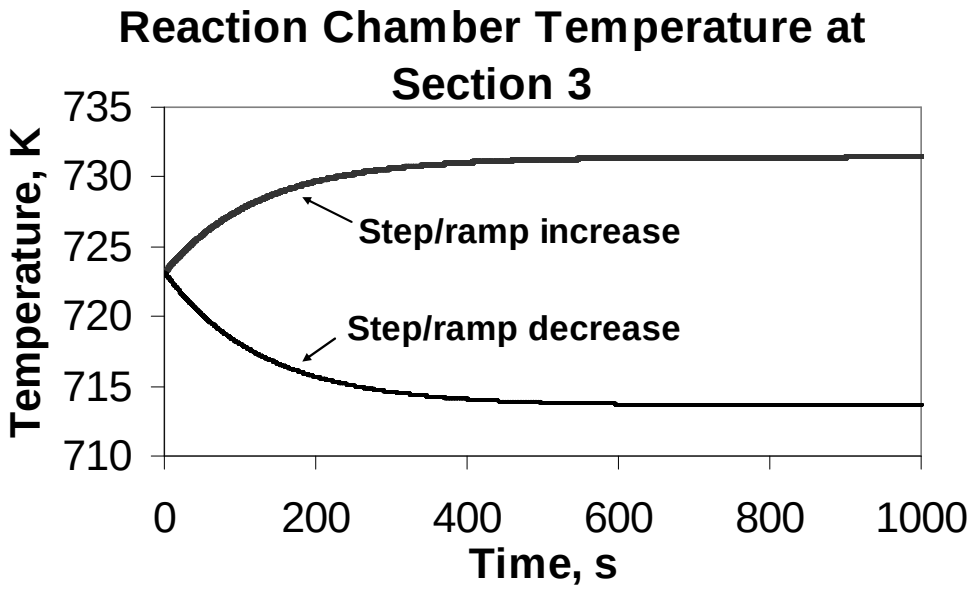

(b)

Figure 5.8 - a) Section 2 b)Section 3, Reaction chamber temperatures for Helium flow change events

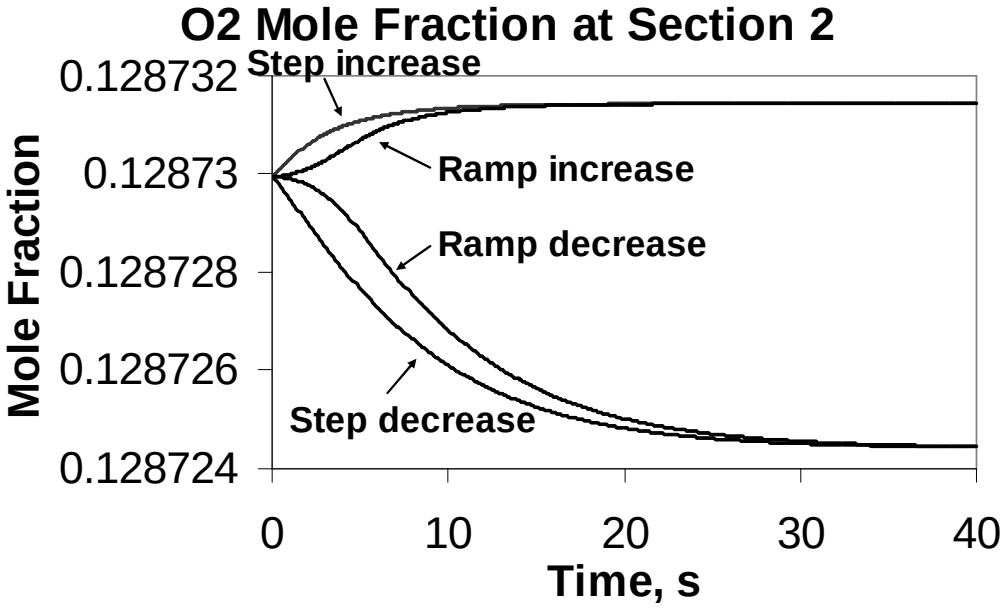

Figure 5.9 - Oxygen mole fraction at Section 2 for Helium flow change events

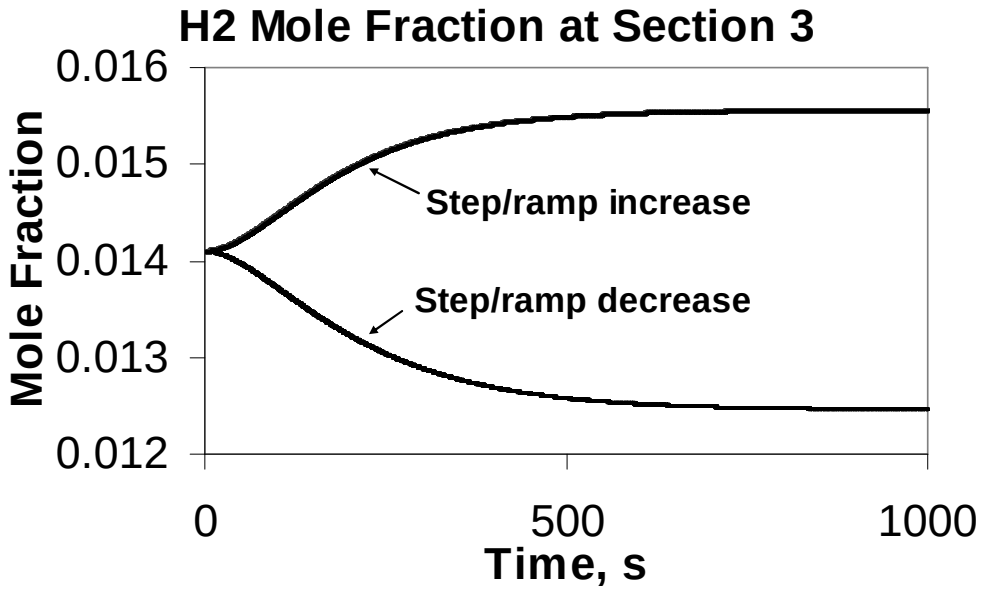

Figure 5.10 - Hydrogen mole fraction at Section 3 for Helium flow change events

5.5 Nomenclature

A chemical species

A_1, A_2 ,, A_3, A_{-3} pre-exponent factor for reaction rate

C concentration in reaction chamber

c_p specific heat at constant pressure volume

c_v specific heat at constant volume

E activation energy of reaction

G Gibbs energy

h enthalpy

H total enthalpy

k rate constant of reaction

m molar flow rate

M number of moles

p partial pressure

P total pressure

Q_{HX} heat transferred in heat exchanger

R universal gas constant

S entropy

t time elapsed

T fluid temperature

U Internal energy

V volume

dX reactant X produced by reaction

y mole fraction of reactant

Z Concentration of chemical species

Greek

v stoichiometric coefficient

ρ density

Subscript

i species type

in in

out out

R reaction

RXN specific reaction

Portions of this chapter were reported in the American Nuclear Society journal, Nuclear Technology.

"Simulation of Sulfur-Iodine Thermochemical Hydrogen Production Plant Coupled to High-Temperature Heat Source," by N. R. Brown, S. Oh, S. T. Revankar, et al., Published in Nuclear Technology, Vol. 167, No. 1, pages 95-106.

6. Nuclear Plant and Interface System Model and Transient Analysis Results

6.1 Introduction

Implementing a nuclear reactor hydrogen production scheme requires robust models of chemical plant and reactor thermal hydraulic behavior and response. Efforts have been conducted in both the transient modeling of the Sulfur Iodine (SI) and Hybrid Sulfur (HyS) thermo-chemical cycles (Brown et al., 2006, 2007).

While several reactor concepts are candidates for use as a high temperature heat source in nuclear hydrogen production, one of the most thoroughly investigated candidates is the Pebble Bed Modular Reactor, or PBMR. Recent work has been performed in benchmarking the THERMIX code to the PBMR 268 and 400 designs (Reitsma et al. 2006, Tyobeka et al. 2007, Hauue et al. 2006, Seker et al. 2005).

In an actual nuclear hydrogen production system, the reactor loop will be coupled to the chemical loop via an Intermediate Heat eXchanger (IHX). This coupling is illustrated in Figure 6.1.

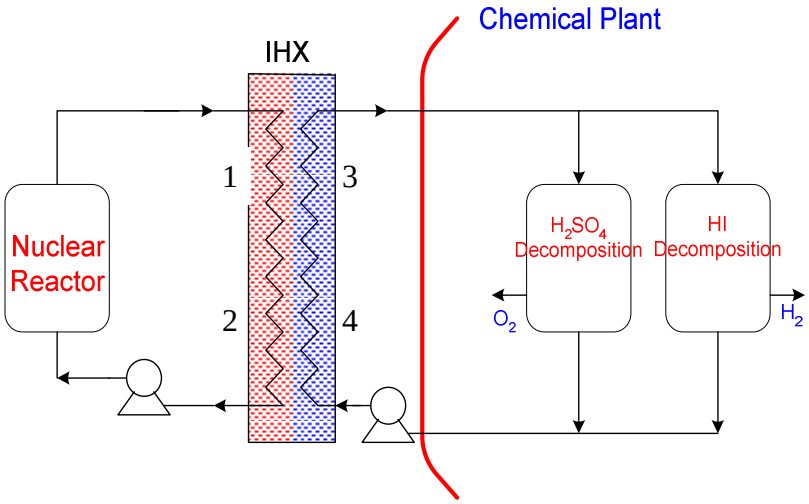

Figure 6.1 - Coupled SI-Cycle Systems

Previous models developed for the SI cycle and HyS cycle initiated transient events at the intermediate heat exchanger inlet to the chemical plant without regard to the response on the nuclear reactor side. The location where transients were initiated in the previous efforts is indicated by location 1 in Figure 6.1. In these models, simple transients were initiated via a

change in flow rate or temperature. For further investigation of severe accident scenarios, a more comprehensive coupling of a detailed PBMR model featuring thermal hydraulic and neutronic characteristics of the reactor is required. A model of the nuclear reactor loop of the coupled system is added to the previous chemical plant models.

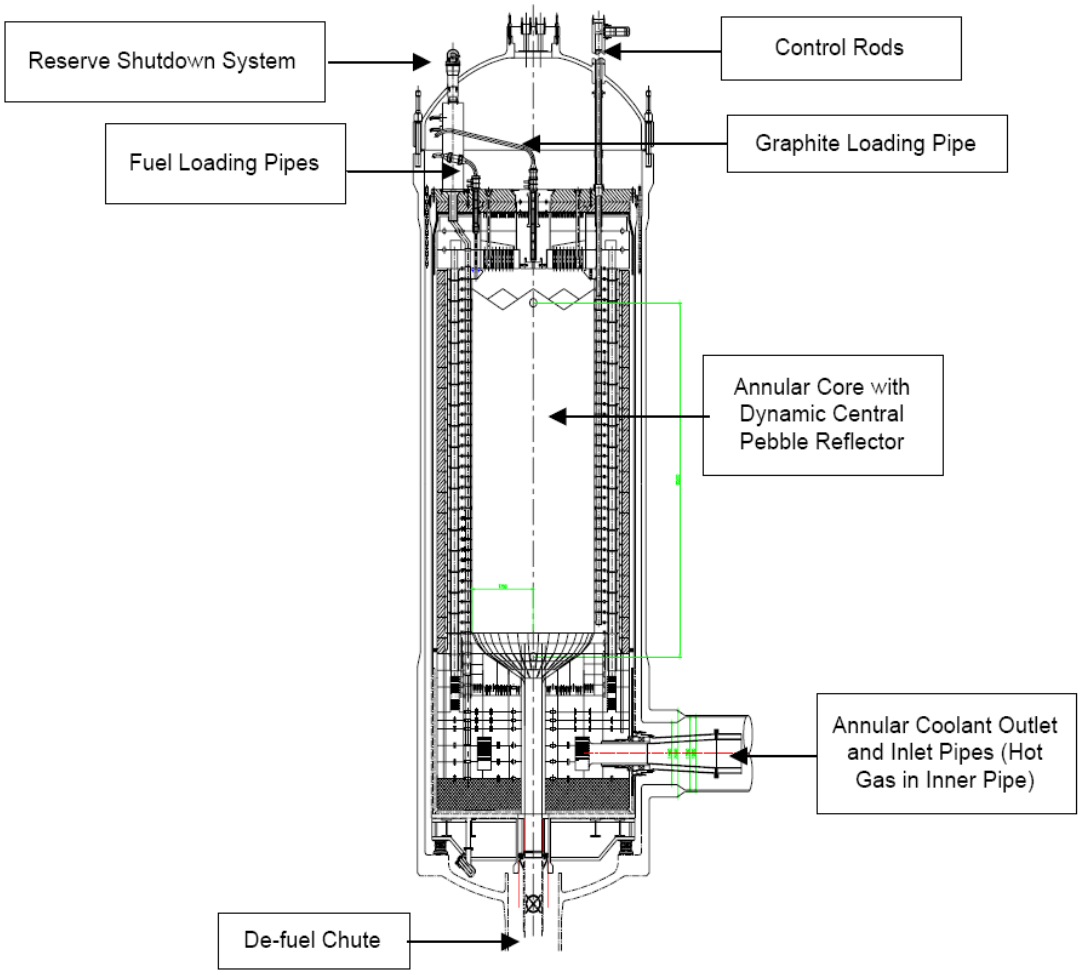

Figure 6.2 - PBMR 268 design schematic (reproduced from Ref. Matzner 2004)

If a nuclear reactor is coupled via heat exchanger to a SI cycle chemical plant, the entire system becomes subject to transients in either the reactor loop or the chemical plant. The IHX serves as a heat exchanger from nuclear plant side to chemical plant side and also acts as an isolation device between two plants. The high temperature helium stream from the IHX outlet is branched into two sub-streams: one for sulfuric acid decomposition process, the other for hydrogen iodide decomposition process. Cold helium streams from each chemical process merge into single stream and return to the IHX.

THERMIX is a thermal-hydraulics analysis code for pebble bed reactors. THERMIX solves the 2-D, steady state and time dependant mass, energy, and momentum balance equations in cylindrical coordinates. The solution is based on the porous media approach. Energy equation is solved considering the two temperature model. The temperature inside the fuel pebble is obtained from 1-D conduction solution in spherical coordinates

6.2 Model Summary

A transient model for the SI cycle has been developed (Brown et al. 2006, 2007). The model utilizes a system of mass balance, energy balance, and chemical kinetics equations which are solved simultaneously to determine system transient behavior during and after a perturbation. In previous analyses, the interface conditions between the chemical plant and the nuclear reactor were described by either:

- Scalar flow conditions in the hot side of the IHX
- Varying flow conditions in the hot side of the IHX

Since a reactor thermal hydraulic and/or point kinetics model was not coupled to the previous analyses, there was no feedback provided via the flow conditions on the hot side of the IHX. Thus, the interface conditions in previous reports were either for fixed scalar or fixed vector IHX conditions.

A more robust model of a coupled nuclear hydrogen production system includes feedback via the interface conditions to the reactor. Thus, as the flow quantities in the chemical plant change, the corresponding flow quantities in the reactor change as well. To achieve a more sophisticated understanding of such a coupled system, a PBMR268 THERMIX model and a simple point kinetics model is coupled to the hydrogen production models. Note: The PBMR-268 model utilized in this chapter was developed by Seker and Downar, as part of a separate research effort. (See: V. Seker, Multiphysics methods development for high temperature gas reactor analysis. Ph.D thesis, Purdue University, 2007.)

The reference design for the PBMR268 benchmark problem is derived from the 268 MW PBMR design (Reitsma et al. 2006, Tyobeka, et al 2007). Numerous assumptions were made regarding the geometry of the PBMR 268 design in the benchmark specification. Some of the most important simplifications are:

- Core is assumed to be 2-D (r,z).
- Flattening of the pebble bed's upper surface
- Flow channels within the reactor parallel

A scaling analysis of the hydrogen production model was completed, and preliminary transient analysis was investigated. In the Purdue SI-cycle model, the steady state power required from the heat exchanger is calculated via an energy balance for a desired hydrogen production rate. For a steady state power of 268 MWth in the heat exchanger, the hydrogen production rate is 1034 mol/s.

In a coupled nuclear hydrogen production system, a transient is initiated on either the nuclear reactor side or the chemical side of the plant. There are many potential transients that occur in a nuclear reactor system. Some examples are,

- Startup –or- shutdown,
- Reactivity insertion or removal,
- Off-normal operation, and
- Design basis accident.

In the chemical plant, examples of transient driving forces are,

- Reaction chamber temperature change,
- Small pipe break or leak,
- Vapor explosion, and
- Chemical plant fire or other event.

In terms of nuclear reactor response, each of these chemical plant events is a loss-of-heat-sink accident.

A preliminary investigation of the coupling of the chemical plant and nuclear reactor consists of evaluating the response of the chemical plant and feedback to the nuclear reactor in a reactivity insertion or removal. By first studying the behavior and response of the plant in simple reactivity transients a formulaic approach is taken to investigation of more serious events.

When unifying two systems which are dynamic and provide feedback to each other the nature of the response is dictated by the relative time constants of the plants. A PBMR is a thermal reactor, thus delayed neutrons are the important factor in reactor response. A thermal reactor has a time constant of about 55 seconds (Lamarsh 1996). In the chemical plant, Section 2

and Section 3 have different response times. This is illustrated in Figure 6.3. Section 2 has a response time on the order of 20 seconds, whereas Section 3 has a response time on the order of 500 seconds. The limiting reaction rate in the chemical plant is that of Section 3. Since the chemical plant is composed of cyclic processes, we know that the slowest reaction rate will occur in Section III, the HI decomposition section. This rate provides at least a first-order approximation of the plant response.

The reason for the large response time of Section III is that HI decomposition requires a very large volume. This large volume is due to the reverse reaction rate of HI decomposition which is on the same order as the forward reaction rate. In the simplified SI model, HI decomposition is the most challenging reaction in terms of chemical kinetics. In contrast, the chemical kinetics of the H_2SO_4 decomposition is straightforward, but there are many material difficulties due to high temperature and the highly corrosive nature of the solution. The long response time of Section 3 slows chemical plant feedback to the nuclear reactor.

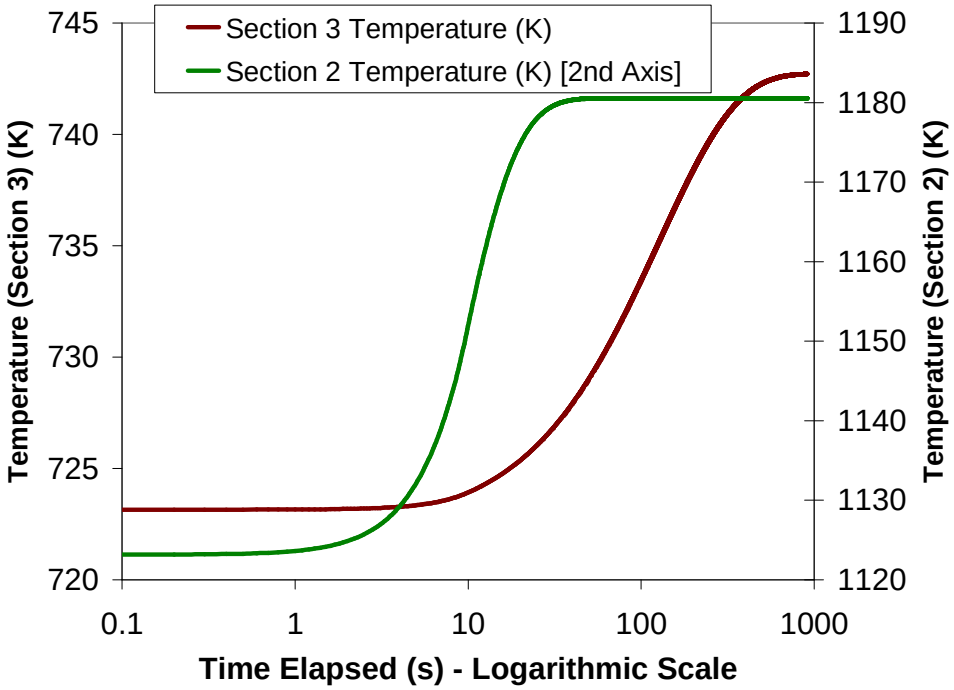

Figure 6.3 - Response time of Section 2 and Section 3 to a transient event

6.3 Model Integration Scheme

The hydrogen and THERMIX codes have three points of interaction:

1. Initial steady-state solution

2. Initiating event coupling
3. In-transient feedback

First, a steady-state solution is attained in both the THERMIX model and hydrogen model. Second, a transient is initiated, either in the chemical plant model or in the point kinetics model. Finally, the THERMIX, point kinetics, and hydrogen generation models all interact in each time step. The integration scheme is shown in Figure 6.4

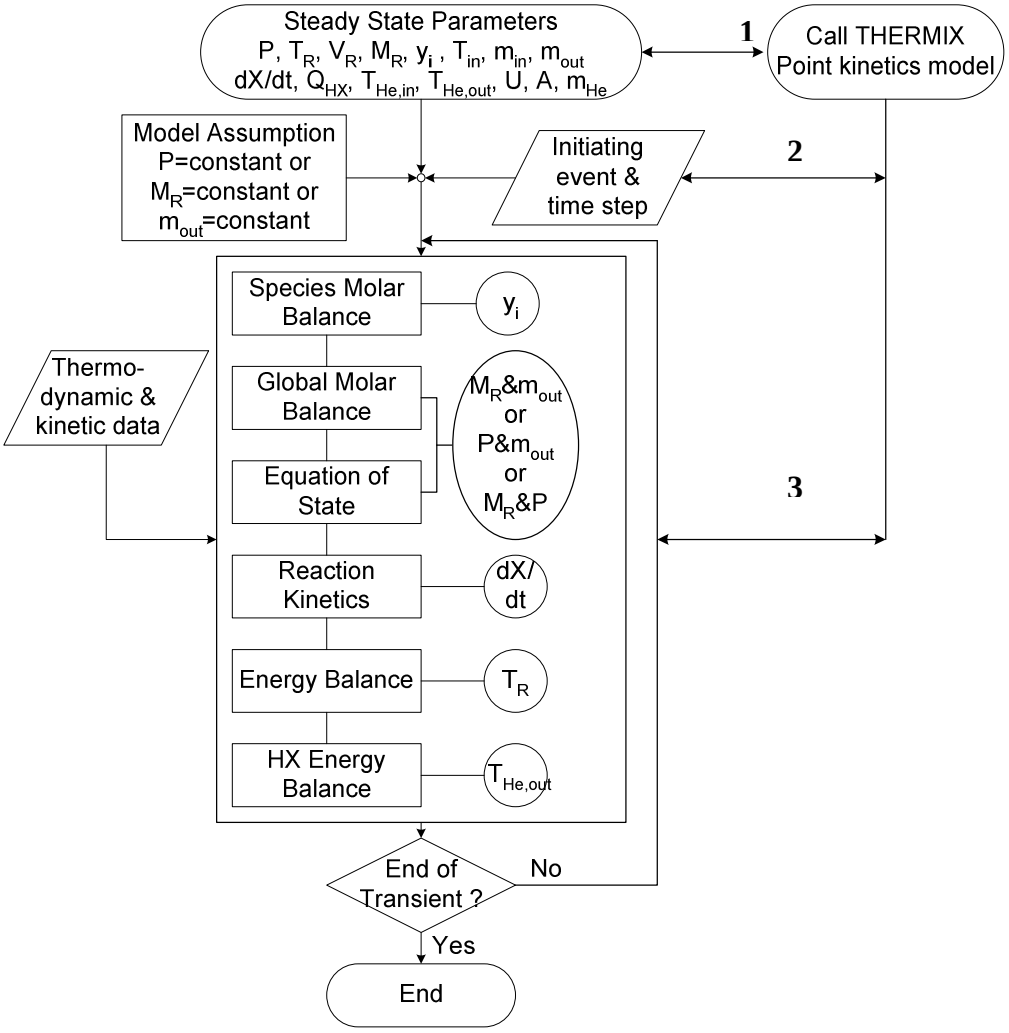

Figure 6.4 - Coupled model flow-sheet

Coupling of the codes is performed through the IHX. The data exchanged between the codes consists of the flow rate and temperature of helium through both hot and cold legs of the IHX. The hydrogen model calls THERMIX and the point kinetics model every time step and then new temperature and flow rate values are returned. This process is repeated each time step.

6.4 Coupled Model Transients

In a coupled nuclear hydrogen production system, many varieties of transients are possible. A transient event which is driven by the chemical plant might consist of a small leak or break in piping. Such an event would be a partial loss of heat sink accident. A more catastrophic chemical plant driven accident, such as an explosion, would cause a complete loss of heat sink for the nuclear reactor.

One interesting reactor driven transient is that of a reactivity removal. As reactivity is removed, nuclear reactor power and coolant temperature will drop. The heat sink for the nuclear reactor is the chemical plant. Section 2 has a very high threshold temperature, around 800 ^{o}C (Le Guigou et al. 2006). Below this threshold temperature, the reaction will not proceed. The heat transferred through the IHX is split into the sensible heat, the latent heat of vaporization, and the heat required for the endothermic chemical reaction.

$$Q_{HX} = Q_{sensible} + Q_{vaporization} + Q_{reaction} \tag{6.1}$$

After a negative reactivity is inserted, such as a control rod insertion, the reactor power and temperature will drop accordingly. As the coolant temperature drops, the value of $Q_{reaction}$ will incur a corresponding drop. Thus, as the reactor coolant temperature drops, the reactor will also lose a portion of its heat sink. The magnitude of the loss of the reaction heat sink should be investigated.

6.5 Model Transient Test

To test the transient integration of the THERMIX and hydrogen production models, a simple step reactivity insertion of \$ 0.20 is used. This reactivity insertion is shown in Figure 6.5. Due to simplicity, a small reactivity insertion is a good candidate for consideration.

The reactor thermal power and the load of the heat exchanger are plotted in Figure 6.6. A relatively small amount of the power increase is actually sent to the chemical plant, since much of the additional heat is used to raise the temperature of the fuel, moderator, and containment of the reactor. After the response from the reactivity insertion, a new steady state is attained within several hundred seconds.

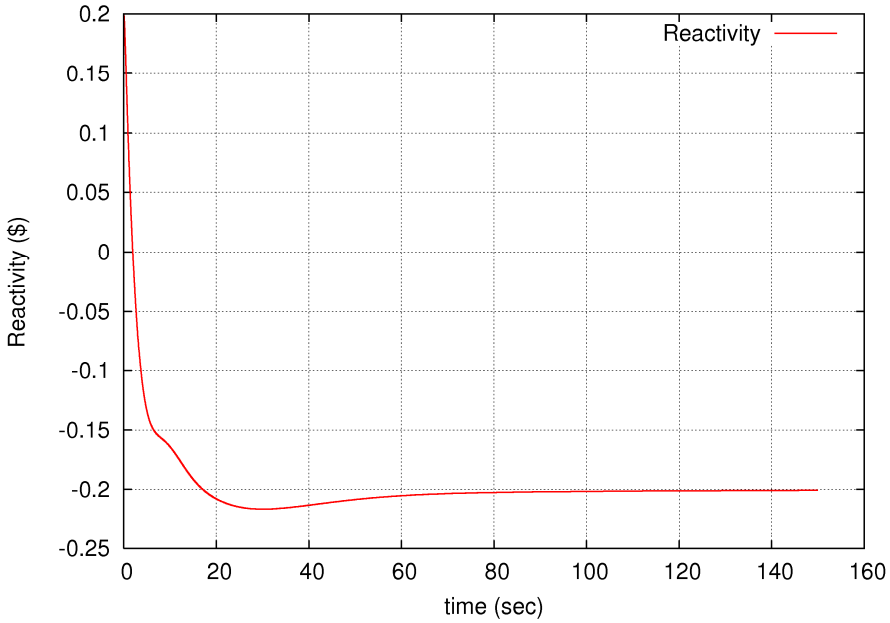

Figure 6.5 - Reactivity insertion of $ 0.20

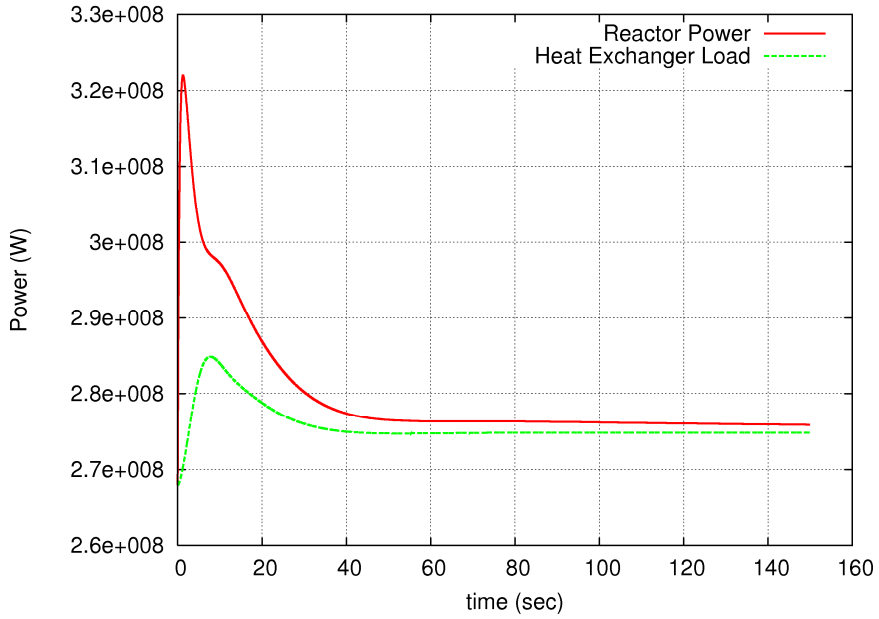

Figure 6.6 - Power response of reactivity insertion

The maximum fuel, average fuel temperature, and average core temperature are plotted in Figure 6.7 and Figure 6.8. Integrating the average core temperature, over the first 20 seconds and comparing the power deposited in the core to the approximate power required to raise the temperature of the reactor core by 41 ^{o}C it is determined that the predicted amount of heat deposited in the core is reasonable.

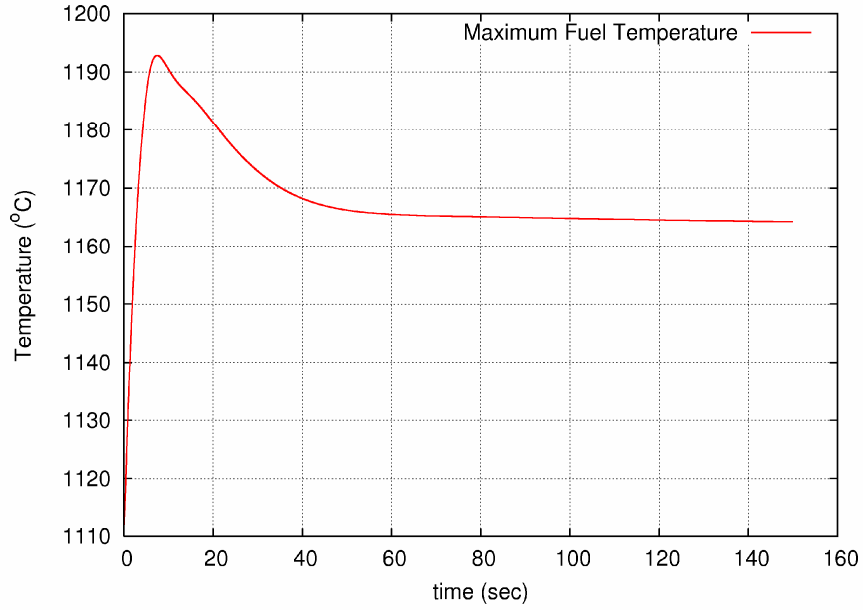

Figure 6.7 - Maximum fuel temperature

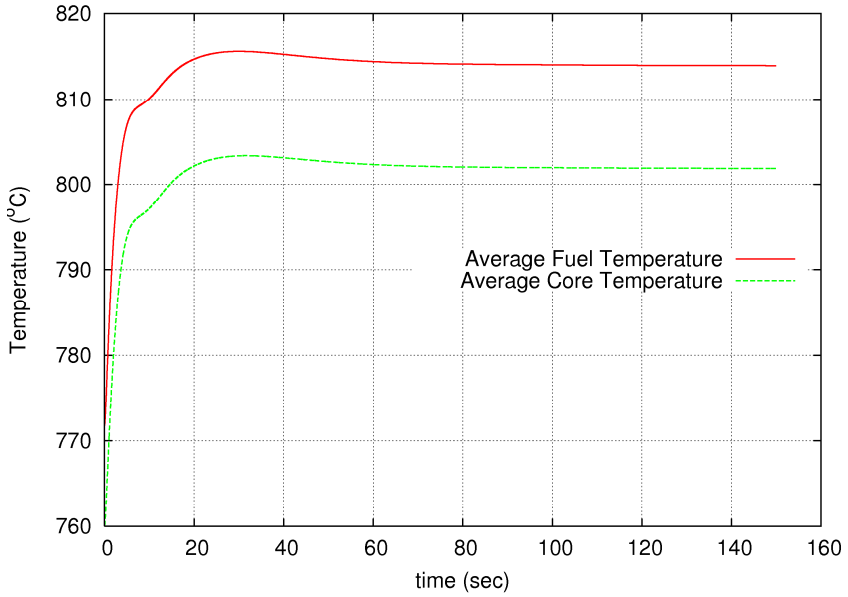

Figure 6.8 - Average fuel and core temperature

The radial and axial fuel and coolant temperatures at the initial steady state, the peak temperature, and the final steady state, are shown in Figure 6.9 and Figure 6.10. Since the reactor neutronics is based on a simple point kinetics model, change in the shape of the plots is not expected, since the basic flux shape will remain the same. The flux shape will change in magnitude, hence the changes seen in Figure 6.9 and Figure 6.10.

Since the reaction rate of Section III is too slow to provide relevant feedback to the reactor side, only the temperature and reaction rate of Section 2 are examined. Since the SI process is cyclical, the Section III reaction rate will also significantly dampen the entire response of the chemical plant. However, since there is some initial concentration of reactants in the Section II reaction chamber, the H_2SO_4 decomposition rate will have a sharp increase, due to the temperature increase in the IHX. In Figure 6.11 the temperature in Section II as well as the reaction rate is plotted. These plots illustrate the quick response of Section II to the temperature in the IHX.

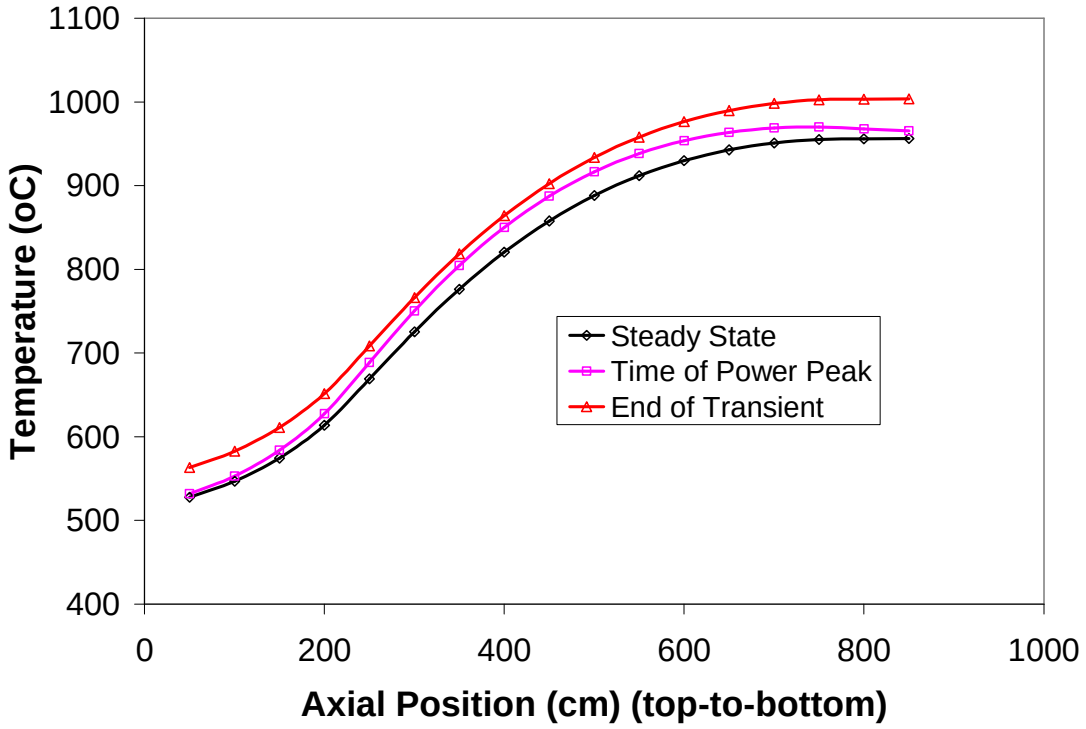

Figure 6.9 - Fuel pebble center axial temperature

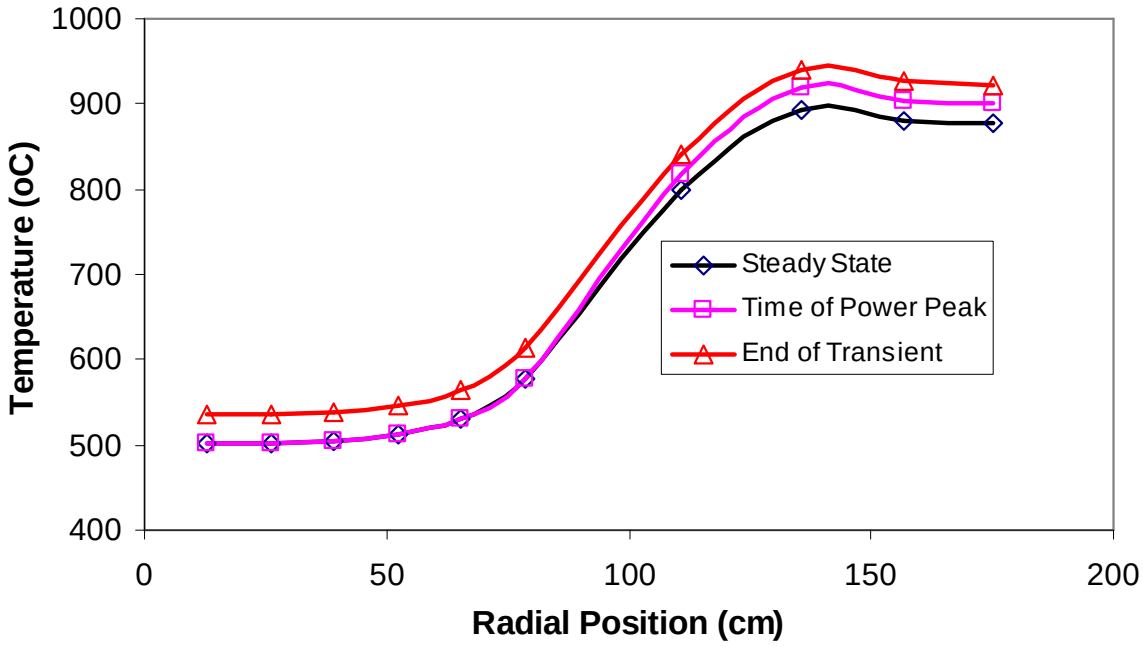

Figure 6.10 - Fuel pebble radial temperature

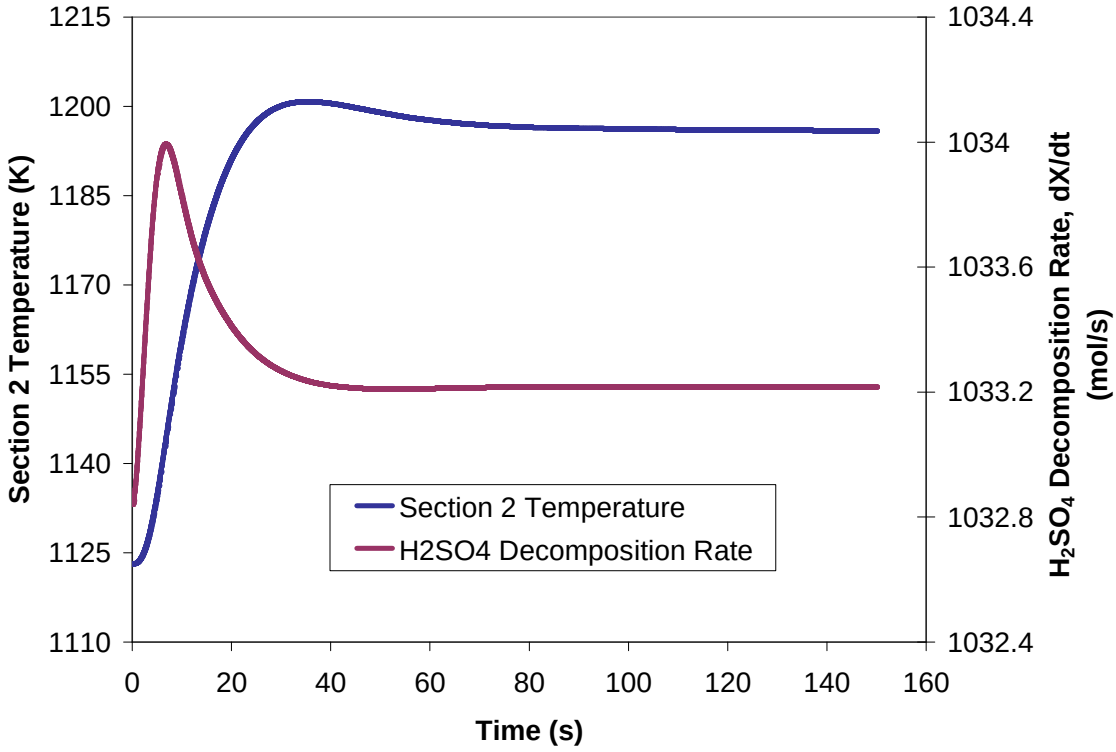

Figure 6.11 - Section 2 temperature and decomposition rate

6.6 Nomenclature

A : Heat transfer area

m : Molar flow rate

M_R : Number of moles in reactor

P : Reactant pressure

$\dot{Q}_{HX}$: Heat transferred in heat exchanger

$Q_{reaction}$: Chemical reaction heat

$Q_{sensible}$: Sensible heat transferred to fluid

$Q_{vaporization}$: Latent heat of vaporization

t : Time elapsed

T : Fluid temperature

T_R : Bulk temperature in reactor chamber

U : Intermediate heat exchanger coefficient

V_R : Reactor volume

dX : Reactant X produced by reaction

y : Mole fraction of reactant

$[Z]$: Concentration of chemical species Z

7. Conclusions

Thermochemical hydrogen production is a method to obtain hydrogen from water by a series of reactions. Many types of thermochemical hydrogen production have been proposed. The Sulfur-Iodine (SI) process is one of water splitting methods using iodine and sulfur as recycling agents. The SI cycle consists of three chemical reactions expressed as the following equations.

Section I (Bunsen reaction): $I_2+SO_2+2H_2O \rightarrow 2HI+H_2SO_4$

Section II (Sulfuric acid decomposition): $H_2SO_4 \rightarrow H_2O+SO_2+1/2O_2$

Section III (Hydrogen Iodide decomposition): $2HI \rightarrow H_2+I_2$

In the SI cycle, all process fluids are recycled and no greenhouse gases are emitted. Also, the SI cycle has been fully flow sheeted and operated at the bench scale in the US and Japan. This cycle has the highest efficiency (~52%) of any process that has been fully flow sheeted. However, the integrated SI cycle is not yet fully demonstrated and the process economics are not yet verified.

In this report, the SI thermochemical cycle was simulated using ASPEN PLUS version 12. The GA's flowsheet (Brown et al. 2003) Section I, II, and III are used as a reference. The present simulations followed the methodology applied to the GA's flowsheet. A step-by-step simulation was performed starting from the single component simulation to the whole Section simulation. For the single component simulation, conversed solutions were obtained and the results were comparable to the GA's results. For the whole Section simulation, the converged solution for Section II was obtained and the results were also comparable to the GA's result. The sensitivity analysis shows the same behavior as in GA's report. For the whole Section simulation, the converged solution for Section I, II and Section III was obtained and the results were also comparable to the GA's result. Various attempts has been tried to resolve the convergence issue in Section I and III.

A simplified model of the SI-cycle for transient analysis was developed. Balance equations for the simplified model were presented and parameters for the model were introduced. An introduction to potential transient scenarios in a nuclear reactor – chemical plant system was detailed. Continuing improvements to the simplified model were outlined.

A mathematical model was developed for simulation of dynamic response of the SI cycle coupled to nuclear heat source. In this model recycling of reactants is accounted for in molar balance. The energy balance considers sensible, latent, and reaction heat. Constant reaction chamber pressure is assumed. The reaction chamber model is used to analyze the reaction chamber of sulfuric acid (H_2SO_4) and hydrogen iodide (HI) decomposition reactor in SI cycle. Steady state concentrations of reactants are obtained from the GA flow sheets and ASPENPlus calculation. Transients are initiated from high temperature helium side such as helium inlet temperature or helium inlet flow rate changes are simulated. The results indicate that the dynamic response of the SI cycle for small perturbation in process heat coolant temperature and the coolant flow rate. The results are useful in assessing the transient behavior of coupled SI plant with nuclear reactor heat exchanger.

A coupling of previously developed chemical plant models to a THERMIX PBMR benchmark is described. Steady state results and preliminary transient results are presented.

From this study, it is concluded that the response of Section III is practically non-existent over the time scale of a nuclear reactor transient. The immediate response of Section II, however, is important to consider. It is concluded that partial and total loss-of-heat-sink accidents categorization and analysis are very important to the safety of any coupled nuclear hydrogen production system.

8. Accomplishments

- The whole Sections I, II and III of the SI cycle were fully flowsheet and the results are similar to the GA's results.
- Specifically the convergence of the Section III (HI decomposition) of the SI cycle was achieved. The convergence was performed by using the GA strategy and data. First, the column was converged without the HI decomposition reaction, then, the value of the equilibrium constant for the reaction was increased gradually. Once the column convergence was obtained, the operating conditions, as the pressure, the boiling rate were varied simultaneously and a production of 1kmol/hr was obtained. The sensitivity analysis was also performed to study the influence of the side liquid flow rate on the hydrogen generation rate. Various attempts has been tried to resolve the convergence issue in Section I.
- A membrane separation technology for the Section III has been considered for efficient separation.
- A simplified transient model for SI cycle was further developed that included recycle of reactants. Various transient cases were studied with initiating event from the chemical plant.
- A model for coupled nuclear reactor (PBMR) and hydrogen plant was developed. The reactor core was modeled with THERMIX code and a point kinetic model was used for the reactor core.
- Transient analysis of the couple nuclear plant and chemical plant was carried out with reactor initiated events.

9. Future Work

- Implement the membrane separation techniques for the HI and H_2SO_4 decomposition processes and modify the flowsheet
- Perform comparative flowsheet analysis of the modified cycles
- Optimize the flowsheet for each sections for process efficiency
- Perform detailed transient analysis of the simplified thermochemical process coupled to nuclear reactor heat transport system for hydrogen generation using SI cycle.
- Operational and Process Control Strategies for the Hydrogen Plant
- Preliminary Guideline for the Control Logic in Both Plant Sides

10. References

1. Arifal, Hwang, G.-J., and Onuki, K. (2002). "Electro-electrodialysis of hydriodic acid using the cation exchange membrane cross-linked by accelerated electron radiation." Journal of Membrane Science, 210(1), 39-44.
2. Besenbruch, G. E. (1982). "General Atomics Sulfur-Iodine Thermochemical Water-Splitting Process." Am. Chem. Soc., Div. Pet Chem(Prepr. 271), 48-53.
3. Brown, L.C., Besenbruch, G.E., Funk, J.E., Marshall, A.C., Pickard, P.S., Schowalter,S.K., (2003), "High efficiency generation of hydrogen fuels using nuclear power", DE-FG03-99-SF21888, Final technical report for the period August 1, 1999 through September 30, 2002, La Jolla, CA: General Atomics Corp. Report GA-A24285.
4. Brown, N., Oh S., Revankar, S. T., (2006)“Simulation of Heat Exchanger Transients In Sulfuric-Acid and Hydrogen-Iodide Decomposition IMECE2006-14566,” Proceedings of the 2006 ASME Congress, Chicago IL. ASME.
5. Brown, N., et al. (2007), “Analysis Model for SI (Sulfur Iodine) and HyS (Hybrid Sulfur) Thermo-chemical Cycle Coupled to High Temperature Gas Cooled Reactor.” Proceedings of Safety and Technology of Nuclear Hydrogen Production, Control and Management (ST-NH2). Boston, MA ANS.
6. Duigou, A. L., Borgard, J.-M., Larousse, B., Doizi, D., Allen, R., Ewan, B. C., H. Priestman, G., Elder, R., Devonshire, R., Ramos, V., Cerri, G., Salvini, C., Giovannelli, A., De Maria, G., Corgnale, C., Brutti, S., Roeb, M., Noglik, A., Rietbrock, P.-M., Mohr, S., de Oliveira, L., Monnerie, N., Schmitz, M., Sattler, C., Martinez, A. O., de Lorenzo Manzano, D., Cedillo Rojas, J., Dechelotte, S., and Baudouin, O. (2007). "HYTHEC: An EC funded search for a long term massive hydrogen production route using solar and nuclear technologies." International Journal of Hydrogen Energy, 32(10-11), 1516-1529.
7. Elder, R. H., Priestman, G. H., Ewan, B. C., and R. W. K. Allen 2005, Process Safety and Environmental Protection. (2005). "The separation of HIX in the sulfur-iodine thermochemical cycle for sustainable hydrogen." 83(B4), 343-350.
8. Engels, H. and Knoche, K.F., (1986), "Vapor pressures of the system HI/H2O/I2 and H2", Int. J. Hydrogen Energy, 11, 703-707.

9. Engels, H., Knoche, K.F., Roth, M., (1987), "Direct dissociation of hydrogen iodide-An alternative to the General Atomic proposal," Int. J. Hydrogen Energy, 12, 675-678.
10. Fogler, H. S. (1999). Elements of Chemical Reaction Engineering, Prentice Hall, Upper Saddle River, New Jersey.
11. Forsberg, C. W. (2003). "Hydrogen, Nuclear Energy and the Advanced High-Temperature Reactor." Int. J. Hydrogen Energy, 28, 1073-1081.
12. Funk, J. E., and Reinstrom, R. M. (1966). "Energy requirements in the production of hydrogen from water." Ind. Eng. Chem. Proc. Des. Develop., 5, 336-342.
13. Gelbard, F., Andazola, J. C., Naranjo, G. E., Velasquez, C. E., and Reay, A. R. (2005). "High Pressure Sulfuric Acid Decomposition Experiments for the Sulfur-Iodine Thermochemical Cycle." SAND2005-5598, US Department of Commerce, National Technical Information Service.
14. Goldstein, S., Borgard, J. M., and Vitart, X. (2005). "Upper bound and best estimate of the efficiency of the iodine sulfur cycle." Int. J. Hydrogen Energy, 30, 619-626.
15. Haque, H., et al., (2006), “Thermal response of a modular high temperature reactor during passive cooldown under pressurized and depressurized conditions.” Nuclear Engineering and Design 236, pp. 475-484.
16. Huang, C., and T-Raissi, A. (2005). "Analysis of sulfur-iodine thermochemical cycle for solar hydrogen production. Part I: decomposition of sulfuric acid." Solar Energy, 78(5), 632-646.
17. Kasahara, S., Kubo, S., Onuki, K., and Nomura, M. (2004). "Thermal efficiency evaluation of HI synthesis/concentration procedures in the thermochemical water splitting IS process." Int. J. Hydrogen Energy, 579-587.
18. Kracek, F. C. (1931). "Solubilities in the system water-iodine to 200 0C." J. phys. Chem., 35, 417-422.
19. Kubo, S., Kasahara, S., Okuda, H., Terada, A., Tanaka, N., Inaba, Y., Ohashi, H., Inagaki, Y., Onuki, K., and Hino, R. (2004b). "A pilot test plan of the thermochemical water-splitting iodine-sulfur process." Nuclear Engineering and Design, 233, 355-362.

20. Kubo, S., Nakajima, H., Kasahara, S., Higashi, S., Masaki, T., Abe, H., and Onuki, K. (2004a). "A demonstration study on a closed-cycle hydrogen production by the thermochemical water-splitting iodine-sulfur process." 233, Nuclear Engineering and Design, 347-354.
21. Lamarsh, John R.. (1966), “Introduction to Nuclear Reactor Theory.” Addison-Wesley Publishing Co. Reading, MA.
22. Le Guigou, Alain, Borgard, Jean Marc, et al. (2006), “HYTHEC: An EC funded search for a long term massive hydrogen production route using solar and nuclear technologies.” Int. J. Hydrogen Energy: doi: 10.1016/j.ijhydene.2006.10.047.
23. Lukas, D. M., Kwang, Y. L., and Ghezel-Ayagh, H. (2001). "An Explicit Dynamic Model for Direct Reforming Carbonate Fuel Cell Stack." IEEE Transac. Energ. Conversion, 16, 289-295.
24. Mathias, P. M. (2005). "Applied thermodynamics in chemical technology: current practice and future challenges." Fluid Phase and Equilibria(228/229), 49-57.
25. Matzner, Dieter. (2004), “PBMR Project Status and the Way Ahead.” Proc. Of 2nd International Topical Meeting on HIGH TEMPERATURE REACTOR TECHNOLOGY Beijing, China, September22-24.
26. Nomura, M., Fujiwara, S., Ikenoya, K., Kasahara, S., Nakajima, H. S., Kubo, G.-J. H., Choi, H.-S., and Onuki, K. (2004). "Application of an electrochemical membrane reactor to the thermochemical water splitting IS process for hydrogen production." Journal of Membrane Science, 240(1-2), 221-226.
27. Nomura, M., Kasahara, S., Okuda, H., and Nakao, S. (2005). "Evaluation of the IS process featuring membrane techniques by total thermal efficiency." Int. J. Hydrogen Energy, Energy, 30(13-14), 1465-1473.
28. Norman, J. H., Besenbruch, G. E., Brown, L. C., O'Keefe, D. R., and Allen, C. L. (1982). "Thermochemical water-splitting cycle, bench scale investigations, and process engineering, Final report for the period February 1977 through December 1981." GA-A16713, General Atomics Corp, La Jolla, CA.
29. O'Keefe, D. R., and Norman, J. H. (1982). "Vapor pressure, iodine solubility, and hydrogen solubility of hydrogen Iodide-iodine solutions." J. Chem. Eng. Data, 27, 77-80.

30. Onuki, K., Hwang, G.-J., Arifal, and Shimizu, S. (2001). "Electro-electrodialysis of hydriodic acid in the presence of iodine at elevated temperature." Journal of Membrane Science, 192(1-2), 193-199.
31. Orme, C. J., and Stewart, F. F. (2007). "Pervaporation of water from aqueous hydriodic acid and iodine mixtures using Nafion(R) membranes." Journal of Membrane Science, 304(1-2), 156-162.
32. Oxtoby D.W. and N.H. Nachtrieb., 1986, "Principles of modern chemistry," Saunders College Publishing.
33. Öztürk, I. T., Hammache, A., and Bilgen, E. (1995). "An Improved Process for H2SO4 Decomposition Step of the Sulfur-Iodine Cycle." Energy Convers., 36, 1-21.
34. Reitsma, F., et al. (2006), "The PBMR steady-state and coupled kinetics core thermal-hydraulics benchmark test problems," Nuclear Engineering and Design 236 pp. 657-668.
35. Revankar S. T. and S. Oh, (2005), "Simulation of Sulfur Iodine Thermochemical water Splitting Process using ASPEN PLUS", PU/NE-05-08, September.
36. Roth, M., and Knoche, K. F. (1989). "Thermochemical water splitting through direct HI-decomposition from H2O/HI/I2/H2 solutions." Int. J. Hydrogen Energy, 14(8), 545-549.
37. Seker, Volkan, Downar, Thomas J., (2005), "Analysis of a PBMR-400 Control Rod Ejection Accident Using PARCS-THERMIX and the Nordheim Fuchs Model." Trans. American Nuclear Society.
38. Smith J. M. and H. C. Van Ness, (1987), "Introduction to chemical engineering thermodynamics," 4th ed., McGraw-Hill, New York.
39. Stewart, F. F., Orme, C. J., and Jones, M. G. (2007). "Membrane processes for the sulfur-iodine thermochemical cycle." International Journal of Hydrogen Energy Path Forward to a Hydrogen Economy, 32(4), 457-462.
40. Tyobeka, B. et al., (2007), "Utilization of two-dimensional deterministic transport methods," Ann. Nucl. Energ. doi:10.1016/j.anucene.2007.01.014.
41. Yalcin, S. (1989). " A review of nuclear hydrogen production." Int. J. Hydrogen Energy, 14, 551-561.

42. Yan, X., Kunitomi, K., Nakata, T., and Shiozawa, S. (2003). "GTHTR300 design and development, Nuclear Engineering and Design." 222(2-3 SPEC), 247-262.
43. Yildiz, B., and Kazimi, M. S. (2003). "Nuclear energy options for hydrogen and hydrogen-based liquid fuels production.", MIT Report: MITNES-TR-001, September.

Appendix.A Sensitivity Analysis

Sensitivity analysis is a tool for determining how a process reacts to varying key operating and design variables. It can be used to vary one or more flowsheet variables and study the effect of that variation on other flowsheet variables. It is a valuable tool for performing "what if" studies. The flowsheet variables that are varied must be inputs to the flowsheet. They can not be variables that are calculated during the simulation. Sensitivity analysis can be used to verify if the solution to a design specification lies within the range of the manipulated variable. It can be also used to perform simple process optimization. Sensitivity blocks are performed to generate tables and/or plots of simulation results as functions of feed stream, block input, or other input variables. Sensitivity analysis results are reported in a table on the Sensitivity Results Summary sheet. The first *n* columns of the table list the values of the variables that are varied, where *n* is the number of varied flowsheet variables entered on the Sensitivity Input Vary sheet; in this study the only flow sheet variable is the side liquid flow rate (SIDELIQ). The remaining columns in the table contain the values of variables that you tabulated on the Tabulate sheet. The tabulated results can be any flowsheet variable or any valid Fortran expression that may depend on flowsheet variables that are either input or calculated. In this study the tabulated variables are the flow rate of water at the bottom tray (BOTFW), the mole fraction of water at the bottom tray (BOTXW) and the hydrogen flow rate at the top of the separator (H2PROD) (Figure 4. 11).

The results (Table A1) can be plotted using the Plot Wizard from the Plot menu to easily visualize the relationships between different variables. Sensitivity blocks provide additional information to base-case results, but have no effect on the base-case simulation. The simulation runs independently of the sensitivity study. Sensitivity blocks with more than one varied variable generate a row in the sensitivity table for each combination of values. The sensitivity analysis to more than one variable should be done by using separate sensitivity block for each varied variable. Sensitivity blocks create loops that must be evaluated once for each row of the sensitivity table. ASPEN PLUS

sequences sensitivity blocks automatically. Accessed scalar flowsheet variables are in the units set selected for the sensitivity block. The units cannot be modified individually for different variables in the sensitivity. The unit set can either be changed for the sensitivity block (on the toolbar of the Data Browser), or enter an expression on the tabulate sheet to convert the variable. Accessed vector variables are always in SI units.

Table A.1 Sensitivity analysis results at 71bars and BR=36kmol/hr

SIDELIQ	BOTXW	BOTFW	H2PROD
50	0.399	29.733	1.002
52	0.389	28.280	0.990
54	0.380	26.811	0.977
56	0.369	25.323	0.964
58	0.357	23.813	0.948
60	0.344	22.281	0.932
62	0.331	20.724	0.914
64	0.315	19.146	0.897
66	0.299	17.556	0.880
68	0.284	16.093	0.878
70	0.284	15.526	0.878